FREEZE-THAW DURABILITY SPECIFICATION FOR HIGHWAY CONCRETE

by

Joseph Dylan O'campo

A thesis submitted to the faculty of
The University of North Carolina at Charlotte
in partial fulfillment of the requirements
for the degree of Master of Science in
Construction and Facilities Management

Charlotte

2022

Approved by:

____
Dr. Tara Cavalline

____
Dr. Brett Tempest

____
Dr. Stephanie Pilkington

ABSTRACT

JOSEPH DYLAN O'CAMPO. Freeze-Thaw Durability Specification for Highway Concrete. (Under the direction of DR. TARA CAVALLINE)

The Super Air Meter (SAM) is a new method of testing that correlates to how well concrete can resist damage from freeze-thaw stresses. This test is a modified Type B pressure meter that undergoes a set of sequential pressure steps. The equilibrium pressure difference between the first and second steps of pressurization provides a number that correlates to both the spacing factor and durability factor of the mixtures tested. The goals of this research were to evaluate how the materials and mixture proportions commonly used by the North Carolina Department of Transportation (NCDOT) affect the SAM number, as well as to identifying SAM numbers that are indicative of durable concrete based on the performance specifications of the NCDOT.

Mixtures from four past NCDOT projects that used a variety of w/cm, fly ash type and replacement percentages, and cementitious material content were included in this study. SAM numbers obtained from fresh concrete tests were correlated to freeze-thaw durability test results (ASTM C666, method A) and air void system parameters determined using manual point count methods (ASTM C457). This analysis provided insight into the performance of NCDOT mixtures in the freeze-thaw durability test, the relationship between the air void system spacing factor of the hardened concrete and historically used performance targets, and a potential SAM number performance target that could be used in shadow specifications by NCDOT in future concrete construction.

ACKNOWLEDGEMENTS

I would like to thank Dr. Tara Cavalline and the other members of my committee, Dr. Brett Tempest, and Dr. Stephanie Pilkington. Firstly to Dr. Tara Cavalline without her sage like patience and guidance I would not be where I am today. She has been a steady guiding presence since I first entered into the program five long years ago. I also would like to thank Dr. Brett Tempest and Dr. Stephanie Pilkington for their calm and practiced guidance and advice through the process. I would also like to thank the companies supporting this research, namely the NCDOT who believed in this project enough to donate time, money, and materials to support it.

I would like to thank everyone who has been involved in the batching process with me both those who taught me how including Blake Biggers, Ross Newsome, and Wes Maxwell as well as those who helped me batch and test my own project including Peter Theilgard, Clarke Summers, Allison Summers, and Brandon Ellis. Without them and their constant support I would never have been able to finish.

Finally, I would like to thank my family who have always pushed me to continue even when I was down. My brother Travis Ocampo has done more to help me through this then I can ever fully articulate. My mother Dianna Perrotto who has been a constant source of help both in general and with my thesis and I am forever grateful to the selfless acts she has done and continues to do. I would also like to thank the friends I made along the way without their help and friendship I would not be half the student I am today.

Table of Contents

LIST OF FIGURES

LIST OF TABLES

LIST OF ABBREVIATIONS

AASHTO	American Association of State Highway and Transportation Officials’
ACI	American Concrete Institute
ACR	Alkali-Carbonate Reaction
AEA	Air Entraining Agent
ASCE	American Society of Civil Engineers
ASR	Alkali-Silica Reaction
ASTM	American Society for Testing Materials
$CaCl_2$	Calcium Chloride
$Ca(OH)_2$	Calcium Hydroxide
CDOT	Colorado Department of Transportation
Cf	Cubic Feet
CH	Calcium Hydroxide
CSH	Calcium Silicate Hydrate
cwt	Hundredweight
DF	Durability Factor
DOT	Department of Transportation
dpi	Dots per Inch
FFT	Fast Fourier Transform
FHWA	Federal Highway Administration
F-T	Freeze-Thaw

g	Gram
in.	Inch
LWA	Lightweight Fine Aggregate
$MgCl_2$	Magnesium Chloride
mm	Millimeter
MOE	Modulus of Elasticity
MOR	Modulus of Rupture
NCDOT	North Carolina Department of Transportation
NYSDOT	New York Department of Transportation
OPC	Ordinary Portland Cement
OSU	Oklahoma State University
oz	Ounce
PC	Superplasticizer
pcf	Pounds per Cubic Foot
pcy	Pound per Cubic Yard
PEM	Performance Engineered Mixtures
PLC	Portland Limestone Cement
psi	Pounds per Square Inch
SAM	Super Air Meter
SF	Spacing Factor
SHA	State Highway Association
W/cm	Water to Cementitious Material Ratio
WisDOT	Wisconsin Department of Transportation

WRA	Water Reducing Admixture
WROS	Wood Rosin Air Entraining Agent
WVDOT	West Virginia Department of Transportation
°F	Degrees Fahrenheit
μm	micrometer

CHAPTER 1: INTRODUCTION

1.1 Background and Significance

According to the American Society of Civil Engineers (ASCE), to address the deterioration of surface transportation infrastructure in the United States is expected to cost the nation $2.2 trillion in lost business sales. In addition to capital costs, damage to the GDP to address these concerns would be on the order of $1.1 trillion through 2025 if the funding gap remains at its current imbalance. It is also estimated that over 1 million jobs will be lost by 2025 due to deteriorating surface transportation infrastructure. As of 2016 the ASCE estimated that to bridge the funding gap between the total needs and the actual funding of surface transportation, an extra $1.1 trillion in funding would need to be allocated through 2025 with $4.3 trillion needed through 2040 (ASCE 2019).

In 2015 the Federal Highway Administration (FHWA) along with several industry partners decided to make efforts to enable state highway agencies (SHAs) to modernize the concrete paving specifications in collaboration with the research community. This meeting provided the first step towards modernizing the specifications with the creation of the American Association of State Highway and Transportation Officials' (AASHTO) PP 84-17, Developing Performance Engineering Concrete Pavement Mixtures (Cackler et. al. 2017). Six critical properties of concrete mix performance were identified as the core of the performance engineered mixtures (PEM). These properties are aggregate stability, fluid transport properties, freeze-thaw resistance, shrinkage, strength, and workability. Workability was included due to poor workability in the field leading to sub-par concrete placement which can affect durability (Cackler et. al. 2017).

Prescriptive specifications had the FHWA dictating exactly how the materials should be constructed or what they should consist of. This stifles the ability of contractors to innovate with the design mixtures and required the FHWA to have a large well-trained workforce to design the specifications. Moving to a performance specification allows for agencies to instead identify characteristics they desire to have in materials or finished products and allows the contractor flexibility the mixture design and other construction approaches. With a performance specification the contractor is allowed to innovate as much as they possible so long as all specified characteristics are achieved in the final product. Performance specifications have the added benefit of removing some of the burden of oversight from the agency that is reviewing the specifications.

By entraining a relatively small amount of air, hardened concrete will be more durable against cracking due to freeze-thaw cycles. However, the degree of durability the hardened concrete will have against these forces cannot be predicted by only knowing the amount (volume) of air that has been mixed into the concrete. To get a more accurate understanding of how the hardened concrete will perform once it has been placed in its environment and during its service life, the spacing factor (which can be used to assess the dispersion of the air-void system) and durability factor of the concrete (which assesses the performance of the concrete in a freezing and thawing test) need to be found. Using conventional freeze-thaw testing (ASTM C666) analysis for the durability factor takes over 3 months for all tests to be completed, while determining the spacing factor (ASTM C457) can take days or weeks to complete. In this time between placing the concrete and getting the results for its final freeze-thaw durability test the concrete has already fully cured. Before curing the contractor and owner have only a vague assurance that the concrete will be durable against the freezing and thawing conditions that they will encounter by having a prescribed volume of air mixed into the concrete. Correlated to both the spacing factor and the durability factor, the SAM (Super Air Meter) test performed per the AASHTO TP 118 standard helps give some assurance that the concrete will hold up in its environment by drawing a correlation between the SAM number and both the durability factor and spacing factor (Ley et al. 2017).

1.2 Objectives and Scope

A study of the relationship between the SAM number and both the durability factor and spacing factor of hardened concrete would help support identification of performance targets for freeze-thaw durable concrete for NCDOT (North Carolina Department of Transportation) use.

The objectives of this study are as follows

- Perform analysis to determine durability factor, spacing factor, and SAM number of a range of NCDOT highway mixtures for bridge and pavement concrete.
- Develop correlations between SAM number, spacing factor, and durability factor for these mixtures
- Develop recommendations for the use of SAM for North Carolina based on a review of other state specifications for freeze-thaw durability, as well as the correlations between SAM number, durability factor, and spacing factor.

CHAPTER 2: LITERATURE REVIEW

2.1 Concrete Durability

Durability is the ability of concrete to survive in its environment without degrading and according to Bryant Mather, formerly of the U.S. Army Corps of Engineers, "There is a misconception that concrete has a property named "durability." This is not the case, since concrete with a given set of properties will endure without noticeable change for centuries or even millennia in one environment and be reduced to fragments in a few years or even a few months in another (TRB, 2013)." As such, when talking about durability it must be discussed in relation to the service conditions, environmental exposure, and life cycle expectations in which the concrete will serve.

Most current mechanical property tests have only a loose correlation with the in-service and end stage performance of concrete. With the current trend of research aimed to better predict performance over the full life cycle of the material, new testing methods are being developed that can be used to assess concrete and better predict the early age and in-service performance of hardened concrete. One such testing method is the Super Air Meter (SAM). The SAM was created in Oklahoma State University (OSU) to provide a quick and easy test that measures the frost durability of the concrete being tested by comparing it to Spacing Factor (Welchel, 2014). The specifics of what information the SAM can obtain, and the method upon which the SAM number is determined will be described in detail later in this thesis.

2.1.1 Performance Requirements for Concrete

To be considered durable, concrete must be able to withstand the environment that it will be placed into. It must do this while withstanding the service conditions along with the life cycle expectations. As these can vary greatly, prescriptive specifications are often too constraining to allow the flexibility in mixture materials and proportions that are needed to provide the durability required to meet today's standards. When allowed to use a performance specification, concrete manufacturers can innovate and provide a mixture that will provide the properties linked to durability that is necessary for that exact environment. The following sections identify and describe the mechanisms of freeze-thaw stresses and the role of deicers in freeze-thaw damage (and mitigation).

2.1.1.1 Freeze-Thaw Stresses

As stated above, the durability of a sample of concrete will largely depend on what conditions it is subjected to, and this is no different for when it is being subjected to a freezing environment. Freezing environments can cause concrete to deteriorate in several different ways, but the most common deterioration method is cracking and spalling from being subjected multiple times to freezing conditions followed by a warm period that thaws the ice located within the concrete. The other deterioration methods that a freezing environment can produce are surface scaling when concrete freezes in the presence of deicing salts and D-cracking when the aggregates within the concrete crack, usually at edges and joints. These other methods will also be discussed in this document, however, when discussing freeze-thaw stresses in this document it will strictly be about cracking and spalling due to water freezing and thawing affecting the hardened paste of concrete (Mehta and Montiero, 2006).

The current specifications from NCDOT require an air content of 5% ± 1.5% in freshly mixed concrete for all concrete pavement and have an air content of 6% ± 1.5% for all concrete that will be used for structures (NCDOT). This specification has supported the construction of many concrete structures across North Carolina that have exhibited adequate freeze-thaw performance for many years. However, the air content alone does not provide a strong correlation with adequatefrost resistance, since the individual air voids still need to be dispersed within the paste closely enough to mitigate damage from water freezing within air voids contained within the paste. For a given total air content (volume %), attaining adequately close spacing between voids requires that the volume of air be dispersed in a network of many small, closely spaced air voids, rather than a network of larger, more distantly spaced air voids. For a given air content, a network of fine air voids will protect far more paste than a network of large, coarse air voids. Figures 2.1, 2.2, and 2.3 illustrate the area of protection surrounding the air voicd as well as the differences between a well-developed air-void system and a poorly developed system.

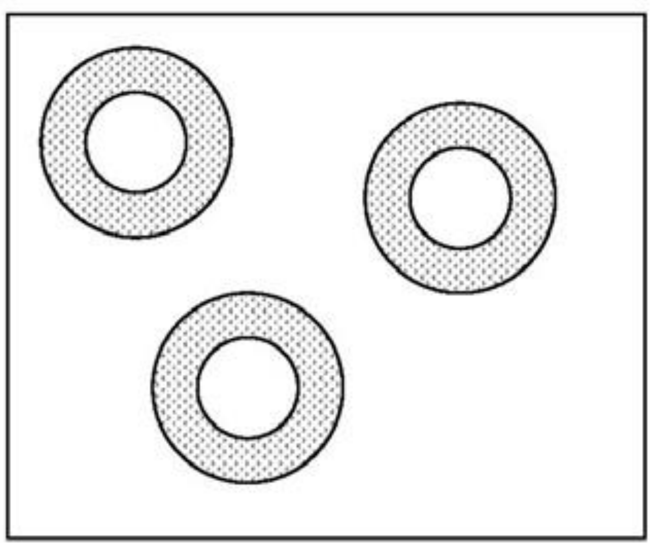

Figure 2.1: 2D Illustration of Protective Zone Surrounding an Air Void

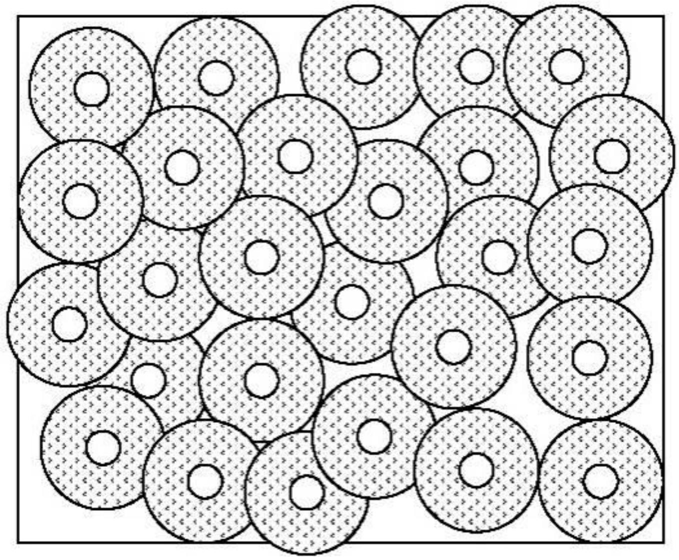

Figure 2.2: 2D Illustration Showing Small Evenly Dispersed Air Voids

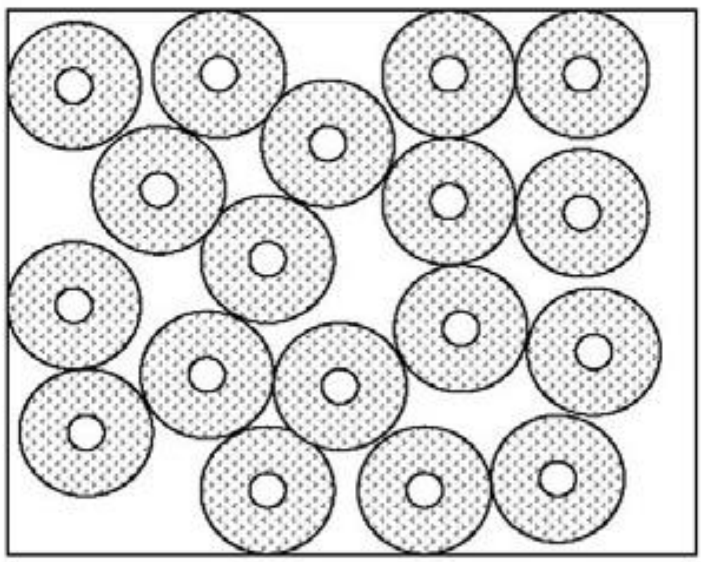

Figure 2.3: 2D Illustration Showing a Sample with a Lower Quality Air Void System

Every concrete mixture includes air whether it was intentionally mixed into the concrete or was simply entrapped by the mixing process. Void space also exists in the network of pores contained in the paste. However, to resist freeze-thaw distress an appropriate air-void network requires the use of an air-entraining admixture to stabilize the smaller air voids and ensure they are not forced out of the (hydrated) cement paste by the act of mixing or placing the concrete. Entrained air voids are generally spherical and smaller than entrapped air voids which can be much larger and coarser (Hover 1993). Figure 2.4 shows an enlarged view of the boundary between an air void and the other components that comprise the hardened cement paste system. These components are calcium silicate hydrate (CSH) gel, calcium hydroxide (CH), calcium sulfoaluminate, and capillary pores.

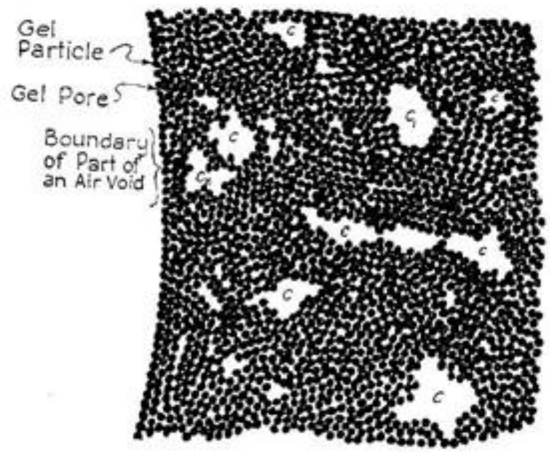

Figure 2.4: Concrete Microstructure (Tanesi and Meininger 2006 originally from Powers and Helmuth 1953)

The damage to concrete in freezing conditions comes not from the temperature but from the water held in the voids of the (hydrated) cement paste. This water contained within the cement paste will freeze within the air voids and exert stresses on the surrounding cement paste. This mechanical damage to the concrete caused by freezing water does not necessarily come from the water freezing within the concrete, but from the rate with which water is being expelled overloading what the concrete can handle. This is influenced by the rate of cooling, permeability, and degree of saturation of the concrete (Mehta and Montiero, 2006). Out of these factors only the permeability can be influenced with the other factors being influenced by the environment that the concrete will be placed into.

Permeability not only controls the hydraulic pressure that comes about from the movement caused by water freezing within the concrete but also is the major factor affecting the critical saturation of the concrete (Mehta and Montiero, 2006).

When the environmental temperature surrounding hardened concrete is below the threshold for water to freeze, freeze-thaw damage to the concrete will not occur until the concrete hits the critical saturation level. This level is dependent on many factors. However, in the critical saturation theory that was proposed by Powers, the critical saturation level of cement paste is reached when the capillary pores of the cement paste are more than 91.7 percent full of water. This is based on the fact that water expands approximately 9 percent when frozen (Tanesi and Meininger 2006). Once the critical saturation level has been achieved the concrete will be damaged through the pressures developed by water freezing within the concrete.

The most accurate factor in determining the freeze-thaw resistance of a particular batch of concrete is the spacing factor as determined by ASTM C457 (Pigeon and Pleau, 1995), which will be discussed in a subsequent section.

2.1.1.2 Deicing Salts

In the 1960's the United States started increasing the use of deicing salts to maintain clean roads after snowfall (Lilek 2017). This rapidly increased the amount of deicing salts that were being applied to the roadways. Figure 2.5 shows graphically the increase in deicing salts used from 1940 to 2014 (Lilek 2017). This increase in roadway deicing is a cause of deterioration in the roadway due to the interaction between the concrete and the deicing salts within a freezing climate.

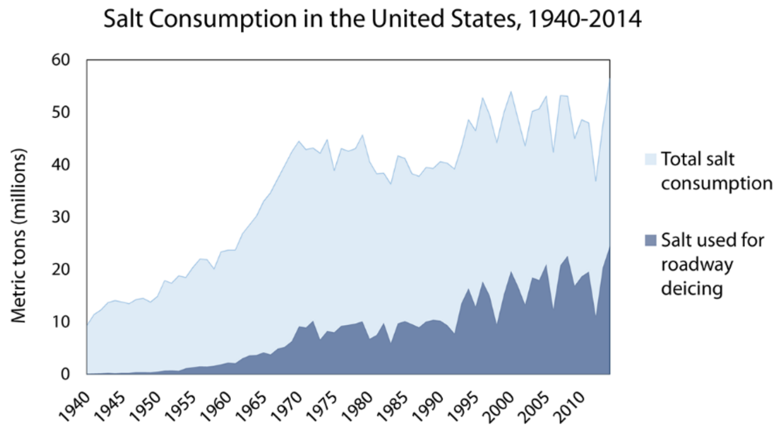

Figure 2.5: Salt Consumption (US) (Lilek 2017)

2.2 Characteristics of Durable Concrete

One of the largest misconceptions about durability is that if the concrete meets the required mechanical properties, it will provide durable performance over the structure's service life. However, there is no one intrinsic property singularly capable of predicting concrete's durability. For concrete to be considered durable it must be able to resist the environment within which it will reside. Each service and exposure environment will be slightly different. Hence, in order to monitor the different parameters that concrete must have in order to resist the most common environmental hazards a list of performance characteristics has been identified by leading concrete experts (Taylor et al., 2013).

All concrete must first and foremost have the mechanical strength required to resist the loads that will be placed upon it. While mechanical strength does not directly correlate to the durability of concrete it has been shown to aid in the concrete's ability to resist some of the stress involved with internal cracking during the freeze-thaw cycle (Pigeon and Pleau, 1995).

- Strength: Strength includes both flexural and compressive strength when dealing with concrete pavement. The flexural strength can vary depending on the specifics of the project design requirements but for many highway concrete mixtures, is usually around 500 to 700 psi at 28 days. Compressive strength can also vary depending on what the design requires, however, for most pavements and structural applications it is usually at least 4000 psi at 28 days (AASHTO, 2019).

- Slab Warping and Shrinkage Cracking: Drying shrinkage is a naturally occurring reaction to a concrete slab losing moisture to the surrounding environment. This can be exacerbated by the bottom of the concrete slab being moister on the top than the bottom, causing differential drying within the slab. This differential drying can cause the slab to curl upwards. This upward warping of the slab can cause problems with the roughness of the road and imparts stresses into the slab. If the slab is restrained these stresses can overcome the tensile strength of the concrete causing cracks within the slab. To help mitigate the susceptibility of a slab warping or cracking AASHTO PP-84 provides an option for either a prescriptive specification or a performance specification. The prescriptive specification states, "the volume of the paste shall not exceed 25 percent." and that "the unrestrained length change should be less than 420 microstrain at 28 days as determined from T 160." The performance specifications provide two separate tests, T 334, and T 363, that can be performed to provide an estimate of the cracking tendency of the concrete samples along with the ability to use a numerical model along with the test results of T 160 (AASHTO, 2020).
- Freeze-Thaw: When a saturated concrete structure is subjected to freezing temperatures the water located within the air voids and capillary system within the structure will freeze and develop tensile stress within the concrete. This stress can cause cracking within the concrete which will grow as the water penetrates deeper

into the cracks with each thawing cycle and then creates more tensile stress with each freezing cycle causing the crack to widen. The two most common requirements currently used to determine the F-T durability of concrete are an air content from 5% to 8% and a water to cementitious material (w/cm) ratio of 0.45 or less. AASHTO PP-84 (now AASHTO R101) has also introduced the Super Air Meter (SAM) into being an acceptable test along with a minimum air content of 4% as long as the SAM number is 0.20 or lower.

- Deicing Salt: The prescriptive and performance specifications used to reduce damage from deicing salt use is only provided when the deicing salts used are either $CaCl_2$ or $MgCl_2$. For the prescriptive specifications either 30 percent of the concrete should be replaced with a SCM, or a topical sealer should be applied that is in accordance with AASHTO standard M 224. The only performance specification that is allowed is to determine if the concentration of calcium oxychloride is lower than 15g per 100g of cementitious paste in accordance with AASHTO T 365.
- Transport Properties: The transport properties of concrete refer to several mechanisms that allow water and ions to pass through into the concrete where they can damage the concrete in several ways. The mechanisms with which fluids can penetrate into concrete include diffusion, thermal gradient, and electromigration (Claisse, 2014). Along with these mechanisms are several factors that can either increase or decrease the transportation of deleterious materials into the concrete. These factors include adsorption, capillary suction, and osmosis (Claisse, 2014). To lessen the effects of the transportation properties of concrete

the w/c ratio should be less than 0.45 for all concrete that will be subjected to either freezing and thawing or deicer salts. Along with the w/c the concrete should have a F_{APP} of greater than or equal to 1000 as determined by the AASHTO TP 119 standard. The F_{APP} can also be used to determine a service life for the concrete.

- Aggregate Stability: The aggregates used must be tested not only for their freeze-thaw durability, but also for resistance to alkali-silica reactions (ASR) and alkali-carbonate reactions (ACR). D-cracking or d-line cracking occurs when a susceptible aggregate goes through repeated freeze-thaw cycles in a critically saturated state causing fractures and/or dilations in the aggregates. ASR is a chemical reaction between the hydroxyl ions of alkalis contained within the pore solution and certain silica containing aggregates. ASR is very common with most highway agencies having reported instances of ASR. While not as common as ASR, ACR is extremely damaging when it occurs. ACR creates significant expansion and can cause significant damage and rapid failure of the concrete. Like ASR, ACR is the result of a reaction between hydroxyl ions and material within the aggregates, however, for ACR it is certain carbonate rocks.
- Workability: The American Society for Testing Materials (ASTM) defines workability as “that property of freshly mixed concrete that affects the ease with which it can be mixed, placed, consolidated, and struck off (ASTM, 2019).” Workability can have a direct effect on the durability of the concrete being placed as this is when the concrete will set up the air-void system contained within the paste. Workability was also a concern as many failures in the field stemmed

directly from poor workability leading to poor placement and consolidation. Low workability can also lead to over working of the concrete which can cause segregation or removal of entrained air. To better evaluate the workability of concrete two tests were designed and have been implemented into PP-84. These tests are the Box test, which is outlined in standard TP 137, and the V-Kelly test outlined in TP 129. For the Box test the slump at the edge should be 0.25 in (6 mm) and its ranking should be 2 or less which means that it has less than 30 percent surface voids. The V-Kelly test should have results between 0.6 and 1.2 in (15 and 30 mm) to be considered adequate.

2.2.1 Materials

Selecting the proper materials for each specific application and environment is a crucial first step to mitigate durability issues in the finished product. It would be highly uneconomical to protect against every deterioration mechanism; therefore, each individual environment will need to be examined to determine what deterioration mechanisms will need to be protected against. This allows for the finished product to be both economical and durable in the environment that it will be placed into (Taylor et al., 2013).

Cementitious materials play a key role in every performance characteristic and must be carefully and thoughtfully balanced against some negative performance, primarily occurring when relatively high amounts of cement are used without use of supplementary cementitious materials. Some performance issues that may be encountered in certain situations include sulfate attack, alkali-silica reactions, as well as providing a capillary system that allows water to travel within the paste.

Sulfate attack occurs when susceptible cements are used in sulfate-containing environments. Alkali-silica reactions (ASR) are caused by alkali and hydroxyl ions contained within the cement paste chemically reacting with reactive siliceous materials in the aggregates. Both issues can be controlled using appropriate materials selection and SCMs (Taylor et al. 2013)

For freeze-thaw durability, both the aggregates and paste components of the concrete need to have the appropriate performance characteristics. According to V. Ramakrishnan, "Aggregates generally make up 70% to 85% of the mass of a concrete mixture. Their grading, size, mineralogical composition, porosity, surface texture, and shape greatly influence the properties of unhardened and hardened concrete (TRB, 2013)." With such a large percentage of concrete being comprised of aggregates special attention needs to be paid to the properties of the aggregate being used.

According to Pigeon and Pleau (1995) "all aggregates with a high porosity (with a 24 h absorption of more than approximately 2%) should be avoided as much as possible." The reasoning behind this is that the water absorbed by the aggregates will be pushed out into the paste surrounding them once temperatures get low enough for freezing to occur. Once the water within the aggregates starts to freeze it will expand and force out the not yet frozen water contained with the aggregate creating a powerful hydraulic pressure within the paste.

2.2.2 Proportions

Mixture proportioning is the process used to determine the various quantities of ingredients that will provide the required characteristics called for in the mixture design. The mixture design is based on the intended use, exposure, size and shape, and physical properties required from the concrete (Kosmatka, et al., 2002). Proportioning needs to account for more than just the required strength of the concrete, it also has to consider the cost, workability, and durability. Many of these characteristics trend in opposite directions when the proportion of each material within the mixture is adjusted. As each material proportion is changed, the proportions of the others must carefully be balanced together (Mehta and Montiero, 2006).

Most of the desired characteristics of concrete depend upon the quality of the cementitious paste which is why the first step in proportioning out a mixture design is to select an appropriate water to cement ratio that will provide adequate strength and durability. The water cement ratio should be kept as low as possible while still maintaining the strength and durability required from the structure (Kosmatka et al., 2002).

The proportioning of the aggregates is based on the workability of the fresh concrete required. Aggregates have two characteristics that will be looked for in most mixtures and those are gradation and the nature of the aggregates. Gradation includes particle size as well as distribution of those sizes and it has the most obvious example of being able to change the workability of a mixture which will be discussed in more depth in the next section. The nature of the aggregates includes shape, porosity, and surface texture.

2.2.3 Construction

The workability of concrete is dependent upon the use of the concrete with slip-formed paving mixtures being stiffer than a mixture that would be used in a structural element with congested reinforcing steel. Getting the proper workability for the desired use of the structure is part of the mixture design and affects the decisions made before it is delivered to the site. The primary concern for contractors has been being able to place the concrete on-site successfully as even a mixture that follows all guidelines will not be worth much if it cannot be transported, placed, and finished. The workability of concrete is broken into two separate properties: consistency which describes the ease of flow of the concrete and cohesiveness which describes the ability for the concrete to not give off bleed water or segregate when placed (Mehta and Montiero, 2006).

While workability does not directly affect the F-T durability of concrete it does directly affect the placement of the concrete which can have a large impact on the F-T durability of concrete. Research done by Ram et al. (2012) showed that a drop in air percentage is likely to happen in fresh concrete after the concrete has been run through the slip-form paver, however their studies were inconclusive if the hardened concrete experiences a decrease of increase in the air content after being run through the slip-form paver.

2.3 Concrete Deterioration Due to Freeze-Thaw Stresses

The true mechanism behind freeze-thaw deterioration is not fully understood; however, there are several theories which may partially explain the forces and could also allow separate theories to work together to better explain the phenomenon (Pigeon and Pleau, 1995).

2.3.1 Theories of Freeze-Thaw Stress Action

The first theory that will be discussed is Powers' hydraulic pressure theory. The next theory being discussed is the osmotic pressure theory put forth by Powers and Helmuth and expanded upon by Litvan to include the physics involved with supercooled water. The final theory this paper will go over is the ice lens growth. These three theories are perhaps the most complete and widely used theories explaining the mechanisms of frost damage in concrete.

2.3.1.1 Hydraulic Pressure Theory

The hydraulic pressure theory was created by Powers in 1945 and further modified in 1949. This theory used a series of equations that related the air void spacing to properties of the cement paste and to the rate at which the temperature is decreasing. All of these equations are based upon the simple mechanism of freezing water expanding and forcing all non-frozen water out of the pore into the paste. Darcy's law of water flow through porous bodies is used to calculate how much pressure the expelled water will exert for the water to travel to the next open-air void.

$$\Delta h = \frac{\eta}{k} Q \frac{l}{A}$$

Equation 2.1: Darcy's Law (Pressure Gradient)

Equation 2.1 shows Darcy's Law as it is applied in Powers' hydraulic pressure theory where, Δh is the pressure gradient, η is the fluid viscosity, k is the permeability of the paste, Q is the flow rate, l is the length of the flow path, and A is the flow area (Tanesi and Meininger 2006).

It is this pressure exceeding the tensile strength of the paste that causes the internal cracking of the concrete. The pressure involved with the hydraulic pressure theory is increased through the distance the expelled water must travel to enter into the next air void and through an increase in the freezing rate (Pigeon and Pleau, 1995).

Powers would reconfigure Darcy's Law based on the flow length to create an equation for the maximum theoretical length of the flow path from one air void to another that would not cause the pressure gradient to be greater than the tensile strength of the cement paste. This maximum spacing between the air voids is called the spacing factor and is shown in Equation 2.2 below (Tanesi and Meininger 2006).

$$l = \Delta h \frac{k}{\eta} \frac{A}{Q}$$

Equation 2.2: Spacing Factor

2.3.1.2 Osmotic Pressure Theory

The hydraulic pressure theory could not explain every phenomenon that occurred within a sample that was undergoing freeze-thaw cycles such as the shrinkage that accompanies freezing concrete samples that have entrained air and some responses the samples had to the change in the rate of cooling they were undergoing (Powers and Helmuth 1953). While Powers and Helmuth saw evidence that the hydraulic pressure theory had a basis in reality, they also saw evidence that it was not the only phenomena that was causing all of the changes they had observed in the samples that were being tested. The theory they developed from their observations regarding the experimental results was that diffusion of water was occurring towards the freezing sites instead of water flowing away from the freezing sites.

A theory supplied by Litvan to supplement the osmotic pressure theory is based on the differences between supercooled water and ice particles. When adsorbed water (water that is held as a thin film on the outside of an internal material) is brought to below its freezing point cannot freeze without redistribution. Adsorbed supercooled water also cannot have freezing initiated by nucleation. These two properties cause the adsorbed water to remain as a liquid when the temperature falls below the freezing point of water. This causes there to be liquid water in the gel pores and ice outside which throws the system out of equilibrium because supercooled water has a higher vapor pressure than ice. Equilibrium is restored to the system by water being expelled out of the gel pore system so that it can freeze in the larger capillaries in the surrounding area. Further cooling of the concrete will cause more water to be expelled as the difference in vapor pressure is increased with a decreasing temperature (Litvan 1973).

2.3.1.3 Ice-Lens Model Theory

The ice-lens model or segregation ice model is a known principle cause of frost heave within soils (Peppin and Style 2013), however most of these models focus on a moving boundary and assume the matrix of the material to be infinitely rigid (Setzer 2001). The micro-ice-lens model created by Setzer was based on a shift in the triple-phase condition, a state where vapor, liquid, and solid water exist simultaneously in a stable condition, and a non-infinitely rigid system (Setzer 2001).

During the freezing stage the pore water will generate a negative pressure following the triple-point shift and the gel matrix will be compressed due to this negative pressure formed. This compression will cause the matrix to shrink in volume and to account for this decrease in volume water will flow out and into the ice forming in the air voids and capillary pores surrounding the gel matrix. If there is still space within the air voids surrounding the gel matrix then the degree of saturation will increase, and the micro-ice-lenses will grow without expansion of the pore. However, if a critical degree of saturation is reached the growth of the ice will cause damage to the pore further speeding up the transport of water to the ice lens forming (Setzer, 2001).

During the thawing stage the pressure difference between water and ice starts to decrease with an increase in the temperature and the ice is transported back into water. This transformation back into water is a slower process than the transportation of water to ice that took place by the gel matrix squeezing out its water during the freezing phase.

While the transportation of water from the micro-ice-lenses is not quick the gel matrix can be replenished by an external source if water is available through the much faster process of viscous flow. While thawing the micro-ice-lenses stay frozen within the pores keeping the saturation constant while the gel matrix increases in the degree of saturation if external water is available (Setzer, 2001).

2.3.2 Distress Mechanisms

There are two primary distress mechanisms that occur due to concrete freezing and thawing: internal cracking and surface scaling. Internal cracking is the more serious of the two as it can weaken the concrete significantly while not showing outward signs that the concrete is weakening. Surface scaling involves the surface layer of concrete flaking off which can lead to the ingress of water and other deleterious materials into the concrete.

2.3.2.1 Internal Cracking

The air-void system within the hardened concrete is an important factor when discussing deterioration due to the freeze-thaw cycle. The air-void system includes all of the air within the hardened concrete, this includes the microscopic and evenly shaped air voids as well as the much larger irregularly shaped air voids (Hover 2006). A properly established system of air voids within hardened concrete consists mainly of microscopic air voids that have been evenly dispersed throughout the mortar fraction of the mixture. According to Hover, an air-void system that will effectively provide frost resistance must have a total volume of empty air voids that is equal or exceeds the overflow volume of water or ice from the capillary pore system. Another factor that is just as important for frost resistance is how well dispersed the air voids are throughout the hardened cement paste. The exact requirements for volume, dispersion, and spacing of the air voids is dependent upon the environment the concrete will be placed in as well as the properties of the concrete.

This air-void system will generally increase the workability, cohesion, and frost resistance of the finished concrete product. However, this can influence the density and strength of the finished concrete by displacing some of the other components within the concrete and by creating a more porous cement paste.

Spacing factor is very important for internal micro cracking. The 0.008 in spacing factor that is generally accepted as durable is a conservative parameter and a spacing factor of up to 0.02 in could be considered durable with regard to internal cracking due to freeze-thaw cycles (Pigeon and Pleau 1995).

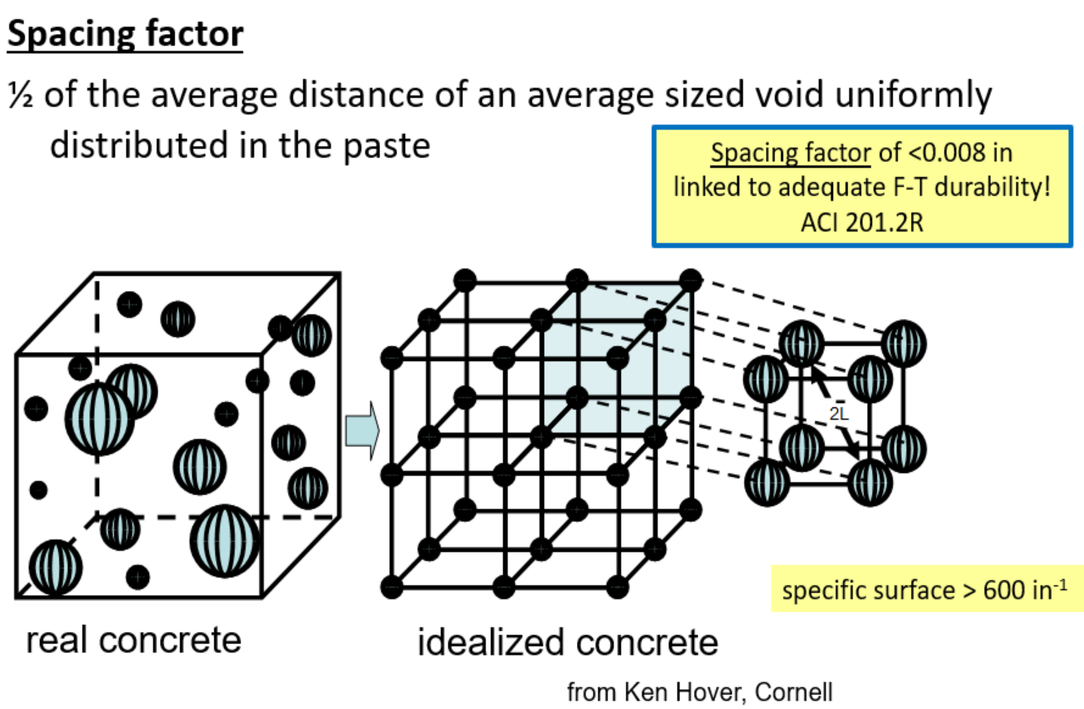

Figure 2.6: Visualization of Spacing Factor

Figure shows a visualization of how the space within real concrete is laid out along with a visualization of how a perfect air void spacing would look like. In the perfect version the space from each void is spaced such that any water being expelled from the capillary void system will have an empty air void to fill rather than increase the pressure exerted on the paste system (Hover 2006).

2.3.2.2 Surface Scaling due to Deicing Salts

Deicing salts affect the concrete in two ways: drawing water to the surface layer of the concrete surface and the leaching of $Ca(OH)_2$. The suggested sequence of events for deicing salt damage is as follows. The deicing salt will melt the snow or ice that it comes into contact with while the surrounding ice and snow keeps the water pooled in that area. The melted ice and snow now have all of the deicing salts dissolved within it turning it into a salt solution which will lower the freezing point of the solution. This solution now gets absorbed into the surface layers of the concrete slab increasing the saturation level of the concrete. The ice surrounding the concrete slab will continue to melt diluting the salt solution within the concrete slab. This dilution will raise the temperature at which the solution can freeze until the solution freezes. This sequence of events can have as many or more freeze-thaw cycles when compared to a slab that has not been treated with deicing salts. Along with the freeze-thaw cycles caused by deicing salts there is a thermal shock that can occur in the subsurface concrete when the surface ice melts and extracts the latent heat of the concrete (Neville 2013).

A lower spacing factor is necessary to aid in creating a concrete that can resist surface scaling, although it alone is not sufficient to ensure that the concrete will be able to resist surface scaling (Pigeon and Pleau 1995). The lower spacing factor with regards to surface scaling is mostly due to the decrease in permeability the paste will have with a much smaller spacing factor.

2.3.3 Mitigation Strategies

The three most important factors concerning the prevention of frost damage are reducing freezable water, having a robust entrained air-void system, and proper design protocols. This thesis will only discuss ways to reduce freezable water and acquire a proper entrained air-void system as design protocols are not within the purview of this work. Reducing freezable water can be achieved by reducing the w/cm which will likely have the added benefits of a higher strength and lower permeability in the hardened concrete. In order to lower the w/cm and still maintain a proper workability supplementary cementitious materials and admixtures can be added that will increase the workability of the concrete without sacrificing the strength required (ACI 2016).

While reducing the amount of freezable water works to mitigate freeze-thaw damage the best way to mitigate freezing damage is to have a proper air-void network in the hardened concrete. A proper air-void network not only encompasses having enough air within the hardened paste to allow for any water within the concrete to flow to when in a freezing environment but also the quality and spacing of air voids involved. To achieve an entrained air-void system an air entraining admixture needs to be used to ensure that the air within the concrete is entrained and not entrapped air which does not help the concrete resist freezing damages (ACI 2016).

2.3.3.1 Concrete Permeability

According to Mehta and Montiero “Permeability is defined as the property that governs the rate of flow of a fluid into a porous solid.” The coefficient of permeability, simply called permeability in this paper, is governed by Darcy’s expression in Equation 2.3 below:

$$\frac{dq}{dt} = K\frac{\Delta HA}{L\mu}$$

Equation 2.3: Coefficient of Permeability

Where dq/dt = rate of fluid flow
μ = viscosity of the fluid
ΔH = pressure gradient
A = surface area
L = thickness of the solid

In hardened cement paste permeability is controlled indirectly by the mixing water used for the mixture as this determines the total space in the hardened cement paste once the mixing water has either hydrated the cement grains or evaporated out during the curing process. As concrete is a composite material the materials that are bound within the hardened cement paste will also affect the permeability of the concrete. Aggregates that are used in typical concrete mixtures will have a porosity, percentage of total volume that consists of voids, of 3 to rarely exceeding 10 percent whereas cement paste has a typical porosity of 30 to 40 percent. With such a difference in porosity it would be expected that the permeability of the aggregates would be much lower than that of the hardened cement paste, however that is often not the case. The reason for this is the size of the capillary pores in aggregates compared to the hardened cement paste, with the capillary pores in aggregates being much larger than those typically found in hardened cement paste. Table 2.1 below shows the permeability of some common types of rocks along with how that permeability compares to a matured cement paste (Mehta and Montiero 2006).

Table 2.1: Comparison between the Permeability of Rocks and Cement Pastes

Type of Rock	**Coefficient of permeability (cm/s)**	**Water-cement ratio of mature paste with the same coefficient**

		of permeability
Dense trap	2.47 x 10^{-12}	0.38
Quartz diorite	8.24 x 10^{-12}	0.42
Marble	2.39 x 10^{-11}	0.48
Marble	5.77 x 10^{-10}	0.66
Granite	5.35 x 10^{-9}	0.70
Sandstone	1.23 x 10^{-8}	0.71
Granite	1.56 x 10^{-8}	0.71

(Mehta and Montiero 2006, originally from Powers 1958)

As concrete continues to cure and produce more CSH and other products the porosity of the concrete will decrease. This decrease in porosity will also generally decrease the permeability with the capillary pores within the hardened paste becoming more disconnected overtime until every mixture that has a w/cm of 0.70 and under will eventually have a discontinuous pore structure. Table 2.2 shows the time required for several w/cm to achieve a discontinuous pore structure along with the hydration that is needed during the curing process to achieve a discontinuous pore structure in these times (Hearn et al. 2006).

Table 2.2: Time Required to Achieve a Discontinuous Pore Structure (Powers et al. 1959)

W/CM	Time Required	Approximate degree of hydration required
0.40	3 days	0.50
0.45	7 days	0.60
0.50	14 days	0.70
0.60	6 months	0.95
0.70	1 year	1.00
>0.70	Impossible	>1.00

The freeze-thaw durability of a sample of concrete largely depends upon its level of saturation and whether its current saturation level is above its critical degree of saturation. The critical degree of saturation is the point at which a concrete sample will be damaged by the stresses generated by freezing. The degree of saturation can be seen expressed as Equation 2.4:

$$S = \frac{V_W}{V_P}$$

Equation 2.4: Degree of Saturation

where S = degree of saturation

V_W = volume of evaporable water

V_P = total pore volume

At a degree of saturation below the critical level there will be little to no frost damage if concrete freezes (Fagerlund 2004).

2.3.3.2 Air Entrainment

"Air is always present in concrete mixes. It is intentionally or unintentionally trapped in fresh concrete as a result of mixing and placing. About the only way to avoid trapping some air would be to mix, transport, and place concrete in a vacuum (Hover 1993)." As all concrete is not made in a vacuum the air that is mixed into a concrete mixture must be mixed in with precision and care to the final product.

Air entrainment first began by accident in the 1930s when some mills had been using beef tallow as a grinding aid when preparing cement. The cement used from these mills produced a less dense concrete that better survived the freezing and thawing cycles that the concrete was placed into (ACI 2012). Most common air entraining agents (AEA) act as a surfactant, molecules that reduce the surface tension of the water, this allows the bubbles formed by mixing to become stabilized within the concrete (Neville 2013).

Air voids are put into two categories depending upon the size of the void with air voids larger than 0.04 in. (1 mm) being considered entrapped air and all voids smaller than 0.04in. (1 mm) being classified as entrained air. The amount and type of air voids is dependent upon many factors such as cement content and characteristics, coarse and fine aggregate size, w/cm ratio, SCMs used, chemical admixtures, and the characteristics of the water itself (Kosmatka et al, 2002). Along with those factors involved in the mixture design several production procedures and construction practices can also have a drastic effect on the air void system. The production factors include how the concrete is batched, the mixing time, speed, and capacity when compared to batched amount. The construction factors include transport and delivery, placement methods, finishing methods, and the environment during placement (Kosmatka et al, 2002).

When the air content of a concrete sample increases it causes the percentage of air voids that are filled to decrease, thus lowering the degree of saturation which will delay the sample from reaching a critical degree of saturation.

2.4 Tests to Evaluate Concrete Freeze-Thaw Durability

The current tests used to evaluate the freeze-thaw durability of a mixture have allowed for durable concrete to be made. However, these tests either provide a very loose correlation to durability or are expensive and take a long time to get results. The tests performed on fresh concrete currently only provide a total air amount and do not provide information about how the air-void system is physically established, which would provide a better look at how the hardened concrete might handle the stresses involved once it starts freezing and thawing in its environment. The tests run on hardened concrete provide a better correlation to the mixture's durability to the freeze-thaw cycle, however, these tests require hardened samples and take much longer to run the tests then the tests done to fresh concrete

2.4.1 Total Air Content of Fresh Concrete

There are three current ASTM approved tests to determine the air content of concrete while it is fresh: ASTM C138 (gravimetric method), ASTM C173 (volumetric method), and ASTM C231 (pressure method) (Concrete.org 2021).

Table 2.3: Recommended air contents (ACI 2016)

Nominal maximum aggregate size, in. (mm)	Air content, percent	
	Exposure Class F1	Exposure Class F2 and F3
3/8 (9.5)	7	7.5
1/2 (12.5)	7	7
3/4 (19)	6.5	7
1 (25)	6.5	6.5
1-1/2 (37.5)	6	6.5
2 (50)	6	6
3 (75)	5	5.5

Table 2.3 is based on earlier work done by Klieger which recommends an air content of 18 percent in the paste. These recommendations are based on using a Vinsol resin air-entraining admixture. These air content recommendations consider not only the exposure class that the concrete will be placed into but also the paste content of the concrete mixture and smaller nominal aggregate size will result in more paste content within the concrete mixture (ACI 2016). Research done by Felice et al. (2014) has shown that these air contents might be excessive with current modern air-entraining admixtures to achieve durable concrete mixtures. Concrete tested with modern AEAs were shown to be durable with a minimum air content of 3.5 percent when tested using ASTM C666/C666M. Research done by Ley et al. (2017) on mixtures that are identical except for one including a water reducer shows that the air content of fresh concrete does not line up with the spacing factor of both concrete mixtures. The mixture with only AEA had a linear trend that it would be under a spacing factor of 200 μm at around 4.5 percent

air while the mixture with the water reducing admixture showed a linear trend of being under 200 µm at 7.5% air. Figure 2.7 shows all of the data points used to acquire the linear trend and determine the estimated fresh air percentage to obtain an adequate spacing factor. This same shift between the two mixtures was also observed when comparing the durability factor using the percentage of air within the fresh concrete (Ley et al. 2017).

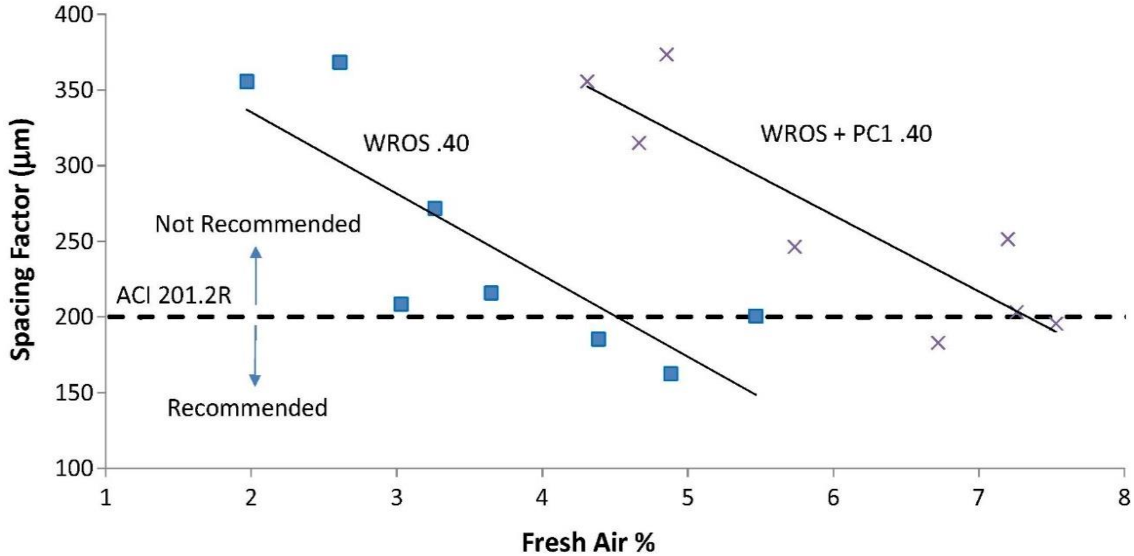

Figure 2.7: Spacing Factor vs. Fresh Air (Ley et al. 2017)

2.4.2 Super Air Meter

While finding the air content in fresh concrete can provide a measure of understanding for how likely the concrete mixture will withstand the environment it will be placed in it cannot provide a measure of the quality of the air-void system. The Super Air Meter (SAM) uses a device similar to the ASTM C231 Type B pressure meter, however the Super Air Meter has six clamps to contain the increased pressure required during the test and a digital pressure gauge. Previous studies done by Ley and Tabb, Ley et al., and Dabrowski et al. have found a correlation between the SAM number and factors that have been shown to affect the durability of concrete (Ley and Tabb 2014, Ley et al. 2017, Dabrowski et al. 2019).

The SAM test goes through three pressurization steps (14.5 psi, 30 psi, and 45 psi) before allowing the chambers to depressurize and the pressurization steps are repeated to the same levels. This multi-step pressurization allows for the equilibrium pressure to be found for each run of pressurizations. The SAM number is the difference between the first and second pressurization's equilibrium pressure (Ley and Tabb 2014).

When the SAM number was used instead of the percentage of air in the fresh concrete both mixtures used by Ley et al. had a better correlation between the SAM number and the spacing factor as show in Figure 2.8. The durability factor created a similar graph when compared to the SAM number with both mixtures having a much closer trend line when compared to using the fresh air content (Ley et al. 2017).

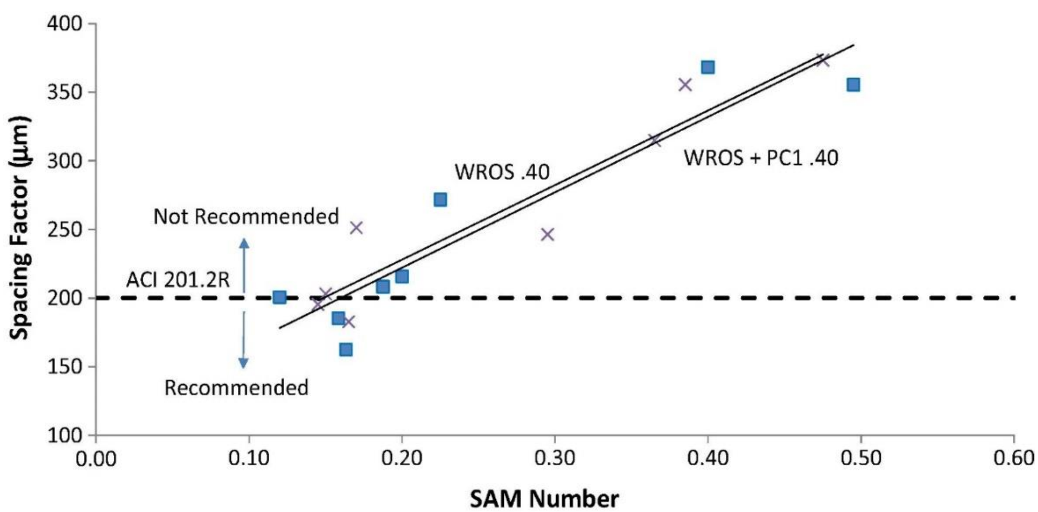

Figure 2.8: Spacing Factor vs. SAM Number (Ley et al. 2017)

A correlation between the SAM number and spacing factor was then completed for 303 mixtures that came from both laboratory settings as well as field data all from the state of Oklahoma. From this data a SAM number of 0.20 was found to have the most data points fall at or below the spacing factor of 200 µm that is recommended to have the best chance of producing durable concrete in an environment that will undergo freezing and thawing. A SAM number of 0.20 was found to have approximately 88 percent of data points fall at or below 200 μm which is shown visually in Figure 2.9 below (Ley et al 2017).

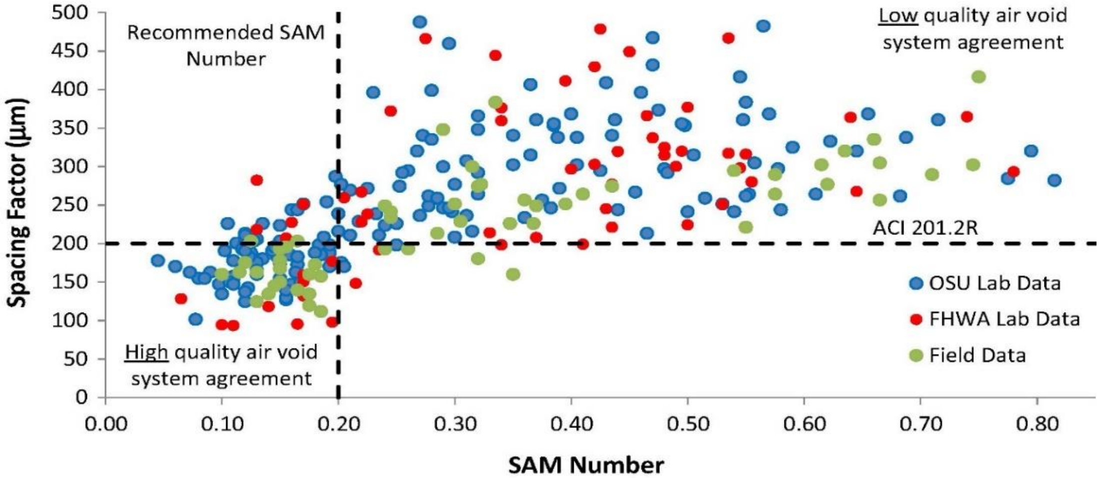

Figure 2.9: Mass Correlation for Spacing Factor vs SAM Number (Ley et al. 2017)

When creating a correlation between the durability factor and SAM number Ley et al. chose a SAM number of 0.32 as it was accurate in the correlation for approximately 90 percent of the mixtures, and it was a more conservative choice over 0.35 which had nearly identical results (Ley et al. 2017).

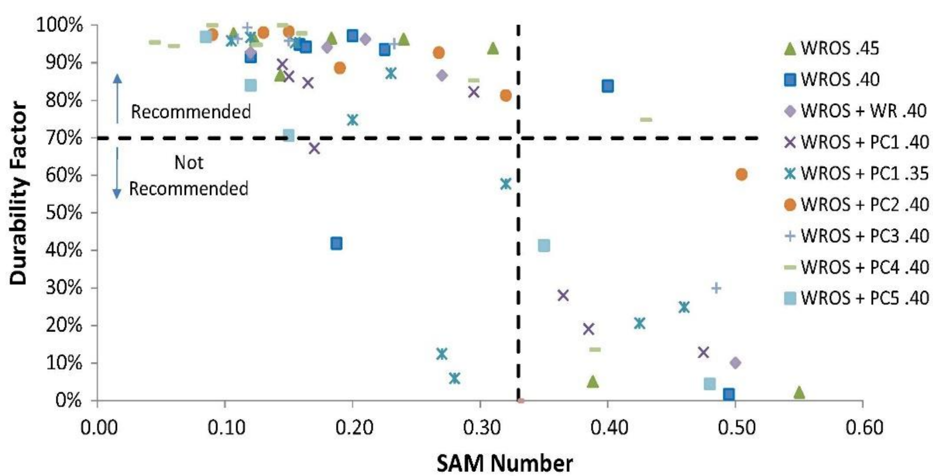

Figure 2.10: Mass Correlation for SAM Number vs Durability Factor (Ley et al. 2017)

Figure 2.10 details the durability factor of all of the chosen mixtures and compares their durability factor to the SAM number of the mixture. After a SAM number of 0.35 the durability factor of the chosen mixtures has a steep decline with almost none of the mixtures having a durability factor recommended for durable concrete (Ley et al 2017).

2.4.3 Freeze-Thaw Testing of Hardened Concrete

ASTM C666/C666M is the definitive test used to determine the resistance to internal damage of concrete going through freeze-thaw cycles. While ASTM C672/C672M is used to evaluate the surface scaling resistance of a concrete mixture. ASTM C672/C672M relies on a visual inspection and numerical rating system and was not used within this study. Several researchers have criticized these tests for not providing an accurate look into what the actual conditions will be for the sample in its placed environment. This disconnects between field conditions and laboratory conditions necessitates heightened caution when using the results from these tests to determine the possible resistance of a particular concrete mixture to freeze-thaw damage (Hallet et al. 1991, ACI 2016).

2.4.4 Hardened Air Void System Analysis

Most of the generally accepted parameters to determine if a sample of concrete has an adequate air-void system come from the hardened air void analysis determined by ASTM C457/C457M (ACI 2016). ASTM C457/C457M can be used to determine the air content, paste content, void frequency, specific surface, spacing factor, and the paste-air ratio if desired. However, most often it is used to determine the hardened air content, spacing factor, and the specific surface in a concrete sample (ASTM 2016, ACI 2016).

There are several procedures that can be followed in ASTM C457/C457M to determine the parameters of the air-void system with this paper using Procedure C which is the contrast enhanced method using a flatbed scanner. This procedure was created by a team of researchers at Michigan Technological University as a way to automate determining the size distribution and volume fraction of air voids, which already had automated methods, along with the volume fraction of hardened cement paste (Peterson et al. 2001).

This procedure uses a number of hand counted samples to provide a basis for the automated program to run off of to determine each component of the concrete sample accurately. The results from these hand counted samples are used to create an optimization file for the software used. The software used for this study is called BubbleCounter which is based off of an open-source National Institute of Health (NIH) software program called ImageJ. The software works on samples that have been colored black and white to allow for easier contrast an example of which can be seen in Figure 2.11. A black and white balance card is used to determine the intensity of the sections colored black and white. This will then be used to normalize the images so that the errors produced by slight variations in the scanning conditions can be reduced (BubbleCounter 2021).

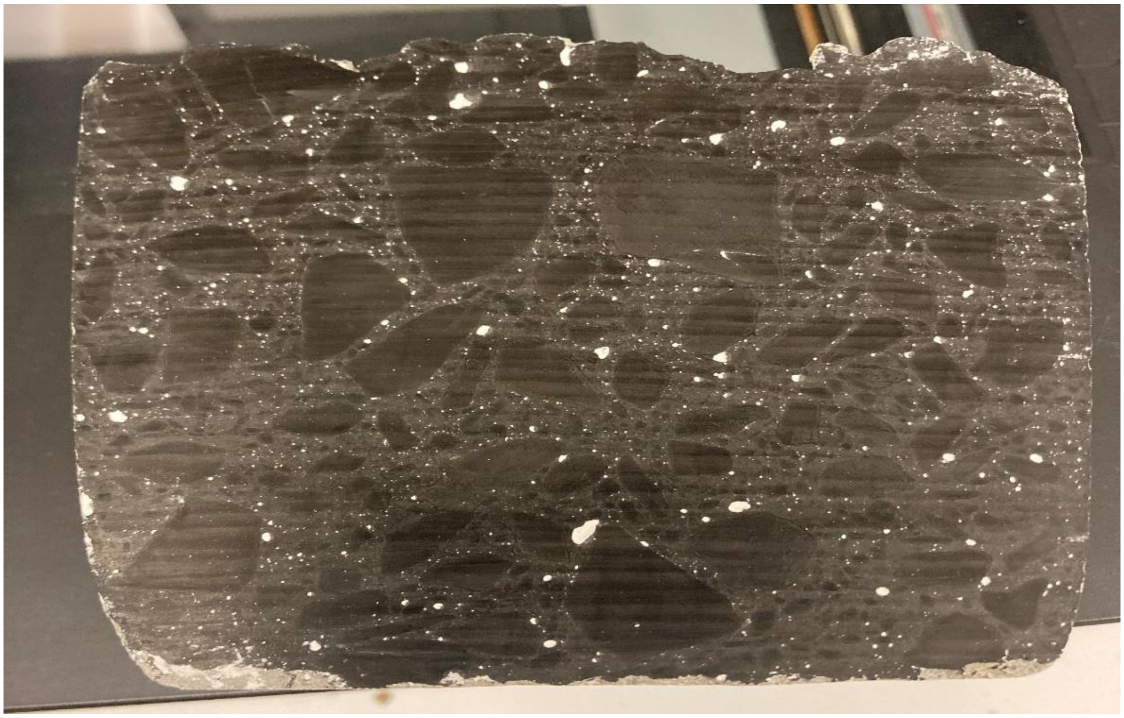

Figure 2.11: Example of color corrected sample

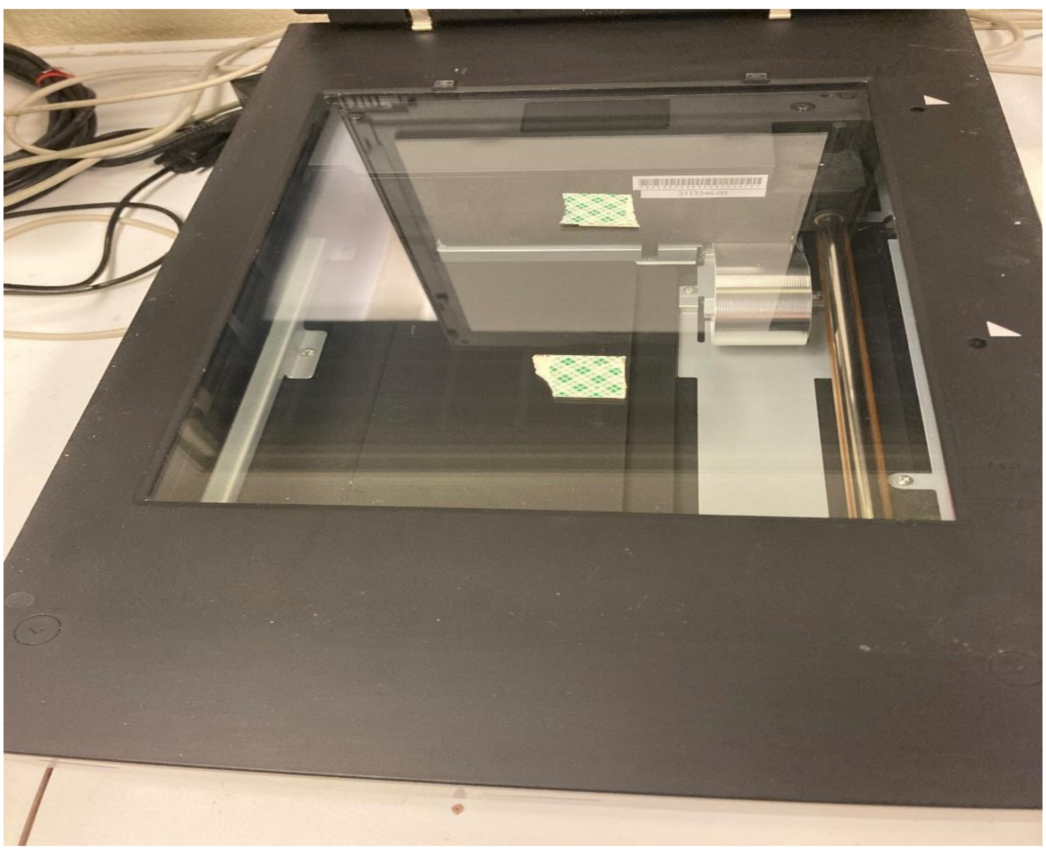

Figure 2.12: Flatbed scanner used to scan samples

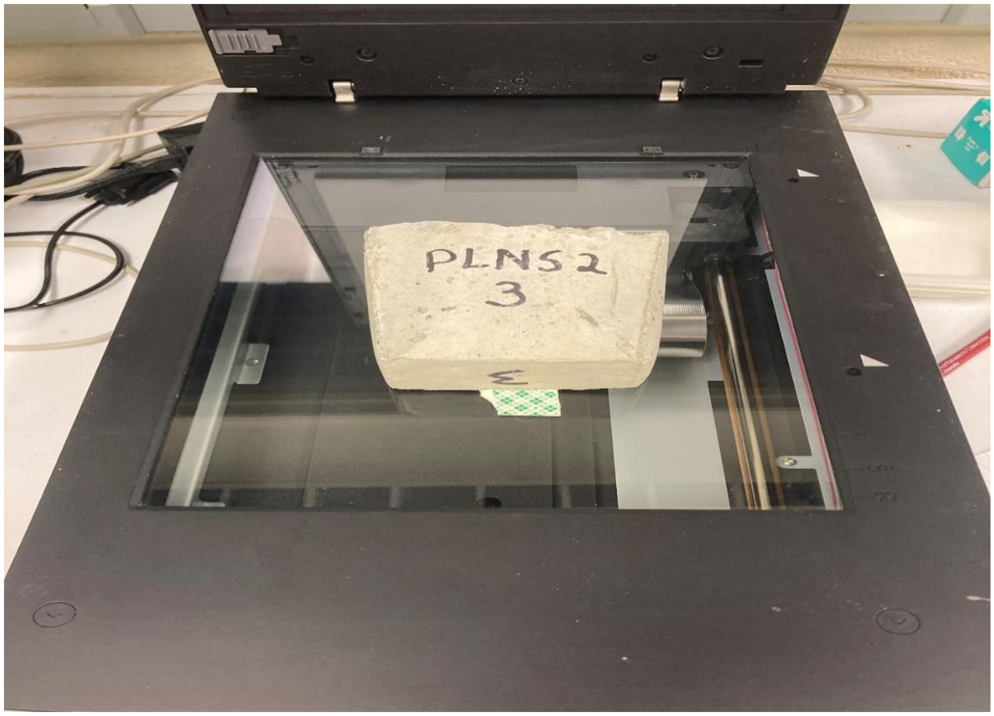

Figure 2.13: Example of a sample being scanned

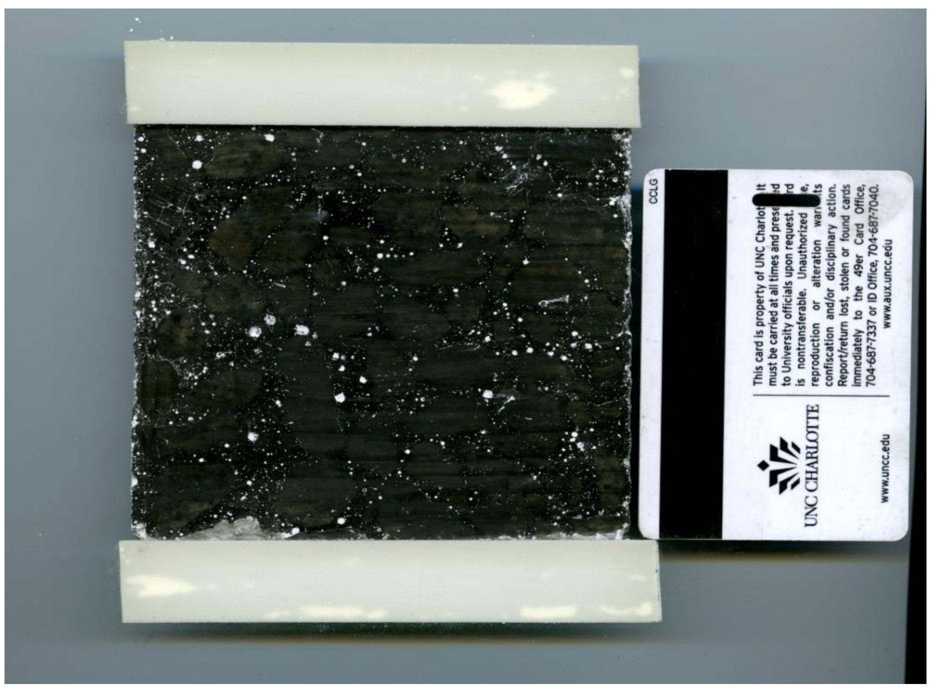

Figure 2.14: Finished scan of a prepared sample

Figure 2.12 shows an example of a flatbed scanner that can be used to analyze samples using Procedure C in ASTM C457. To protect the scanner from damage padded tape is placed on the scanning surface so that the sample is not in direct contact with the surface as seen in Figure 2.13. An example of a properly scanned sample can be seen in Figure 2.14.

Once the image has been normalized a section is chosen to be analyzed and the software will remove strips of pixels from the base image to comply with the point and length traversal requirements from ASTM C457. These strips taken from the base image are used to create a composite image that will then be analyzed by the program. Each pixel within the composite image is scanned and will be separated into either solid or air void depending upon values determined by calibrating the program using the hand counted samples (BubbleCounter 2021). The formula used to determine the spacing factor is based on whether the paste-air ratio is greater than or less than or equal to 4.342. If greater than 4.342 the formula will be Equation 2.5 below:

$$4.342\bar{L} = \frac{3}{\alpha}\left[1.4\left(1+\frac{p}{A}\right)^{\frac{1}{3}} - 1\right]$$

Equation 2.5: Spacing Factor (p/A > 4.342)

where:

L = Spacing Factor

α = Specific Surface

p = Paste Content, in %

A = Air Content, in %

The formula used to determine the spacing factor if p/A is less than 4.342 is shown in Equation 2.6 below:

$$4.342\bar{L} = \frac{T_p}{4N}$$

Equation 2.6: Spacing Factor (p/A < 4.342)

where:

L = Spacing Factor

T_p = traverse length through paste

N = total number of air voids intersected

All calculations and equations to determine the spacing factor have been laid out in ASTM C457 (ASTM, 2016).

2.5 Research Needs

The durability of a concrete sample depends upon many different factors with the most important factor being the quality of the air-void system within the paste of the concrete. Historically there have been two primary ways to determine the likely durability of a concrete sample, ASTM C666 and ASTM C457. However, both of these tests are time consuming and can only be performed on hardened concrete samples after the concrete has already been placed and cured on site. Currently the only test performed on fresh concrete that is used to evaluate the possible durability of the concrete mixture is determining the total air content (volume %) within the mixture. As evidence from Ley et al. (2017) shows that the dispersion of this air is highly dependent upon the mixture itself. Only by evaluating the characteristics of this air void system (dispersion, coarseness) will actually provide an indication if the air void system of high enough quality to withstand the environment it will be placed in.

The Super Air Meter (and associated test method, AASHTO TP 118) have provided a reasonable means of testing fresh concrete to evaluate the air void system characteristics. Research has shown correlation with both the air void spacing factor and freeze-thaw durability tests via ASTM C666. However, the characteristics of an air void system and, ultimately, the performance of hardened concrete under freeze-thaw cycles depends on materials and mixture proportions, which vary across the country. In an effort to develop specifications for freeze-thaw durable concrete, many states have been performing work to determine the SAM number corresponding to adequate freeze-thaw performance via ASTM C666. North Carolina has not yet performed this work, which is the subject of this thesis.

CHAPTER 3: METHODOLOGY

3.1 Introduction

The implementation of performance specifications including a test that could provide a quick and inexpensive correlation to the freeze-thaw durability of the mixture on site is of interest to NCDOT. The development and implementation of this performance specification requires that the SAM threshold be identified using test data from concrete using local materials and mixture designs that comply with NCDOT specifications. The testing program for this project will use four different concrete mixture matrices, three from past projects and one from a currently ongoing project. In this chapter, the methodology behind the laboratory and testing programs will be discussed. Identification of mixture types and proportions, batching of fresh concrete, and testing procedures will be presented.

3.2 Development of Past Concrete Mixture Matrices

This work benefits from data collected as part of three previous concrete materials research studies performed for NCDOT. Each of the three studies had a separate mixture matrix developed to support different research objectives. Each matrix and the corresponding mixtures were approved by NCDOT. All concrete mixtures included in each of the three matrices included mixtures with a design typical of those accepted by NCDOT in use for either pavement construction or as a Class AA (structural) mixture, along with materials selected for their common use in North Carolina concrete.

The first concrete mixture matrix was created in order to test and develop a catalog of inputs that could be used in the AASHTOWare Pavement ME design. The materials in this project were chosen based on recently constructed concrete pavements, as well as possible future construction, in the three regions of North Carolina. These regions are the Piedmont, Coastal, and Mountain regions and each region has different natural aggregates that can be found within the regions (Cavalline et al. 2018, Blanchard 2016).

This matrix consisted of 18 mixtures all of which had a consistent 0.48 w/cm and air content of 5.5% ± 0.5% for an air range of 5% to 6%. The mix matrix can be seen in Figure 3.1This base mixture used a combination of coarse aggregate that are commonly found in different sections of the state and were labelled as Piedmont, Coastal, and Mountain to show what region of the state they were from. This project also used two types of sand, manufactured and natural, two class F fly ashes from different locations, and two Portland cements (OPC) along with a Portland limestone cement (PLC). Table 3.1 shows how each component of the mixture was utilized to craft the 18 mixtures (Cavalline et al. 2018).

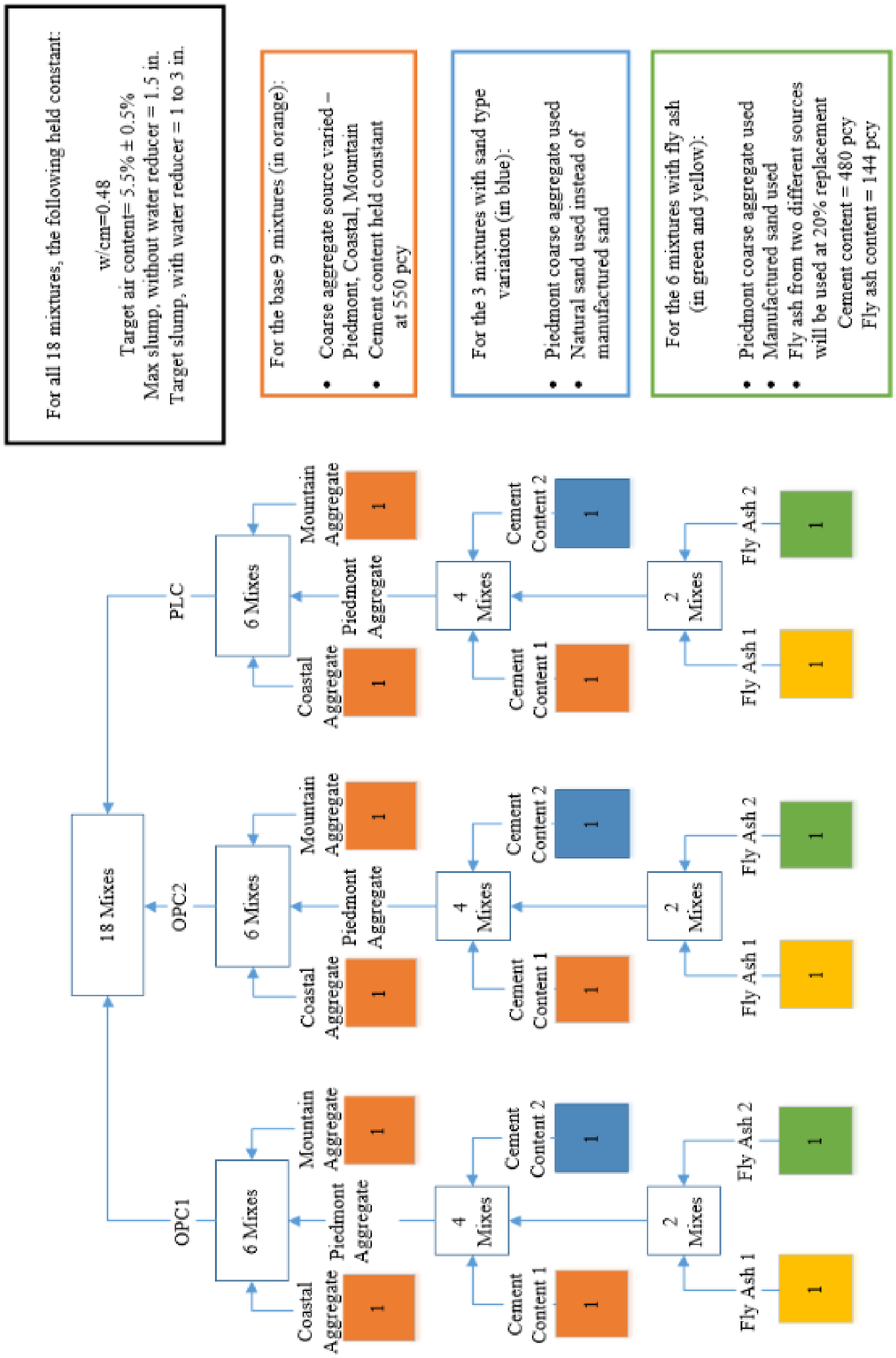

Figure 3.1: NCDOT Research Project 2015-03 Mixture Matrix (Cavalline et al. 2018)

Table 3.1: NCDOT Research Project 2015-03 Mixture Proportions (Cavalline et al. 2018)

Mixture ID*	Material Types				Mixture Proportions, pcy				
	Cement Type and Source	Coarse Aggregate	Fine Aggregate	Fly Ash	Cement	Fly Ash	Coarse Aggregate	Fine Aggregate	Water
C.A.N.M	OPC Source A	Coastal	Manufactured Sand	None	573	0	1661	1260	275
M.A.N.M		Mountain	Manufactured Sand	None	573	0	1798	1260	275
P.A.N.M		Piedmont	Manufactured Sand	None	573	0	1798	1260	275
P.A.N.N			Natural Sand	None	573	0	1798	1184	275
P.A.A.M			Manufactured Sand	Source A	460	137	1798	1260	304
P.A.B.M			Manufactured Sand	Source B	460	137	1798	1260	304
C.B.N.M	OPC Source B	Coastal	Manufactured Sand	None	573	0	1661	1260	275
M.B.N.M		Mountain	Manufactured Sand	None	573	0	1798	1260	275
P.B.N.M		Piedmont	Manufactured Sand	None	573	0	1798	1260	304
P.B.N.N			Natural Sand	None	573	0	1798	1184	304
P.B.A.M			Manufactured Sand	Source A	460	137	1798	1260	275
P.B.B.M			Manufactured Sand	Source B	460	137	1798	1260	275
C.BL.N.M	PLC (produced using OPC from Source B)	Coastal	Manufactured Sand	None	573	0	1661	1260	275
M.BL.N.M		Mountain	Manufactured Sand	None	573	0	1798	1260	275
P.BL.N.M		Piedmont	Manufactured Sand	None	573	0	1798	1260	275
P.BL.N.N			Natural Sand	None	573	0	1798	1184	275
P.BL.A.M			Manufactured Sand	Source A	460	137	1798	1260	304
P.BL.B.M			Manufactured Sand	Source B	460	137	1798	1260	304

*Note: Explanation of Mixture ID coding:

First letter, coarse aggregate type: C = Coastal, P = Piedmont, M = Mountain

Second letter, cement type: A = OPC source A, B = OPC source B, BL = PLC

Third letter, fly ash type: N = None, A = fly ash source A, B = fly ash source B

Fourth letter, fine aggregate type: M = manufactured sand, N = natural sand

The second concrete mixture matrix was created to test the benefits of internally cured concrete particularly in bridge decks and pavement applications. To achieve this internal curing two separate prewetted lightweight fine aggregates (LWA) were used along with the normalweight control aggregates. NCDOT required a moderate LWA replacement level along with a high replacement level to get a better understanding of the optimal level of LWA replacement to use in the future (Leach 2018, Cavalline et al. 2019).

This mixture matrix included 18 different concrete mixtures with ten being designed to meet bridge deck Class AA specifications. Five had a latex-modified concrete overlay with these being broken into three using lightweight aggregates and the other two using the normalweight control aggregates. Two mixtures were using very high early strength mixtures which were also split into an LWA and control group. The final mixture was an internally cured pavement mixture that used a previously batched concrete mixture from NCDOT RP 2015-03 as its control (Cavalline et al. 2019). All of the mixes can be seen in Figure 3.2 below with Table 3.2 showing the proportions used in each mixture.

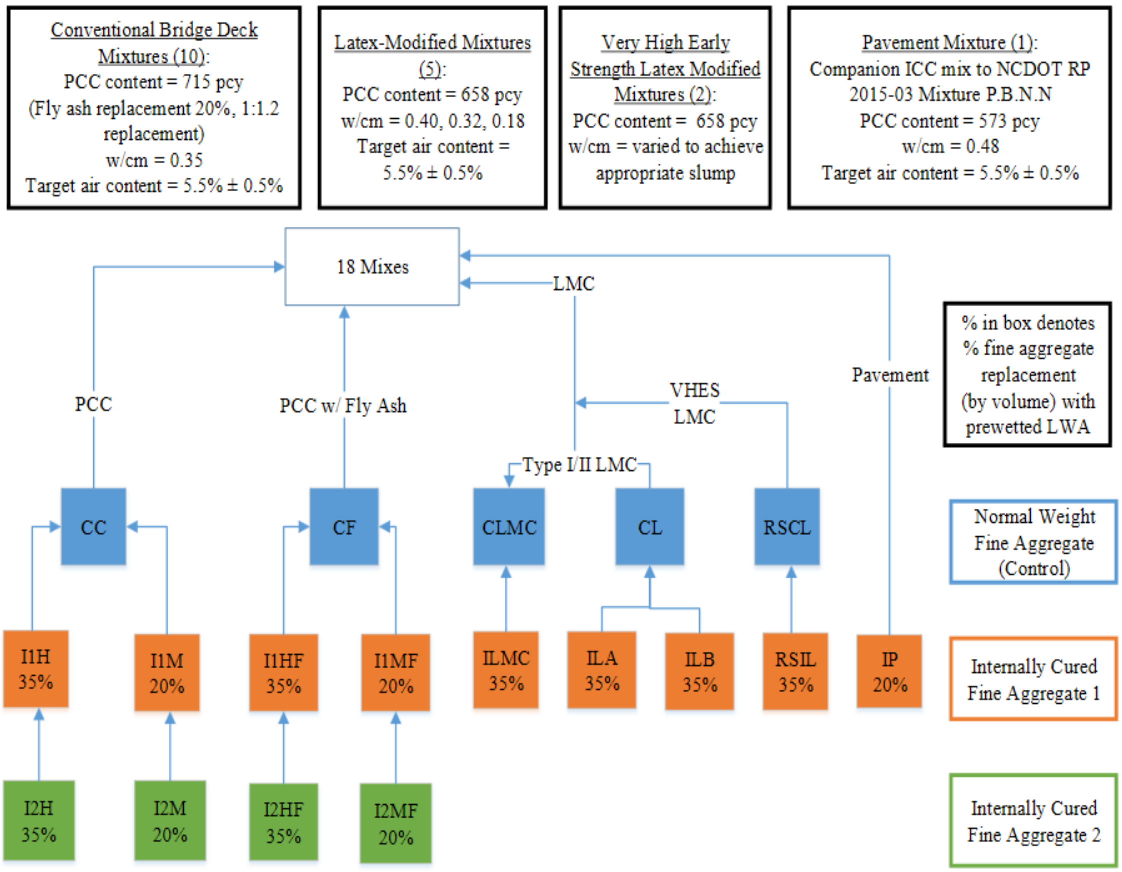

Figure 3.2: NCDOT Research Project 2016-06 Mixture Matrix (Cavalline et al 2019)

Table 3.2 NCDOT Research Project 2016-06 Mixture Proportions (Cavalline et al 2019)

Mixture Type	ID	Description	Weight (lb/cy)					
			Cement	Fly Ash	Water	CA	NWFA	PWLA
Conventional Bridge Deck	CC	Conventional concrete	715	0	266.0	1720	1113	0
	I1M	Internal curing, LWA #1, moderate replacement	715	0	265.6	1720	890	154
	I2M	Internal curing, LWA #2, moderate replacement	715	0	265.6	1720	890	139
	I1H	Internal curing, LWA #1, high replacement	715	0	265.3	1720	723	270
	I2H	Internal curing, LWA #2, high replacement	715	0	265.3	1720	723	243
	CF	Conventional concrete, with fly ash	572	172	266.0	1720	1113	0
	I1MF	Internal curing, LWA #1, moderate replacement, with fly ash	572	172	265.6	1720	890	154
	I2MF	Internal curing, LWA #2, moderate replacement, with fly ash	572	172	265.6	1720	890	139
	I1HF	Internal curing, LWA #1, high replacement, with fly ash	572	172	265.3	1720	723	270
	I2HF	Internal curing, LWA #2, high replacement, with fly ash	572	172	265.3	1720	723	243

LMC	CLMC	Conventional latex-modified concrete	658	0	153.3*	1304**	1510	0
	ILMC	Internally cured latex-modified concrete, LWA #1, high replacement	658	0	153.3*	1304**	921	345
	CL	Conventional latex-modified concrete, w/cm to achieve desirable slump	658	0	101.3*	1304*	1510	0
	ILA	Internal curing latex-modified concrete, LWA #1, w/cm to match mixture CL	658	0	101.3*	1304*	921	345
	ILB	Internal curing latex-modified concrete, LWA #1, high replacement, w/cm to achieve desirable slump	658	0	9.1*	1304*	921	345
VHES LMC	RSCL	Very high early strength conventional latex-modified concrete	658	0	121.0*	1304*	1510	0
	RSIL	Very high early strength internal curing latex-modified concrete, LWA #1, high replacement	658	0	81.5*	1304*	921	345
Pavement	P.A.N.N	Conventional pavement mixture from RP 2015-03	573	0	298.2	1798	1184	0
	IP	Internal curing pavement mixture, LWA #1, moderate replacement	573	0	298.2	1798	770	252

The final mixture matrix was created to support the identification of appropriate methods and performance criteria needed to implement performance specifications that would improve concrete durability. The primary focus characteristics of the mixture matrix included the w/cm, total cement/supplementary cementitious material (SCM) content, and percentage replacement of fly ash. These parameters were chosen as they were found to be highly influential on the development and integrity of the paste structure (Biggers 2019). This testing program focused on developing recommendations to the specification provisions of surface resistivity, shrinkage, opening to traffic at an early age (Cavalline et al. 2020).

This mixture matrix consisted of 24 mixtures which encompassed three w/cm ratios, three cement contents, and two levels of fly ash replacement. The three w/cm ratios were 0.37, 0.42, and 0.47 with seven mixtures each of 0.37 and 0.47 and 0.42 having ten different mixtures. These mixtures are laid out in more detail in Figure 3.3 below. The three cement contents were 700 lbs. per cy (pcy), 650 pcy, and 600 pcy. The

700 pcy and 650 pcy mixtures are typical of NCDOT Class AA design specifications while the lower cement content (600 pcy) is typical of a lower cement content NCDOT Class AA design or a pavement mixture. The fly ash in these mixtures is being replaced at either 20% or 30% with the 30% replacement level being utilized only for the lowest cement content mixtures. Figure 3.3 provides the details of how each mixture used in this project was proportioned out per cubic yard to meet the specifications set.

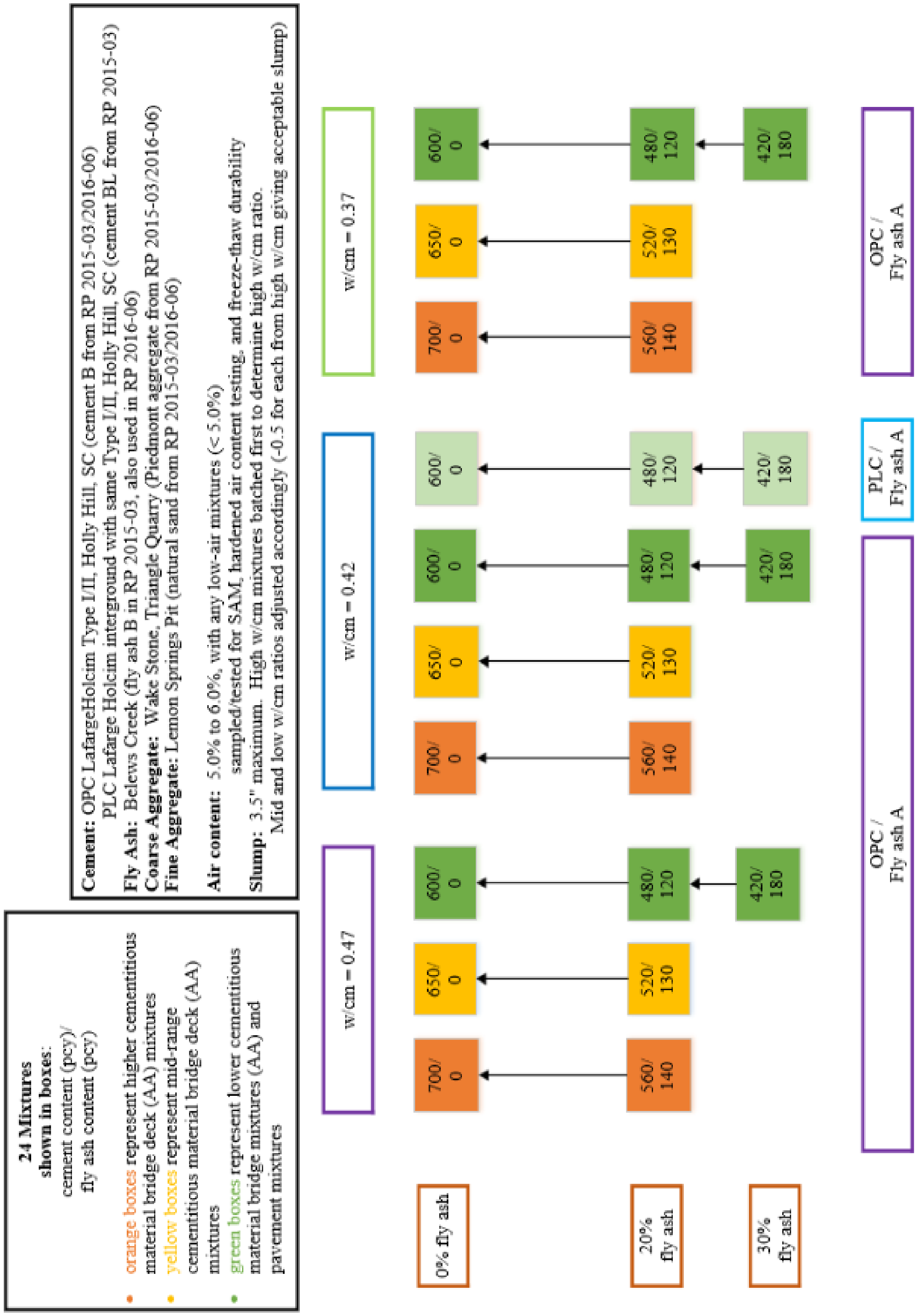

Figure 3.3: NCDOT Research Project 2018-04 Mixture Matrix (Cavalline et al 2020)

Table 3.3: NCDOT Research Project 2018-04 Mixture Proportions (Cavalline et al 2020)

Mixture ID W-XXX-YYY, where **W** is w/cm ratio, **XXX** is cement content, **YYY** is fly ash content	**Mixture Characteristics**			**Mixture Proportions, pcy**					
	Mixture type	**Cement type**	**w/cm**	**Fly ash replacement (%)**	**Cement**	**Fly ash**	**Coarse aggregate**	**Fine aggregate**	**Water**
H-700-0	AA (high and medium cm content)	OPC	0.47	0	700	0	1659	1072	329.0
H-560-140				20	560	140	1659	1022	329.0
H-650-0				0	650	0	1659	1175	305.5
H-520-130				20	520	130	1659	1129	305.5
H-600-0				0	600	0	1659	1277	282.0
H-480-120				20	480	120	1659	1235	282.0
H-420-180				30	420	180	1659	1214	282.0
M-700-0			0.42	0	700	0	1659	1163	294.0
M-560-140				20	560	140	1659	1114	294.0
M-650-0				0	650	0	1659	1259	273.0
M-520-130				20	520	130	1659	1214	273.0
M-600-0				0	600	0	1659	1356	252.0
M-480-120				20	480	120	1659	1313	252.0
M-420-180				30	420	180	1659	1292	252.0
M-600P-0		PLC		0	600	0	1659	1356	252.0
M-480P-120				20	480	120	1659	1313	252.0
M-420P-180				30	420	180	1659	1292	252.0
L-700-0	AA (low cm content) and	OPC	0.37	0	700	0	1659	1254	259.0
L-560-140				20	560	140	1659	1205	259.0
L-650-0				0	650	0	1659	1344	240.0
L-520-130				20	520	130	1659	1298	240.0
L-600-0				0	600	0	1659	1434	222.0
L-480-120				20	480	120	1659	1392	222.0
L-420-180				30	420	180	1659	1370	222.0

3.3 Development of Concrete Mixture for Current Project

The mixture matrix was developed to allow a comparison between itself and the previously batched mixture matrix from NCDOT 2018-14. This allows for as close to a direct comparison as possible between a concrete mixture and that concrete mixture with optimized aggregate gradation. The differences between the paste content for NCDOT 2018-14 and NCDOT 2020-13 is shown in Table 3.4 and shows the difference in paste content between a mixture design without optimized gradation and one that has been optimized.

Table 3.4: Paste content difference between optimized and non-optimized gradation mixtures

Mixture ID	Paste Content (volume % of mixture)	
	RP 2018-14 (completed)	RP 2020-13 (this project)
H-700-0	33%	29%
H-560-140	34%	30%
H-650-0	30%	27%
H-520-130	31%	28%
H-600-0	28%	25%
H-480-120	29%	26%
H-420-180	29%	26%
M-700-0	31%	28%
M-560-140	32%	28%
M-650-0	28%	26%
M-520-130	29%	26%
M-600-0	26%	24%
M-480-120	27%	24%
M-420-180	28%	25%
L-700-0	28%	26%
L-560-140	30%	27%
L-650-0	26%	24%
L-520-130	27%	25%
L-600-0	24%	22%
L480-120	25%	23%
L-420-180	26%	23%

3.3.1 Development of Mixture Design

24 target mixtures were identified to be within the parameters set out by the NCDOT for testing and batching as part of the laboratory program. These 24 mixtures were designed to meet Class AA bridge deck specifications with 12 having cement content that could be considered usable for paving applications. These mixtures are

shown in Figure 3.4 below. Table 3.5 shows the mixture proportions used in NCDOT research project 2020-13.

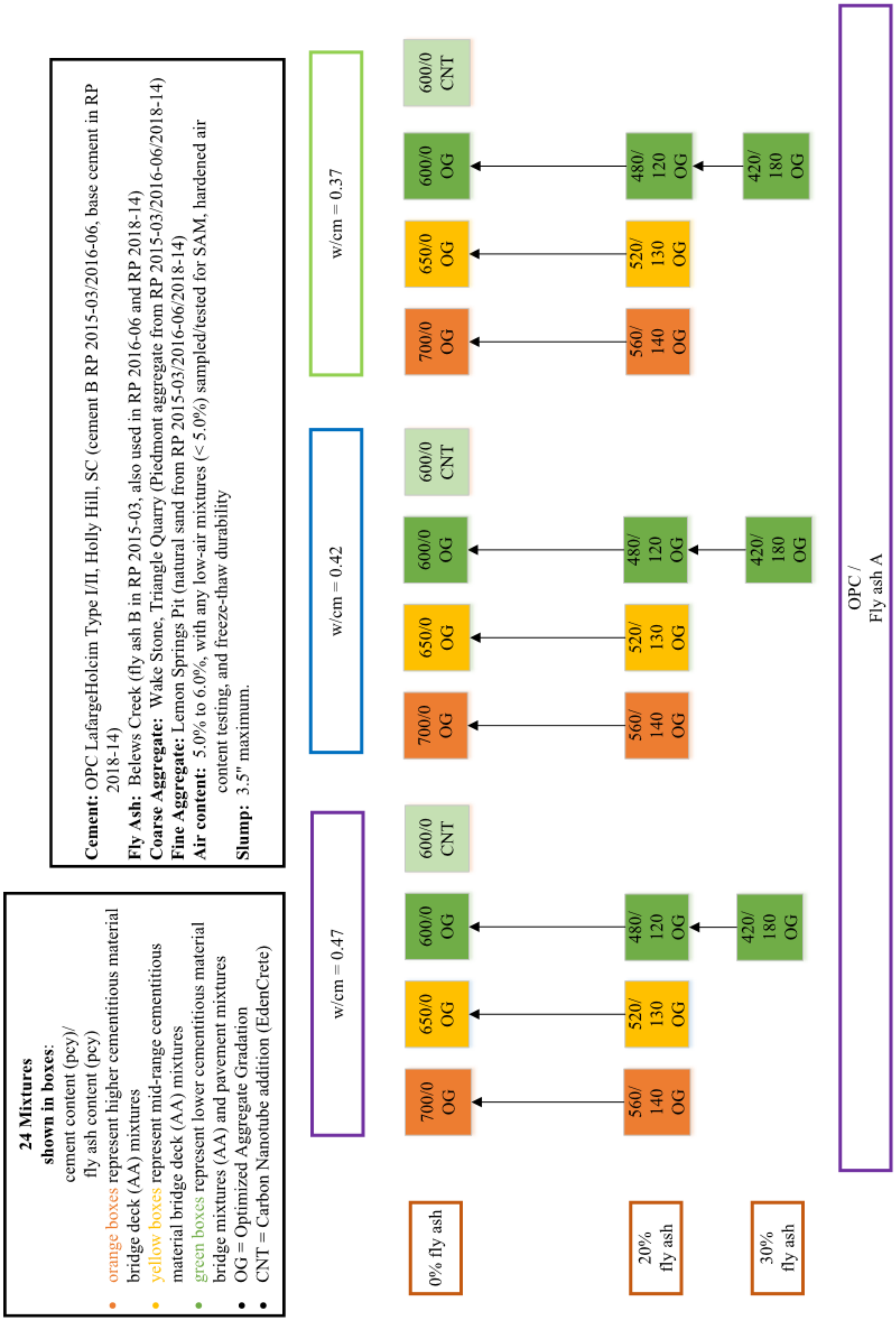

Figure 3.4: Mixture Proportions for NCDOT Research Project 2020-13

Table 3.5: Concrete Mixture Characteristics and Proportions

Mixture ID W-XXX-YYY, where W is w/cm ratio, XXX is cement content, YYY is fly ash content	Mixture Characteristics		Mixture Proportions, pcy					
	Mixture Type	w/cm	Fly Ash Replacement (%)	Cement	Fly Ash	Coarse Aggregate	Medium Aggregate	Fine Aggregate	Water
H-700-0		0.47	0	630	0	1175	620	1065	296.1
H-560-140		0.47	20	504	126	1158	615	1055	296.1
H-650-0		0.47	0	585	0	1215	640	1105	275
H-520-130		0.47	20	468	117	1204	632	1088	275
H-600-0		0.47	0	540	0	1261	662	1130	253.8
H-600C-0		0.47	0	540	0	1261	662	1130	253.8
H-480-120		0.47	20	432	108	1243	652	1125	253.8
H-420-180		0.47	30	378	162	1227	652	1124	253.8
M-700-0		0.42	0	630	0	1206	636	1107	264.6
M-560-140		0.42	20	504	126	1193	626	1093	264.6
M-650-0		0.42	0	585	0	1248	658	1130	245.7
M-520-130		0.42	20	468	117	1235	650	1115	245.7
M-600-0		0.42	0	540	0	1284	678	1162	226.8
M-600C-0		0.42	0	540	0	1284	678	1162	226.8
M-480-120		0.42	20	432	108	1277	672	1141	226.8
M-420-180		0.42	30	378	162	1270	590	1211	226.8
L-700-0		0.37	0	630	0	1252	658	1122	233.1
L-560-140		0.37	20	504	126	1224	650	1123	233.1
L-650-0		0.37	0	585	0	1279	675	1159	216
L-520-130		0.37	20	468	117	1270	668	1140	216
L-600-0		0.37	0	540	0	1316	697	1186	199.8
L-600C-0		0.37	0	540	0	1316	697	1186	199.8
L-480-120		0.37	20	432	108	1297	688	1177	199.8
L-420-180		0.37	30	378	162	1293	684	1173	199.8

3.4 Materials

In the following sections the information surrounding the materials sourced for batching of concrete mixtures included in this study will be provided. Information on the materials used in previous studies is included in the mixture matrix diagram figures, as well as in the referenced project reports.

3.4.1 Cementitious Material

The two cementitious materials used for batching in this project were an OPC and a class F fly ash from a single source. The characteristics of these cementitious materials along with a general description, and source will be provided in the next sections

3.4.1.1 Portland Cement (OPC)

The OPC used is typical of those specified by the NCDOT on paving projects. This OPC was produced by LafargeHolcim at their Holly Hill, SC manufacturing plant and was then transported to UNC Charlotte. This cement is classified as a Type I/II cement as defined by ASTM C150, "Standard Specification of Portland Cement" (ASTM 2020). Mill reports can be found in the Appendix of the accompanying thesis prepared by Peter Theilgard (Theilgard 2022).

3.4.1.2 Fly Ash

To maintain consistency across this mixture matrix and the previously batched mixture matrix from NCDOT 2018-14 fly ash replacements of 20 and 30 percent were used. NCDOT Standard Specifications for Roads and Structures allows for 30% replacement of cement for fly ash at a 1:1.2 ratio for weight (NCDOT 2018). This fly ash is a Type F fly ash, from Belews Creek Power Plant located in Belews, NC, as defined by ASTM C618-19 "Standard Specification for Coal Fly Ash and Raw or Calcined Natural Pozzolan for Use in Concrete" and the composition results can be found in the Appendix can be found in the Appendix of the accompanying thesis prepared by Peter Theilgard (Theilgard 2022).

3.4.2 Coarse Aggregate

The coarse aggregate used for this study and for RP 2018-14 was selected for use in batching of concrete to allow continuity from the previous research projects. A No.67 aggregate was sourced from Wake Stone's Triangle Quarry located in Cary, NC which is just outside of Raleigh, NC.

3.4.3 Intermediate Aggregate

The intermediate aggregate was used to allow the gradation of the aggregates to be optimized. A No.89 aggregate was chosen to be included in the batching of the concrete for this project. This No.89 aggregate was sourced from Wake Stone's Moncure Quarry located in Moncure, NC.

3.4.4 Fine Aggregate

The fine aggregate sourced for the current study is one that has been previously used for past research projects, unless noted in the mixture matrix diagram figures. The fine aggregate is a natural silica sand obtained from a sand pit in Lemon Springs, NC controlled by GS Materials. The physical properties of the fine aggregate can be found in the Appendix.

3.4.5 Chemical Admixtures

An air entraining admixture (AEA) along with a mid-to-high range water reducing admixture (WRA) were used as part of this study. A carbon nanotube admixture was also used in three mixtures as part of a study on the benefits of carbon nanotubes being used as an admixture. The AEA and WRA were used to achieve the project requirements of a fresh air content of 5.5 ±0.5% and a maximum slump of 3.5 in. with reasonable variations to meet the w/cm.

The AEA utilized for batching the concrete in this study was MasterAir AE 200 which is produced by BASF. This AEA was used in batching all mixtures besides one where it could not be used while maintaining the fresh air requirements. The WRA used was MasterPolyheed 997 which is a mid-range WRA produced by BASF. 22 out of 24 concrete mixtures included this WRA to achieve the workability needed. The other two mixtures had sufficient workability without the aid of a WRA mainly due to the w/cm.

3.5 Testing Program

The full testing program developed will be included in Table 7 below, however this testing program has been split between two separate studies and only those that directly relate to this study will discussed in detail in this thesis. All testing of fresh and hardened concrete was done in accordance with the standard test procedures listed in Table 3.6. All mixtures that contain the lowest level of cementitious materials (bottom row of Figure 3.4) had beams cast for flexural strength, modulus of rupture (MOR).

Table 3.6: Testing Program

	Test name	Standard	Testing age(s), days	Replicates
Fresh	Air Content	ASTM C231	Fresh	1
	SAM	AASHTO TP 118	Fresh	1
	Slump	ASTM C143	Fresh	1
	Fresh density (unit weight	ASTM C138	Fresh	1
	Temperature	AASHTO T 309	Fresh	1
Hardened	Compressive strength	ASTM C39	3, 7, 28, 56, 90	3 per age
	Modulus of rupture	ASTM C78	28	2
	Modulus of elasticity	ASTM C469	28	2
	Hardened air content	ASTM C457	N/A	2
	Freeze thaw durability	ASTM C666	14	3
	Resistivity	AASHTO T 358	3, 7, 28, 56, 90	3 per age
	Formation factor (Bucket test)	Protocol by J. Weiss at Oregon State University	35	2

	Shrinkage	ASTM C157	4, 7, 14, 28, 56, 112, 224, 448	3
	Rapid chloride permeability	ASTM C1202	28, 90	2

3.6 Mixing and Batching of Concrete

Concrete batches were mixed within a six cubic foot (cf) portable drum mixer. The batch size required was calculated from the volume specimens needed for the required testing program along with an additional factor to account for SAM testing, air content testing by ASTM C231, and a waste factor. The batches requiring modulus of rupture beams were determined to need 4.5 cf and the remaining mixes required 2.8 cf. The batches requiring the modulus of rupture beams were split into two 3.0 cf batches after discussion on the usable capacity of the drum mixer and ability to fill all molds within a reasonable time. The non-paving mixtures were batched as one mixture in 3.0 cf batches to account for waste. Compressive cylinders were prepared for each batch as a quality check between different batches of the same mixture.

Batching of concrete was performed under the guidelines of ASTM C685, “Standard Specification for Concrete Made by Volumetric Batching and Continuous Mixing” and specimens were created under the guidelines of ASTM C192, “Standard Practice for Making and Curing Concrete Test Specimens in the Laboratory” (ASTM 2017, ASTM 2019). Paving mixtures were split into cylinder mixtures and beam mixtures, however the beam mixtures still contained compressive strength cylinders.

3.7 Tests on Fresh Concrete

Several key properties were tested for directly after batching each mixture of concrete. These properties include slump, fresh air content, temperature, unit weight, and the SAM number. The procedures and standards used to obtain these properties will be described in the following sections.

3.7.1 Slump

The slump test's procedure is outlined in ASTM C143, "Standard Test for Slump of Hydraulic Cement Concrete" and this procedure was performed on every batch of concrete prepared for this study (ASTM 2020). The procedure for slump is to place concrete into a slump cone in three even layers with each layer being rodded 25 times in between layers. The slump cone is then brought up at a steady pace with only vertical motion and placed besides the pile of fresh concrete upside down. The tempering rod is then placed on top of the cone and the pile of concrete is measured from its center up to the bottom of the rod to determine the slump of the concrete mixture.

3.7.2 Fresh Air Content and SAM Number

Fresh air content of the concrete was measured with a Type B air pressure meter in conformance of ASTM C 231, "Standard Test Method for Air Content of Freshly Mixed Concrete by the Pressure Method" (ASTM 2017). This standard entails filling up the bowl in three equal layers with each layer being rodded 25 times and then struck 9-15 times with a mallet between layers. The top layer is the struck off and cleaned to allow for a tight seal when the top chamber is placed on and latched. Once the top is placed on and latched the remaining space inside is filled with water by slowly injecting water through the petcocks with a bulb syringe. Once all remaining air is removed, the petcocks are sealed, and the chamber is pressurized with the pump. Once the pressure has stabilized on the gauge, the needle gauge lever is held, and the bottom chamber is struck with a mallet. The air meter gauge is lightly tapped until it stabilizes, and the air pressure is read.

The procedure for the SAM test is outlined in AASHTO TP 118 and initially follows the same sample preparation procedure as ASTM C231 until pressurization. Figure 3.5 below shows the apparatus used during the SAM test. This apparatus is modeled after the Type B Pressure meter used in ASTM C231; however, the SAM test uses a greater pressure than the Type B Pressure meter and has six clamps to seal the chamber to deal with the increase in pressure. The SAM test uses three pressure steps and two sets of pressurization to determine the SAM Number. Once the bottom chamber has been injected with water through the petcocks and sealed the chamber will need to be pressurized to 14.5 psi. This pressure step can also be used to determine the fresh air content of the concrete if desired. The next pressurization step is to 30 psi and the final pressure required is 45 psi. The system is then purged of pressure and refilled with water before starting the second set of pressurizations. This second set of pressurizations follow the first set exactly (14.5 psi, 30 psi, and 45 psi) and at the final step the difference between equilibrium pressures is calculated as the SAM number (Ley et al. 2017).

It is noted that the SAM test results included in this thesis were obtained over the course of approximately 8 years using two SAM devices and approximately 10 different operators. Additionally, over the course of the project, both SAM devices received service from the OSU technician at several points, including reprogramming of the gauge with updated software as it became available. Additionally, lightweight sand used in RP 2016-06 as an internal curing agent was porous and may have influenced the SAM measurements for these mixtures. These changes in equipment, operator, materials, and computational algorithm each likely influenced the accuracy and the uncertainty of SAM number measurements. Evaluating the influence of these changes on the SAM measurements was not included in the scope of this study, but the likely influence of these changes is acknowledged.

Figure 3.5: Super Air Meter (SAM)

3.7.3 Unit Weight

The fresh unit weight was determined in accordance with ASTM C138, “Standard Test Method for Density (Unit Weight), Yield, and Air Content (Gravimetric) of Concrete” (ASTM 2017). The concrete sample used to determine the unit weight was the same one that the fresh air content test would be run on as the chamber for the air test is a known weight and volume.

3.8 Preparation and Curing of Test Specimens

All test samples were prepared in accordance with ASTM C192, “Standard Practice for Making and Curing Concrete Test Specimens in the Laboratory” (ASTM 2018). All molds were first coated in form release to allow for the samples to be taken out after the initial curing phase. As several research team members were involved with the preparation of the samples continuity of sample making was ensured when possible. After initial curing was achieved the samples were demolded and placed into a moist curing room that adheres to ASTM C511, “Standard Specification for Mixing Rooms, Moist Cabinets, Moist Rooms, and Water Storage Tanks Used in the Testing of Hydraulic Cements and Concretes” (ASTM 2019).

3.9 Testing of Hardened Concrete

Mechanical property testing on the samples mixed as part of this study were performed but are the subject of a thesis by another group member (Theilgard 2022), and therefore will not be discussed in detail within this thesis. The mechanical property tests include compressive strength, MOR, MOE, Poisson’s ratio, and shrinkage. For the convenience of the reader, a summary of results will be provided in this thesis for selected tests. Several properties related to the freeze-thaw durability are the focus of this work, including, spacing factor, durability factor, and hardened air content, which will be described in more detail.

3.9.1 Mechanical properties

The mechanical properties of a sample are traditionally the ones used in specifications and as acceptance. ASTM C39, “Standard Test Method for Compressive Strength of Cylindrical Concrete Specimens” were used to determine the compressive strength of the concrete mixture by testing cylindrical samples at 3, 7, 28, 56, and 90 days after the concrete has been placed in molds (ASTM 2021). The Modulus of Rupture (MOR) was obtained in accordance with ASTM C78, “Standard Test Method for Flexural Strength of Concrete (Using Simple Beam with Third-Point Loading)” (ASTM 2021). The Modulus of Elasticity (MOE) and Poisson’s Ratio were found in accordance with ASTM C469, “Standard Test Method for Static Modulus of Elasticity and Poisson's Ratio of Concrete in Compression” (ASTM 2014).

Shrinkage properties for the samples were determined using an unrestrained shrinkage test in accordance with ASTM C157, “Standard Test Method for Length Change of Hardened Hydraulic-Cement Mortar and Concrete” (ASTM 2017). Three specimens were fitted with gauge studs during the molding process and then wet cured for 28 days before being transferred to an environmental chamber.

3.9.2 Durability Performance

Concrete pavement and structures rely on properties relating to durability being at a sufficiently high level so that the concrete can have a long service life. The durability performance tests of focus for this work are the spacing factor, the hardened air content, and durability factor.

3.9.2.1 Spacing Factor and Hardened Air Content

The spacing factor for this study was found using Procedure C from ASTM C457 using a flatbed scanner and color contrasted samples. In this research only an automated method was used to determine the spacing factor as well as the hardened air content. This scanner-based method and BubbleCounter algorithm were developed at Michigan Technological University and details are provided in several publications (Carlson et al. 2005, Peterson et al. 2002, Peterson et al. 2009).

The automated method to determine these parameters of the air-void system requires that a calibration set be developed, with the air void system parameters manually counted with per ASTM C457 procedures before it can be used. This calibration set of samples was developed during previous research (Ojo 2018). It is noted that the calibration set used for this study was not enhanced or modified from that of Ojo (2018), and additional accuracy of the approach could potentially have been achieved by optimizing the calibration set to include additional samples that were more representative of the range of mixtures included in all studies.

The specimens used in the automated method require special preparation starting with being cast in cardboard food containers, since this shape was found to have the surface area required by ASTM C457 for analysis, while also being easier to cut into a usable sample. Figure 3.6 and Figure 3.7 below show a typical sample being cast into this shape. The specimens were cut in half vertically once curing was complete which was 14 days for the samples used to calibrate the automated method (Ojo 2018). The preparation of the surface of the samples began by applying a silicon carbide polishing powder with a nominal size of 150 µm, which will be referred to by its grit size of no.100. The sample was previously polished with an automated polisher for approximately 15 minutes before it was taken off and cleaned to remove all of the silicon carbide grit. Once the sample and polisher were clean the sample was returned to the polisher and this procedure was repeated for grits of 240, 320, 600, and 1000. Once the sample was fully polished it was examined to determine that a sufficiently mirrored finish was created to allow for the sample to reflect a distant light in its surface. Once the polishing was complete the sample was cleaned in an ultrasonic cleaner to remove any grit trapped on the surface or in any air voids.

Figure 3.6: Sample being cast in takeout container

Figure 3.7: Takeout container after being filled with concrete

Once the sample is polished and has been fully cleaned to be free from any leftover silicon carbide grit, the surface treatment of the sample can begin. The first step in preparing the surface of the sample is darkening the surface with a Pigma BB black marker created by Sakora Color Products Corporation. The surface is darkened horizontally by gently and evenly drawing the marker over the surface in overlapping lines following the same path (Ojo 2018). The sample is then rotated 90 degrees and darkened again in the same manner as the first time. Once the sample has been fully darkened, a 2-micron wollastonite powder manufactured by Nyco is used to fill the air voids and provide a contrast to the darkening agent. This wollastonite powder is spread over the surface of the sample and spread into the air voids using a flat piece of metal. All air voids should be completely filled, and if not, then the wollastonite powder should be applied to the specific areas until the air voids are filled. Once all air voids were completely filled the samples surface were lightly darkened again making sure to not interfere with the air voids. This darkening will help add back the contrast to the sample by removing the excess white wollastonite powder from the surface of the sample (Ojo 2018).

Once the color contrast surface treatment is complete the sample was scanned, with a black and white sample card, in 8-bit grayscale at 125 dpi to a TIFF format using a flatbed scanner. An example of a sample being scanned after the color treatment is shown in Figure 3.8 below.

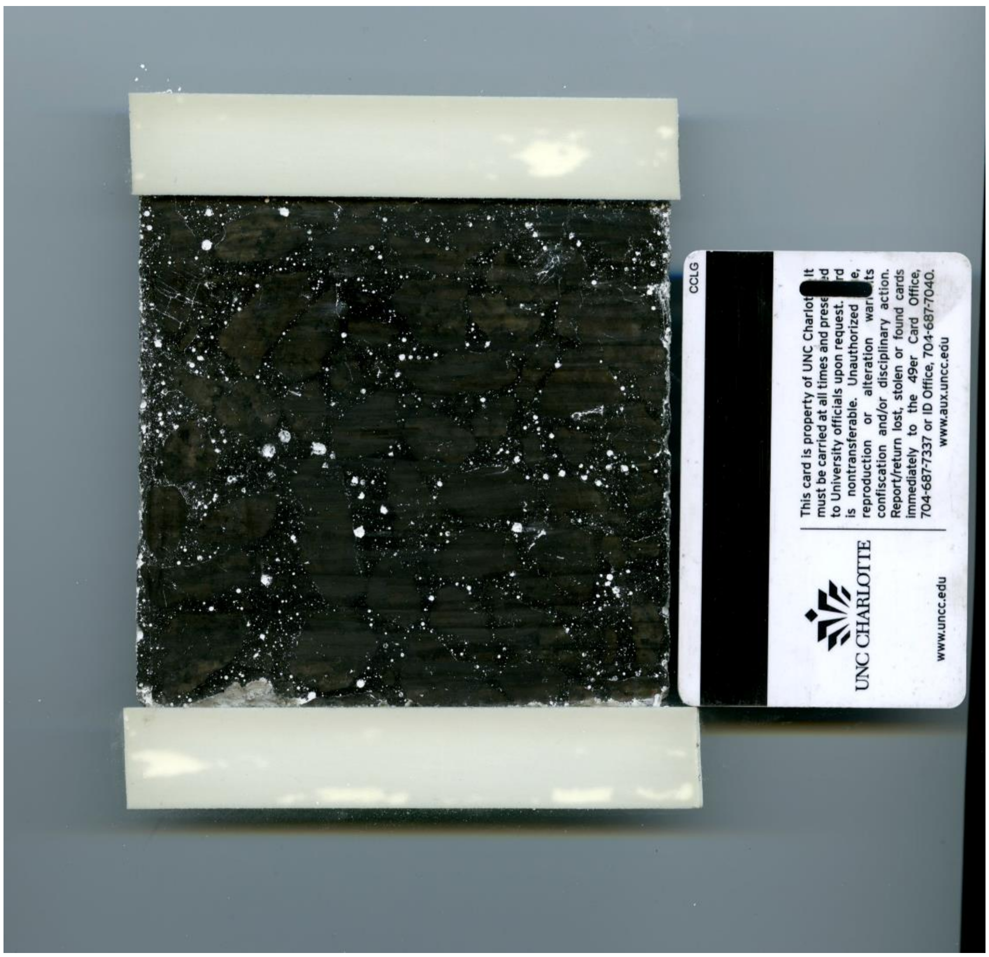

Figure 3.8: Completed Sample being Scanned

Once scanned the sample was opened in BubbleCounter and the black and white sample card was used to determine the white balance in the scan for the program. After the white balance has been calculated for that sample a representative area of the sample was chosen and the program ran a prompt for input of properties of the mixture. This process is shown below in Figure 3.9 below. The properties used for this work were aggregate top size of 0.75 in (19mm), 57 transverses performed per specimen, and a paste fraction of 0.25 of the whole mixture. With these parameters inputted the program extracted the transverses from the sample and counted the white pixels as air voids and black pixels as either paste or aggregate (Ojo 2018, Bubblecounter 2021). A sample of what the software will output from scanning a sample is shown in Figure 3.10.

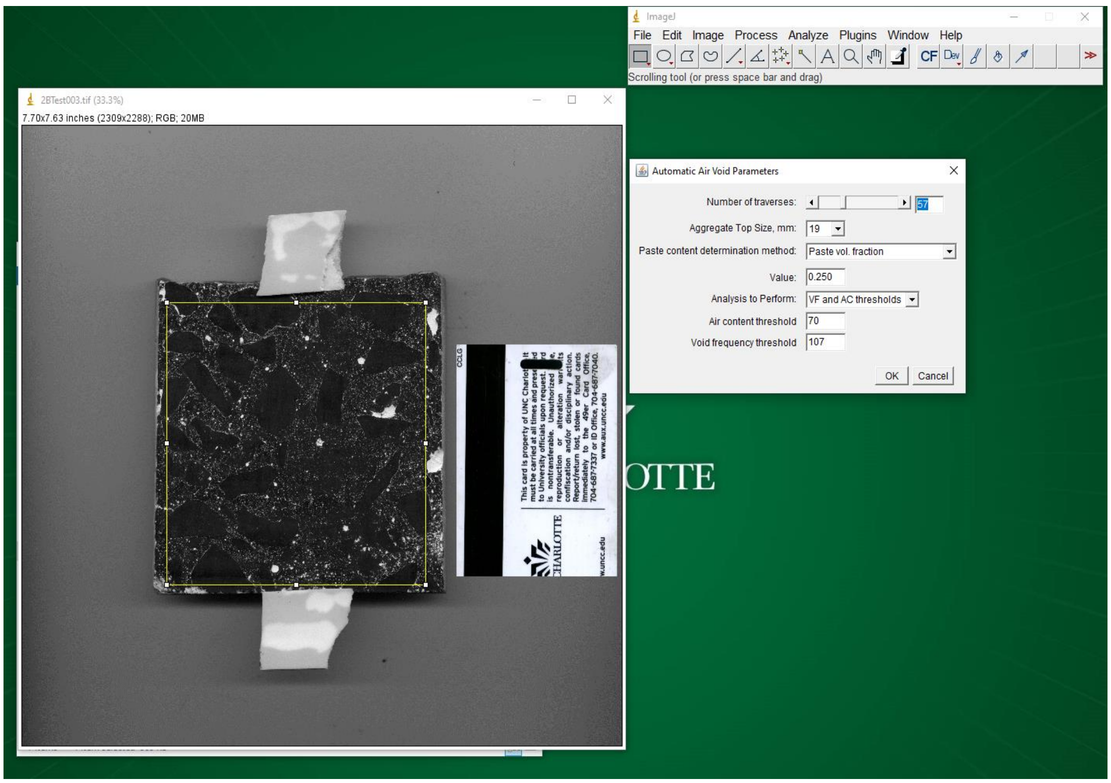

Figure 3.9: BubbleCounter Software

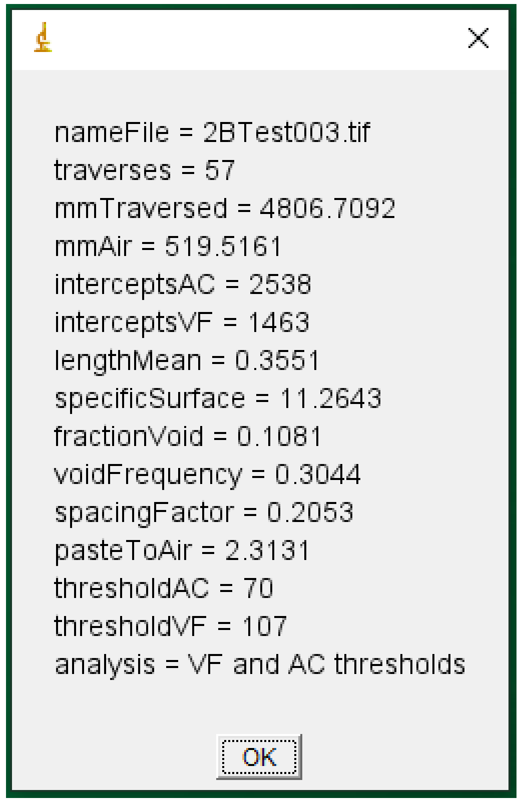

Figure 3.10: BubbleCounter Software Output

The variability associated with the scanner-based approach was explored by the developers. As described (Carlson et al. 2005), the variability expected is approximately 10% with both scanners tested having approximately a 90% agreement between what the scanner and manual point count called an air pixel. ASTM C457 also mentions the variability expected when the sample has both been made and measured in the lab that was performing the study. The coefficient of variation for this was found to be 8% in this case, however, when the sample was prepared and measured in a separate lab the coefficient of variation increased to 17.5% (ASTM 2016). The variability in the scanner approach to determining the parameters of the air-void system seems to come not only from the variability in the scanner but also from the variability from polishing and preparing the surface of the sample. Although every effort was made to keep the same user preparing the samples due to the nature of the study several users were involved for each step of preparation.

3.9.2.2 Durability Factor

The durability factor was determined using Procedure A in accordance with ASTM C666. For each concrete mixture, three 3" x 4" x 16" concrete samples were cast into steel molds. The specimens were then moist cured for 14 days after which they were wrapped in plastic film and placed into a freezer to stop the curing process. Once 17 specimens were accumulated over the batching period, they were placed into a water tank and allowed to fully thaw.

Once all the samples were fully thawed the mass and fundamental transverse frequency were measured using a Rigol DS1052E digital oscilloscope, Omega Engineering ACC-PS2 accelerometer, and digital scale. The digital oscilloscope was set to Fast Fourier Transform (FFT) mode and the fundamental transverse frequency was determined in accordance with ASTM 215, "Standard Test Method for Fundamental Transverse, Longitudinal, and Torsional Resonant Frequencies of Concrete Specimens" (ASTM 2019). It should be noted that during the course of RP 2020-13 (this study) the settings on the oscilloscope were such that the fundamental frequency measurements were only captured to the hundredths of a kHz (e.g., 2.1 kHz) rather than additional resolution (e.g., 2.13 kHz). This source of resolution loss is acknowledged as a limitation of the durability factors computed for specimens tested in this study, many of which were greater than 100 at the completion of the study. A full analysis of the impact of this change in measurement resolution on the uncertainty of the measurements was beyond the scope of this study but would likely also need to consider the combined uncertainty of all sources (calibration, frequency, length, mass, etc.).

After the initial mass and fundamental transverse frequency was determined the samples were placed into stainless steel trays with a small steel rod placed in the bottom of the tray to raise the sample off of the bottom of the tray. The samples were then placed into the freeze thaw chamber along with one control specimen. The control specimen was a beam of the same dimensions as the test beam, cast of a similar concrete mixture, but also had a hole drilled in it to allow for a thermocouple probe to be inserted and read the internal temperature of the sample. This beam was used to help monitor the temperature of the specimens over the course of each cycle, and to control the equipment driving the freeze-thaw process.

The samples then had a plastic spacer placed in either the front or back of the tray and were clipped together with steel clips to maintain a proper distance between the sides of the container and the sample. Once all samples had been clipped together the trays were filled with water, as per Procedure B from ASTM C666, and the chamber was turned on to cycle between 40°F and 0°F in a cycle that should be no less than 2 hours or more than 5 hours in accordance with ASTM C666 (ASTM 2015). After 30 cycles within the freeze thaw chamber the specimens were taken out in a thawed state to get a new reading for the mass and fundamental transverse function. Each time the samples were tested, the stainless-steel trays were cleaned of any debris and the samples are returned and covered with fresh water.

CHAPTER 4: TEST RESULTS

4.1 Introduction

This section of the document will serve as a summary of all data collected based on the testing methodology discussed in Chapter 3. The mixture designations for the previous projects used in this document are different from one another except for the two most current projects (NCDOT RP 2018-14 and RP 2020-13). These mixture designations can be found in section 3.2 of this document as well as in this section.

The mixture ID coding scheme for NCDOT research project 2015-03 is as follows: the first letter designates the coarse aggregate type: C = Coastal, P = Piedmont, and M = Mountain. The second letter designates the cement type: A = OPC source A, B = OPC source B, and BL = PLC. The third letter designates the fly ash: N = none, A = fly ash source A, and B = fly ash source B. The fourth letter designates the fine aggregate used: M = manufactured and N = natural.

The mixture designation coding scheme for NCDOT research project 2016-06 was named based on if the samples were internally cured and which fine aggregate was used. Mixtures marked with a “C” are part of the control mixtures which did not contain internal curing agents while those marked with an “I” were internally cured mixtures. The “1” and “2” within the designation identifies the mixture as using the first or second internal curing fine aggregate. Mixtures marked with an “M” indicate that the mixture had a moderate level of internal curing fine aggregate replacement while “H” indicate a high replacement level. Mixtures marked with an “F” indicate that part of the cement was replaced with fly ash.

The mixture designations for NCDOT RP 2018-14 and RP 2020-13 use the same ID convention and are as follows: the first designation indicates the w/cm ratio with “H” being high at 0.47, “M” being medium at 0.42, and “L” being low at 0.37. The second designator indicate the cement content in pcy and the third designator indicates the fly ash content in pcy. As the mixture IDs of these project are identical 2020-13, will be marked with “*” to designate optimized gradation and “NO” for not optimized when appropriate. NCDOT 2020-13 also had several mixes which used a carbon nanotube admixture which will be marked with a “C” on the second ID designator.

4.2 Testing Fresh Concrete

This section presents the results obtained from the fresh concrete property tests discussed in Section 3.7 from every project previously listed. Tests for fresh concrete included slump, fresh air content, SAM, and unit weight. These tests were performed on each mixture to ensure that the acceptance criteria for the project was being met. Air content was held to a strict requirement of 5.5% ± 0.5% to ensure consistency between all projects outlined. Table 4.1 below provides a summary of all fresh properties obtained. The only mixtures that will be explicitly discussed in this section will be those included in NCDOT 2020-13. Further information on other mixtures can be obtained from previous project reports (Cavalline et al. 2017, Cavalline et al. 2018, Cavalline et al. 2020). The dosage of WRA and AEA used varied based on the mixture characteristics and environmental factors encountered when mixing.

A target slump of 3.5 in. was set for project 2020-13, which is identical to the target slump set for 2018-14. Although this target was established, no mixture was discarded for failing to achieve this slump, since holding the w/cm constant was more important to project objectives. However, if a mixture failed to meet the air content requirements, it was rejected, and additional batches produced until the target was met.

Table 4.1: Fresh Concrete Test Results

Project ID	Designation	Slump (in.)	Air Content (%)	SAM Number	Unit Weight (pcf)
2015-03	P.A.N.M	1.4	5.4%	0.19	145.0
	P.B.N.M	1.9	6.0%	0.23	143.0
	P.BL.N.M	2.2	5.6%	0.28	144.0
	C.A.N.M	1.1	5.8%	0.80	138.0
	C.B.N.M	1.4	5.6%	0.35	139.0
	C.BL.N.M	1.1	5.5%	0.19	139.0
	M.A.N.M	2.0	5.3%	-	145.0
	M.B.N.M	2.4	5.4%	-	144.0
	M.BL.N.M	2.3	5.1%	-	145.0
	P.A.A.M	2.7	5.7%	0.88	141.0
	P.B.A.M	2.3	5.2%	0.42	142.0
	P.BL.A.M	2.5	5.2%	0.29	142.0
	P.A.B.M	2.4	5.6%	0.29	142.0
	P.B.B.M	2.3	5.7%	0.22	141.0
	P.BL.B.M	2.3	5.6%	0.19	141.0
	P.A.N.N	1.9	5.3%	0.10	143.0
	P.B.N.N	3.3	5.4%	0.27	142.0
	P.BL.N.N	2.8	5.5%	0.19	143.0
2016-06	CC	2.5	5.5%	0.32	144.6
	I1M	2.5	5.3%	0.21	141.0
	I1H	3.2	5.8%	0.24	138.8
	I2H	3.0	5.0%	0.39	139.1
	CF	3.2	6.0%	0.30	140.2
	I1MF	2.0	5.0%	0.25	141.0
	I2MF	2.0	5.0%	0.19	141.0
	I1HF	2.2	5.0%	0.29	139.4
	I2HF	2.0	5.1%	0.27	138.7
	IP	7.5	5.2%	0.30	136.8
	ILA	11.0	10.4%	0.50	127.5
	ILB	3.5	6.2%	0.76	140.2
2018-14	H-700-0	8.0	5.2%	-	137.1
	H-560-140	8.0	5.2%	0.19	136.4
	H-650-0	6.5	6.0%	0.38	141.4
	H-520-130	7.0	5.5%	-	138.0
	H-600-0	2.5	5.8%	-	138.7
	H-480-120	3.0	6.0%	0.28	139.4
	H-420-180	3.8	6.0%	0.22	136.1
	M-700-0	5.0	5.5%	0.25	141.6
	M-560-140	4.3	6.0%	-	136.6
	M-650-0	2.5	5.7%	0.23	142.4
	M-520-130	3.0	5.5%	-	139.7
	M-600-0	1.0	6.0%	-	140.5
	M-480-120	1.5	5.0%	-	139.6
	M-420-180	2.0	6.0%	0.24	138.1
	M-600P-0	0.8	5.5%	-	141.1
	M-480P-120	1.0	5.1%	-	140.5

	M-420P-180	1.5	5.9%	-	137.0
	L-700-0	2.3	6.0%	-	143.9
	L-560-140	1.8	5.0%	-	140.3
	L-650-0	1.0	6.0%	-	141.8
	L-520-130	1.0	5.0%	-	141.6
	L-600-0	1.0	5.5%	0.06	142.6
	L-480-120	0.8	5.5%	-	142.0
	L-420-180	1.0	5.2%	-	142.0
2020-13	H-700*-0	5.0	5.8%	0.29	144.5
	H-560*-140	3.5	5.0%	0.40	142.3
	H-650*-0	5.0	6.0%	0.13	140.9
	H-520*-130	2.2	5.2%	0.30	143.1
	H-600*-0	0.0	6.0%	-	142.2
	H-480*-120	4.0	6.0%	0.18	142.7
	H-420*-180	1.5	5.0%	0.24	142.7
	M-700*-0	3.7	5.5%	0.62	142.9
	M-560*-140	6.0	5.0%	0.74	142.1
	M-650*-0	2.5	6.0%	0.43	144.2
	M-520*-130	1.7	5.0%	0.41	145.8
	M-600*-0	1.0	5.6%	-	142.5
	M-480*-120	1.5	5.9%	0.53	144.4
	M-420*-180	1.0	5.1%	-	145.0
	L-700*-0	1.5	5.9%	0.20	144.5
	L-560*-140	0.5	5.7%	0.39	142.9
	L-650*-0	1.0	6.0%	0.42	144.2
	L-520*-130	0.5	5.3%	0.27	144.1
	L-600*-0	0.0	5.3%	-	142.2
	L-480*-120	0.0	5.6%	0.51	144.0
	L-420*-180	0.5	5.7%	-	144.0
	H-600C-0	2.2	6.0%	0.55	141.8
	M-600C-0	1.0	5.6%	0.38	143.6
	L-600C-0	0.5	6.0%	0.50	142.7

4.2.1 Slump

The results from each slump test are shown in Table 4.1 above. Going forward a direct comparison between the non-optimized mixtures from NCDOT project 2018-14 and 2020-13 will be shown and discussed. In general, the mixtures with optimized aggregate gradation had a lower slump than the non-optimized mixture with the slump decreasing for both as the w/cm ratio decreased. Several of the optimized mixtures had no or negligible slump when measured with those having a low w/cm (0.37) having the most mixtures which achieved low slump. All mixtures used for testing were deemed to have adequate workability to create properly consolidated specimens. While most of the least workable mixtures were those with lower w/cm ratios two mixtures with a high w/cm ratio, H-600*-0 and H-420*-180, also had a low slump. The only two optimized mixtures that did not require a WRA were H-700*-0 and H-560*-140 which achieved or exceeded the target slump. While six non-optimized mixtures required no WRA, H-700-0, H-560-140, H-650-0, H-520-130, H-600-0, and M-700-0. The difference between optimized and non-optimized mixtures can be seen in Table 4.2 below.

Table 4.2: Non-Optimized vs. Optimized Mixtures

Mixture ID	Slump (in)		Air		Unit Weight	
	Non-optimized	Optimized	Non-optimized	Optimized	Non-optimized	Optimized
H-700-0	8.0	5.0	5.2%	5.8%	137.1	144.5
H-560-140	8.0	3.5	5.2%	5.0%	136.4	142.3
H-650-0	6.5	5.0	6.0%	6.0%	141.4	140.9
H-520-130	7.0	2.2	5.5%	5.2%	138	143.1
H-600-0	2.5	0.0	5.8%	6.0%	138.7	142.2
H-480-120	3.0	4.0	6.0%	6.0%	139.4	142.7
H-420-180	3.8	1.5	6.0%	5.0%	136.1	142.7
M-700-0	5.0	3.7	5.5%	5.5%	141.6	142.9
M-560-140	4.3	6.0	6.0%	5.0%	136.6	142.1
M-650-0	2.5	2.5	5.7%	6.0%	142.4	144.2
M-520-130	3.0	1.7	5.5%	5.0%	139.7	145.8
M-600-0	1.0	1.0	6.0%	5.6%	140.5	142.5
M-480-120	1.5	1.5	5.0%	5.9%	139.6	144.4
M-420-180	2.0	1.0	6.0%	5.1%	138.1	145.0
L-700-0	2.3	1.5	6.0%	5.9%	143.9	144.5
L-560-140	1.8	0.5	5.0%	5.7%	140.3	142.9
L-650-0	1.0	1.0	6.0%	6.0%	141.8	144.2
L-520-130	1.0	0.5	5.0%	5.3%	141.6	144.1
L-600-0	1.0	0.0	5.5%	5.3%	142.6	142.2
L-480-120	0.8	0.0	5.5%	5.6%	142.0	144.0
L-420-180	1.0	0.5	5.2%	5.7%	142.0	144.0

4.2.2 Air Content

The results for the fresh air content of each mixture are shown in Table 4.2 above. While the SAM can provide a measure of the fresh air content fresh air content tests were done only with a Type B air meter. Due to the varying characteristics of each mixture the amount of AEA needed to meet the air requirements of 5.5% ± 0.5% varied between mixtures. The dosage of AEA required to meet air requirements varied between 0.06 – 0.76 fl oz/cwt. Eight optimized mixtures required a dose of AEA higher than the average dose given. Of these eight mixtures five utilized a fly ash replacement, seven had a low w/cm ratio (0.37), and seven required larger than average doses of WRA.

4.2.3 SAM Testing

All SAM testing was done in accordance with AASHTO TP 118. SAM testing was performed on every batch of every mixture. However, only the SAM test done on the batch used to create samples for freeze-thaw testing was be used in the analysis. Table 4.3 below shows all of the SAM numbers gathered from optimized graded aggregate mixtures.

Due to a limited amount of fresh concrete batched, each SAM test could only be performed once for each mixture. As a result of this when a SAM test had an error occur during the testing it was not able to be performed again without losing the ability to make all required samples so some mixtures do not have a SAM number. A more in-depth analysis of SAM numbers will be performed in section 4.4 of this document.

Table 4.3: SAM Numbers for Optimized Mixtures

Mixture ID	SAM
H-700-0	0.29
H-560-140	0.40
H-650-0	0.13
H-520-130	0.30

H-600-0	Error
H-480-120	0.18
H-420-180	0.24
M-700-0	0.62
M-560-140	0.74
M-650-0	0.43
M-520-130	0.41
M-600-0	Error
M-480-120	0.53
M-420-180	Error
H-600C-0	0.55
M-600C-0	0.38
L-600C-0	0.50
L-700-0	0.20
L-560-140	0.39
L-650-0	0.42
L-520-130	0.27
L-600-0	Error
L-480-120	0.51
L-420-180	Error

4.2.4 Unit Weight

The optimized gradation mixtures had a higher unit weight on average than their non-optimized counterpart mixtures. The optimized mixtures ranged from 140.9 pounds per cubic foot (pcf) to 145.8 pcf while having an average of 143.3 pcf. The non-optimized mixtures ranged from 136.1 pcf to 143.9 pcf and averaged 140.0 pcf. This variation within the unit weights is expected as the mixture proportions varies from mixture to mixture. The optimized gradation mixtures being a higher unit weight is also expected as they have a denser aggregate packing than the non-optimized gradation mixtures. The optimized gradation mixtures had 11 mixtures that were above average unit weight and of those, six utilized fly ash and five had the lowest w/cm ratio (0.37) used.

4.3 Testing of Hardened Concrete

This section will briefly present the results of mechanical tests performed on the optimized aggregate gradation mixtures. A more detailed version of this analysis along with different durability testing is available from a companion thesis prepared as part of NCDOT RP 2020-13 (Theilgard 2022).

4.3.1 Compressive Strength

This section will provide a summary of compressive test results from Theilgard (2022). A 28-day compressive strength of 4500 psi is required for paving and Type AA mixtures according to the NCDOT's 2018 Standard Specifications. Only H-420*-180 failed to reach this compressive strength out of all optimized gradation mixtures. This mixture is a 30 percent fly ash replacement, which can be slower to gain strength and did meet its 56-day strength requirement. Optimized and non-optimized mixtures were observed performing similarly on most compressive strength test dates and across each w/cm ratio used. The difference in compressive strength between optimized and non-optimized mixtures was more prevalent at the early age (3-day) with the non-optimized mixtures having a higher compressive strength on average with this difference lessening as the concrete samples aged (Theilgard 2022).

4.3.2 Modulus of Rupture (MOR)

Modulus of rupture testing was done at 28-days on pavement mixtures only and a more detailed analysis can be found in (Theilgard 2022). MOR ranged from 581 psi to 840 psi with an average of 715 psi for the optimized aggregate gradation mixtures. The non-optimized mixtures ranged from 715 psi to 822 psi with an average of 766 psi. All optimized mixtures passed the requirement of 650 psi except for H-420*-180 and M-

420*-180 which have a replacement level of 30 percent fly ash. In general, the optimized mixtures with 30 percent fly ash showed lesser MOR when compared to their non-optimized counterparts. The MOR of all optimized mixtures was lower than their non-optimized counterparts except for L-600-0 and L-480-120 (Theilgard 2022).

4.3.3 Modulus of Elasticity (MOE) and Poisson's Ratio

Modulus of elasticity was also tested on samples at 28 days of age with the optimized mixtures ranging from 2,894,000 psi to 4,932,000 psi with an average of 3,839,000 psi. The non-optimized mixtures had a range of 2,461,000 psi to 4,317,000 psi and an average of 3,323,000 psi. The samples with a lower w/cm ratio tended to be higher MOE than those of a higher w/cm ratio. The MOE gathered from testing showed every fly ash mixture besides M-560*-140 and L-560-140 as being lower than their straight cement mixture counterpart (Theilgard 2022).

Poisson's ratios for optimized mixtures ranged from 0.14 to 0.24 with an average of 0.19 while, non-optimized mixtures ranged from 0.17 to 0.24 and an average of 0.20. Optimized mixtures showed a noticeable difference when looking at cementitious content of 650 pcy while those that had 700 pcy and 600 pcy showed a difference of less than 10 percent when compared to the non-optimized mixtures. This could be skewed by two mixtures in the 650 pcy of cementitious content mixtures as M-650*-0 achieved a 0.14 and L-520*-130 had a Poisson's ratio of 0.15.

4.4 Durability Testing

This section provides an overview of the durability testing results for all previously mentioned projects rather than just RP 2018-14 and RP 2020-13. This testing includes SAM testing, freeze-thaw durability testing, and spacing factor. As some mixtures do not have all data points for every test, the results will use all available data points. Test results will be compared to specification targets proposed by AASHTO PP 84 (AASHTO R 101-22) and previous research studies completed for NCDOT. As spacing factor, freeze-thaw durability factor, and the SAM number have an established correlation, due to previously completed work, all three will need to be looked at together to form a cohesive analysis. Table 4.4 below lists all mixtures used in the analysis of this thesis as well as the durability characteristics found for each mixture along with the mass loss (%) which is used in ASTM C666 as a factor in stopping the testing. As stated by Peter Theilgard in his companion thesis for this research:

> It should again be noted that the high (0.47) w/cm ratio mixtures were originally batched as non-optimized aggregate gradation mixtures to provide test results that are indicative of poor concrete mixtures that are not typical to NCDOT use. Optimized aggregate gradation concrete mixtures at the high w/cm ratio were batched and tested for a direct comparison between the optimized and non-optimized aggregate gradation mixtures. However, as these mixtures are representative of a higher w/cm ratio than typical NCDOT concrete mixtures, these results may not be as valuable (Theilgard 2022).

Table 4.4: Durability Characteristics for all Mixtures

Project Number	Mixture ID	Df	Mass Loss (%)	SAM	SF (in.)	SF (μm)
2015-03	Piedmont based coarse aggregate					
	PANM	95.73	-0.08%	0.19	0.0212	539
	PAAM	95.59	0.79%		0.0217	552
	PABM	94.65	1.51%	0.29	0.0313	794
	PANN	81.7	0.94%	0.1	0.0239	608
	PBLNM	100.06	-0.27%	0.28	0.0409	1040
	PBLBM	94.34	1.11%	0.19	0.0175	444
	PBLAM	94.65	2.43%	0.29	0.02	508
	PBLNN	74.2	1.60%	0.19	0.016	407
	PBAM	95.9	1.25%	0.42	0.0196	497
	PBBM	94.65	0.72%	0.22	0.0179	454
	PBNM	98.02	-0.29%	0.23	0.0217	551
	PBNN	81.03	1.09%	0.27	0.0221	560

	Coastal based coarse aggregate					
	CANM	96.63	0.52%		0.0186	472
	CBNM	99	-0.09%	0.35	0.0215	545
	CBLNM	98.99	0.00%	0.19	0.0187	474
	Mountain based coarse aggregate					
	MANM	77.92	1.41%		0.0413	1048
	MBNM	78.69	2.22%		0.0226	575
	MBLNM	79.52	2.48%		0.0198	503
2016-06	Conventional concrete, no fly ash					
	CC	85.22	-0.39%	0.32	0.0243	617
	Internally cured concrete, no fly ash					
	I1M	88.39	-0.17%	0.4	0.0211	536
	I2M	100.96	0.23%	0.12	0.0219	557
	I1H2*	91.67	-0.20%	0.24	0.0215	546
	I2H	83.8	-0.48%	0.39	0.0323	821
	Internally cured pavement mixture					
	IP	84.39	0.66%	0.3	0.0138	351
	Conventional concrete, fly ash					
	CF	80.15	-0.29%	0.3	0.0221	560
	Internally cured concrete, fly ash					
	I1MF	87.2	-0.23%	0.25	0.016	408
	I2MF	38	1.57%	0.19	0.0242	615
	I1HF	83.19	0.39%	0.29	0.0196	497
	I2HF 2	52.26	2.99%	0.27	0.023	585
2018-14	H-series (high w/cm ratio, 0.47)					
	H-560-140			0.19	0.0228	580
	H-650-0			0.38	0.0227	576
	H-480-120			0.28	0.0111	281
	H-420-180			0.22	0.0167	424
	M Series (moderate w/cm ratio, 0.42)					
	M-700-0			0.25	0.0237	601
	M-650-0			0.23	0.0208	528
	M-420-180			0.24	0.0159	403
	L Series (low w/cm ratio, 0.37)					
	L-600-0			0.06	0.0196	499
2020-13	H-series (high w/cm ratio, 0.47)					
	H-700*-0	103.46	1.22%	0.29		
	H-560*-140	105.19	0.96%	0.4	0.0246	626

	H-650*-0	103.46	1.12%	0.13	0.0209	532
	H-520*-130	101.73	1.03%	0.3	0.0204	519
	H-600*-0	100	2.05%		0.0236	599
	H-480*-120	103.46	1.93%	0.18	0.0158	402
	H-420*-180	103.46	1.22%	0.24	0.0209	530
	M Series (moderate w/cm ratio, 0.42)					
	M-700*-0	100	1.28%		0.022	559
	M-560*-140	93.65	1.08%		0.026	660
	M-650*-0	103.25	-0.15%	0.43	0.0156	395
	M-520*-130	100	2.30%	0.41	0.0205	520
	M-600*-0	100	1.93%		0.0124	315
	M-480*-120	100	3.20%	0.53	0.0116	295
	M-420*-180	100	3.49%		0.0197	502
	L Series (low w/cm ratio, 0.37)					
	L-700*-0	100	0.98%	0.2	0.031	786
	L-560*-140	96.83	0.54%	0.39	0.0226	574
	L-650*-0	100	0.17%	0.42	0.0208	529
	L-520*-130	106.5	0.41%	0.27	0.0195	496
	L-600*-0	100	1.37%		0.0214	544
	L-480*-120	98.53	0.50%	0.51	0.0205	520
	L-420*-180	100	3.20%		0.0206	523
	CNT Series, containing carbon nanotube mixtures, w/cm designated H, M, L as defined above					
	H-600C-0	96.71	1.77%	0.55	0.0157	400
	M-600C-0	100	0.11%	0.38	0.0248	630
	L-600C-0	98.9	0.15%	0.5	0.0197	500
	CNT Series, containing carbon nanotube mixtures, w/cm designated H, M, L as defined above contains Non-Optimized Aggregate Gradation					
	HNO-600C-0	95.06	0.57%		0.031	788
	MNO-600C-0	95.06	0.31%		0.0176	447
	LNO-600C-0	100	0.09%		0.0241	612

All SAM numbers of 0.60 or greater were discarded as these were found to be more likely the result of a leak during testing then a true SAM number. AASHTO TP 118-17 recommends a range of 0.01 to 0.82 for acceptable SAM numbers so to ensure the integrity of the SAM testing was upheld a more conservative threshold of 0.60 was used as the upper limit.

4.4.1 Fresh Air

As mentioned previously, the research study supporting this effort was configured to support evaluation of optimized aggregate gradation concrete mixtures and identification of performance targets for multiple PEM tests, including surface resistivity and shrinkage in addition to SAM. To support these objectives, a range of 5.5% ± 0.5% air was chosen as the required range for all mixtures tested as part of this project, as NCDOT specifications for concrete is 5.0% ± 1.5%. As such, the fresh air contents for mixtures produced as part of this project were limited to a tight range (5 to 6%) to minimize the variation in the mechanical properties and durability performance test results both within this current project and between projects. The range of 5.0% to 6.0% air should encompass most mixtures being accepted on job sites across North Carolina's highway system.

With such a narrow band of fresh air encompassed by the project mixtures the spacing factors associated with these air contents are also a narrower band then in other projects dealing with the SAM. Therefore, it is likely that the limited range of air contents allowed in most mixtures included in this work did not allow for the full spectrum of spacing factors seen in similar evaluations of the SAM or hardened air void systems. Nevertheless, this chapter presents an analysis of the air void systems of a range of NCDOT structural and pavement concrete mixtures, comparing test results of different mixtures to one another and to published data on air void systems from other state DOT and FHWA research studies.

4.4.1.1 Fresh Air vs. Spacing Factor

Figure 4.1 shows a downward trend of the spacing factor as the fresh air % increases. This is consistent with findings of other researchers. When Figure 4.1 is compared to a similar figure from Ley et al. (2017) a trend in the spacing factor decreasing as the percentage of fresh air increases can be observed. If a wider ranging fresh air content had been allowed in these studies, a broader range of spacing factor values may have been provided and the trend could have potentially been more strongly exhibited.

Figure 4.2 shows the spacing factor in μm for a better comparison to the graph published by Ley et al. (2017). This modified graph uses the same unit of measurement for the spacing factor as well as the same air percentages to show the band of air percentages being used for this project. Figure 4.3 shows two mixtures chosen by Ley et al. (2017) to show case the correlation between fresh air percentage and the spacing factor.

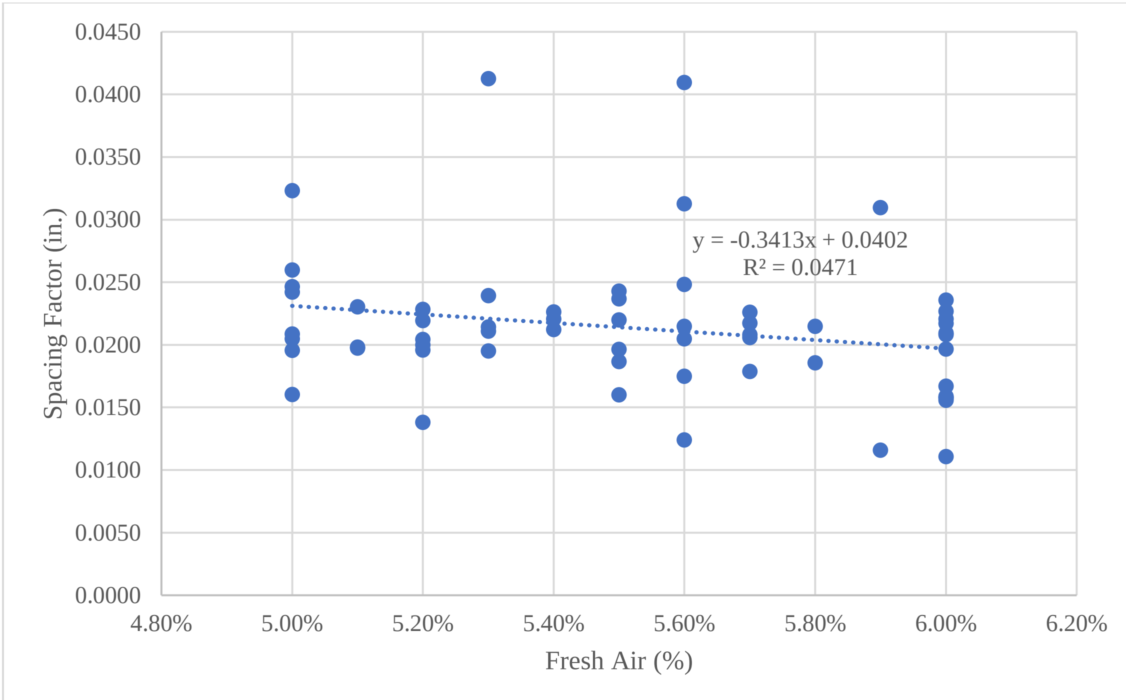

Figure 4.1: Fresh Air (%) vs. Spacing Factor (in.)

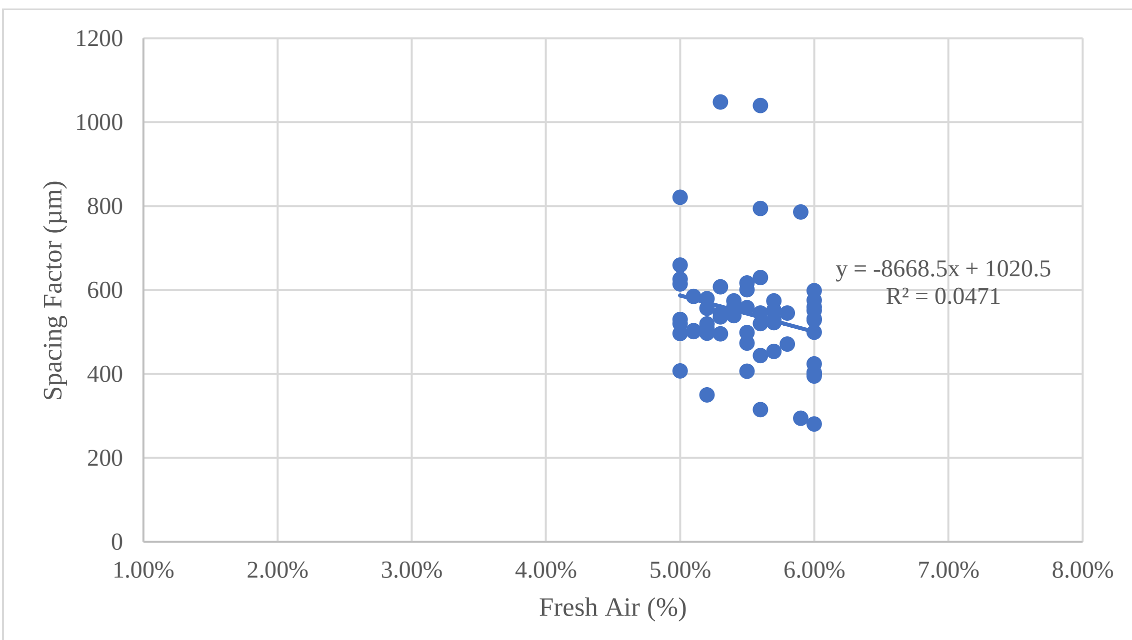

Figure 4.2: Fresh Air (%) vs. Spacing Factor (μm)

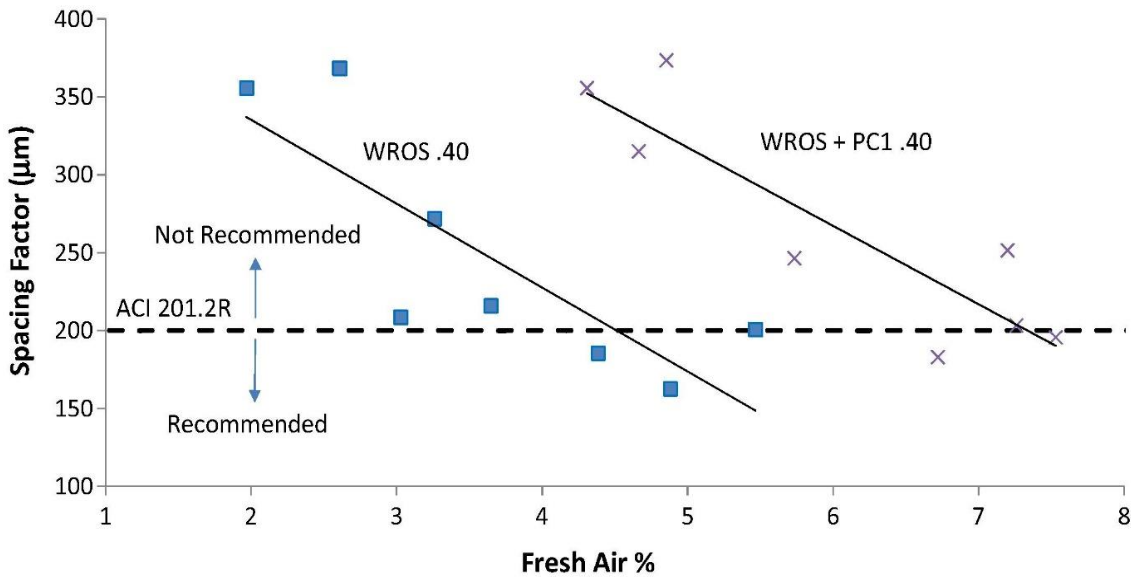

Figure 4.3: OSU Fresh Air (%) vs. Spacing Factor (μm) (Ley et al. 2017)

To further explore whether the data obtained as part of this NCDOT study align with that obtained by OSU, the data provided in the Appendix of Ley et al. (2017) was mined and plotted. Data from this NCDOT-funded study was then plotted with the data from Ley et al. (2017) in the same figure to facilitate comparison. The first of these graphs is shown below in Figure 4 comparing the data obtained from the OSU data sets and comparing it to the data obtained from this NCDOT project. As seen in Figure 4.4 below the data gathered from this NCDOT study are contained fully within an air content range of 5% to 6%. While the spacing factors from some NCDOT mixtures are within the range seen in the OSU data most mixtures spacing factors are between 2 and 3 times the average seen by the data plotted from Ley et al. (2017).

There are several factors that could be affecting the difference in spacing factors seen between the data provided by Ley et al. (2017) and the NCDOT projects such as different AEAs used, using a different class of fly ash, and differing WRAs being used for the different studies. Determining the causes of the general increase in spacing factor was not within the scope of this study and as such will not be evaluated at this time.

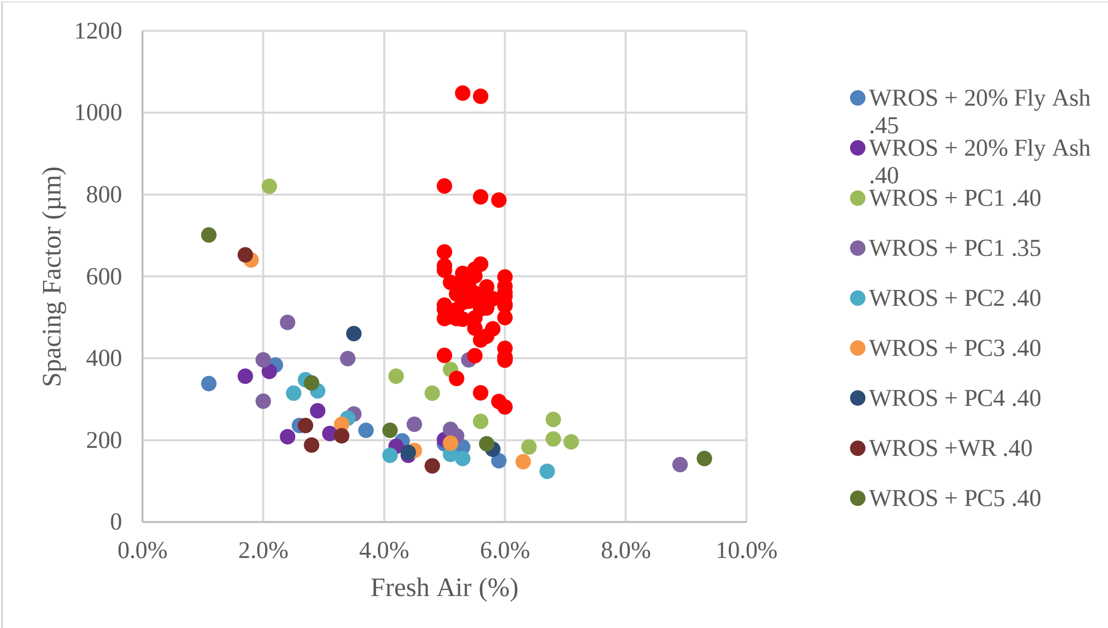

Figure 4.4: Fresh Air (%) vs. Spacing Factor (µm) – OSU data from Appendix of Ley et al. (2017) with NCDOT mixtures overlaid (red data markers)

For similar mixtures dispersion in the SAM numbers could be attributed to the change in users, change in SAM device, different temperatures, or changes in cementitious material chemistry. Interactions between the admixtures may also have coarsened the air voids system, causing larger air bubbles and therefore larger spacing factors.

For the mixtures included in this study, the rodding procedure was used to consolidate the concrete into the base of the SAM unit. In recent years, the developer of the SAM has recommended a vibration procedure that could potentially be used to improve the quality of SAM data collected. A daily leak check procedure has also been developed recently and could also be used to improve the accuracy of SAM measurements.

4.4.1.2 Fresh Air vs. Durability Factor

Figure 4 is a plot from Ley et al. (2017) showing the fresh air content of selected mixtures plotted against the durability factor of the mixtures obtained during freeze thaw testing. The data plotted in Figure 4.5 are for mixtures containing an air entraining admixture (WROS) and an air entraining admixture and a water reducer (WROS + PC1), respectively. Note that in Figure 4.5, “Recommended” and “Not Recommended” are targets established by OSU for use in their work and do not reflect the current targets of NCDOT or the targets used by a number of other agencies, which range from 60 to 80%.

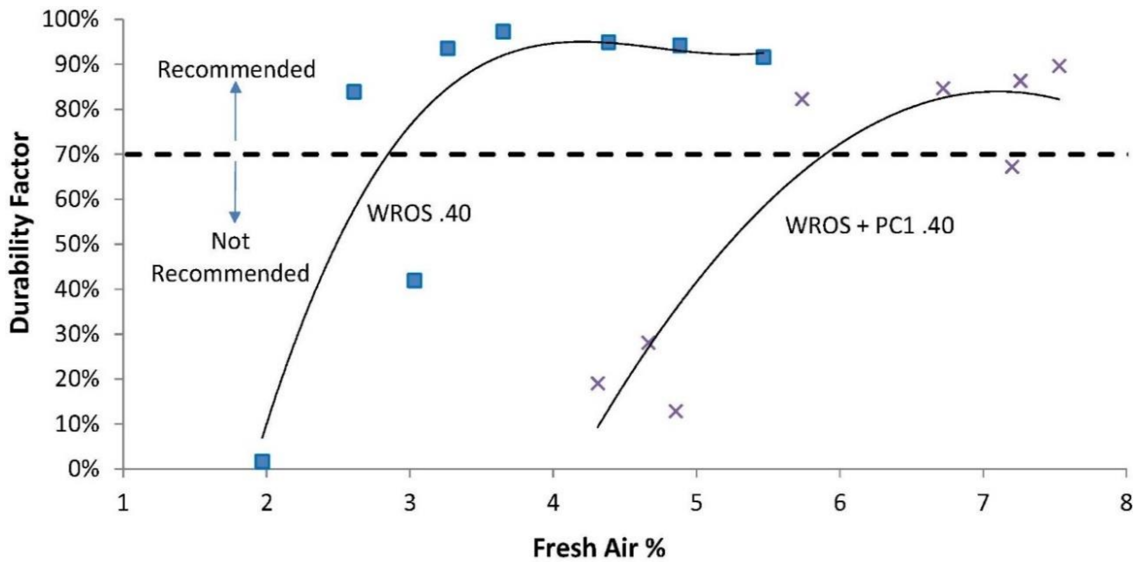

Figure 4.5: Ley et al. (2017) Fresh Air (%) vs. Durability Factor

Figures 4.6 and 4.7 show similar plots of the NCDOT mixtures included in this study, with the durability factor of each mixture plotted against the measured percentage of fresh air. When compared to Figure 4.8 (data collected by Ley et al. (2017)) several trends become apparent. One trend setting the NCDOT mixtures batched and tested for this project apart from the OSU data is the fact that NCDOT mixtures exhibited particularly good durability performance in this test. In fact, only two NCDOT mixtures included in this analysis had durability factors lower than the recommendation provided by Ley et al. (2017), while only six NCDOT mixtures fell below a more conservatively recommended durability factor of 80. In both graphs there is a trend upwards in the durability factor as the fresh air content percentage increases, as could be expected.

Figure 4.7 shows the same data from Figure 4.6 with the same range of fresh air percentage used in the graphs created by Ley et al. (2017) to show a more accurate comparison between the sets of data.

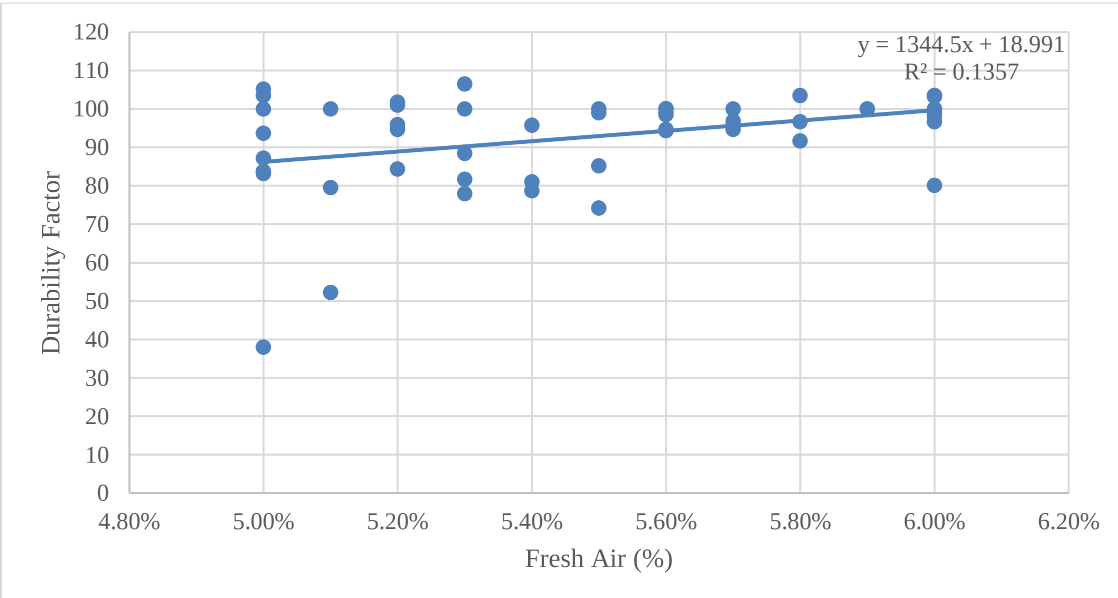

Figure 4.6: Fresh Air (%) vs. Durability Factor

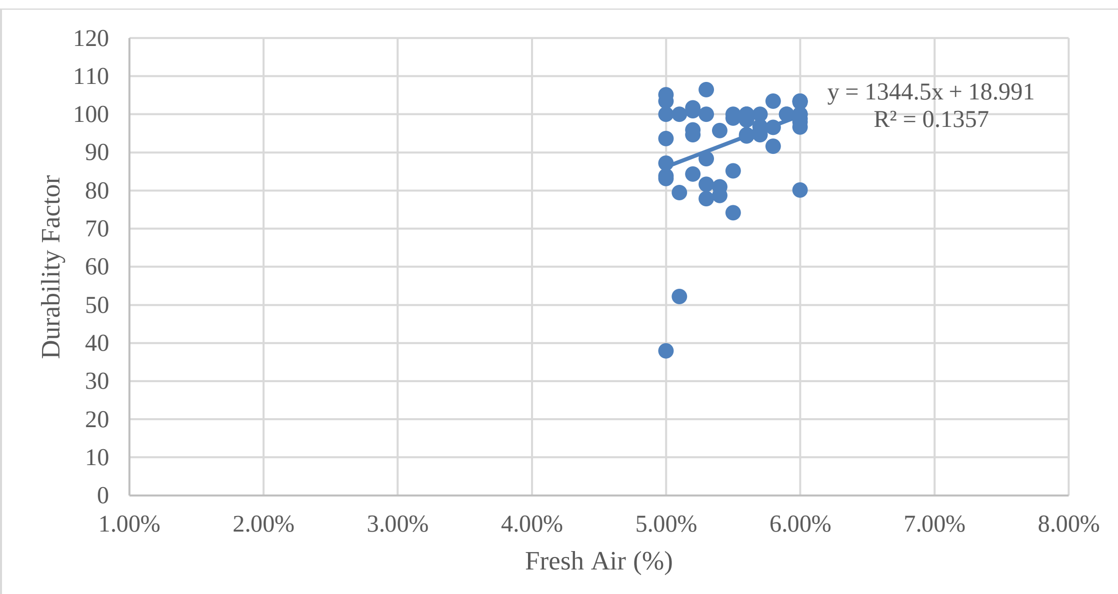

Figure 4.7: Fresh Air (%) vs. Durability Factor

Figure 4.8 shows the selected mixtures from OSU's data along with how those data points tended as the fresh air percentage increased. As can be observed in Figure 4.8, the durability factor generally increased as the fresh air percentage increased, which correlates with the general understanding that an adequate quantity of void space is needed to provide freeze thaw durability. The mixtures all follow a similar trend except for OSU's WROS + PC1.40. This trend is an increase in the durability factor as the fresh air percentage increases. The same trend can be seen on a condensed scale (mixtures containing only 5-6% air) for the mixtures included in this project. Figure 4.9 shows test results for several different mixtures batched and tested as part of this project, comparing the fresh air percentage measured to the durability factor from data points contained within the Appendix of Ley et al. (2017).

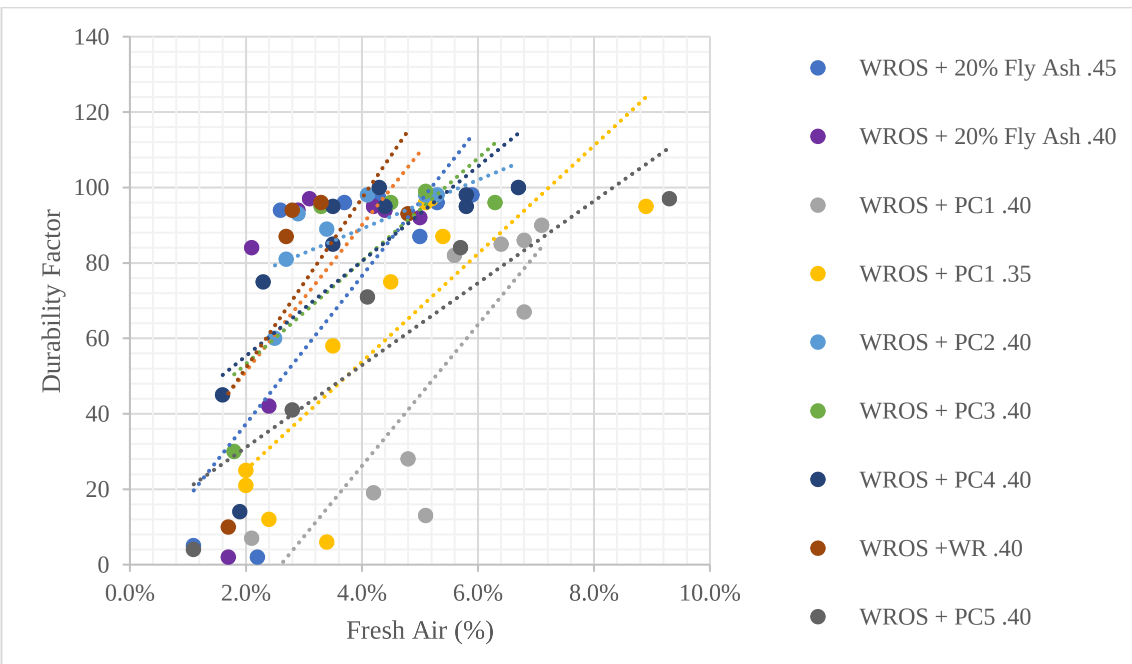

Figure 4.8: Fresh Air (%) vs. Durability Factor – OSU data from Appendix of Ley et al. (2017)

The test results for mixtures used for this NCDOT project have been overlayed on the test results of the mixtures used by Ley et al. in Figure 4.9. The NCDOT mixtures used for this project (plotted using red markers in Figure 4.9) align well with the OSU data based on the expectations from the data provided by Ley et al. (2017) in this category.

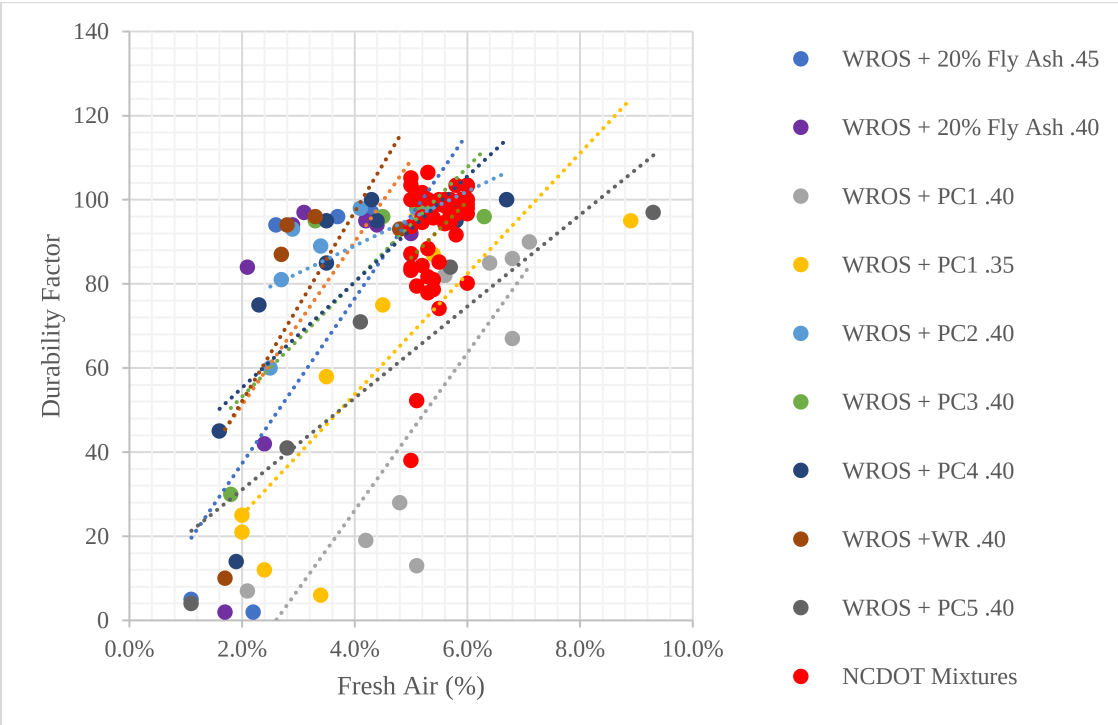

Figure 4.9: Fresh Air (%) vs. Durability Factor – OSU data from Appendix of Ley et al. (2017) with NCDOT mixtures overlaid (red data markers)

4.4.1.3 Fresh Air vs. SAM Number

Figures 4.10 and 4.11 below show the general trend seen in the data acquired from the NCDOT mixtures. The general trend observed shows a slight increase in the SAM number as the fresh air percentage increases. Figure 4.11 displays the same data that is shown in Figure 4.10; however, the data is plotted using the same x and y axis ranges as the data from OSU. As previously stated, the mixtures used for all NCDOT project analysis were designed with mechanical properties and other durability concerns in mind. This focus on particular properties, along with a guiding criterion of maintaining a tight air content range to facilitate comparisons of mixture properties/test performance without undue effects of air content, has left the range of fresh air allowed as a very narrow range when compared to the OSU data. Based on the limitations of this dataset, and the dispersion that could be expected based on the wide range of mixtures tested, the poor correlation shown in Figure 4.11 could be expected.

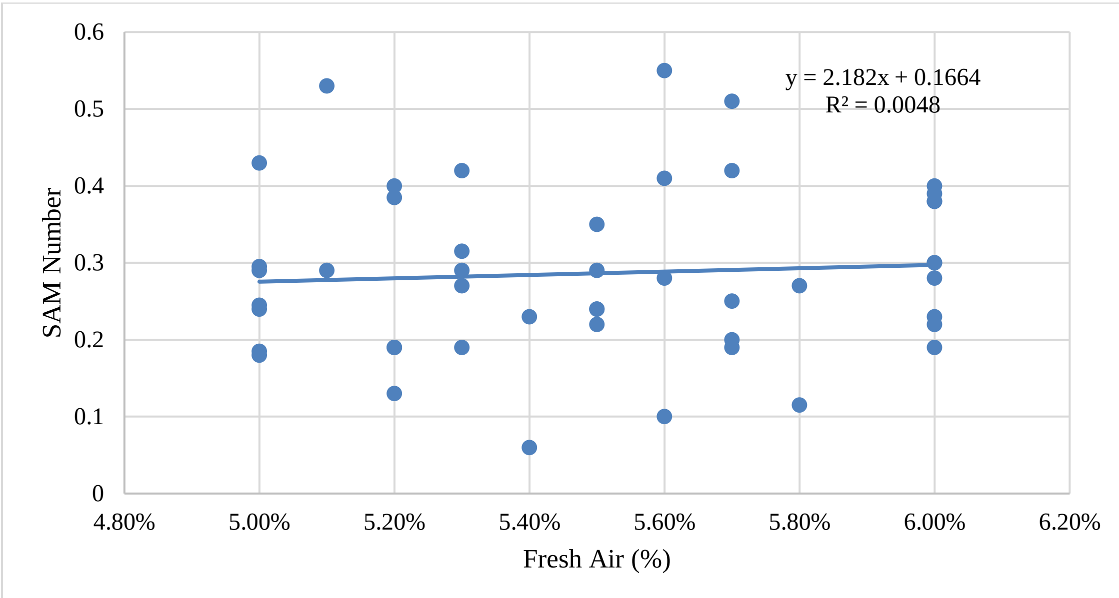

Figure 4.10: Fresh Air (%) vs. SAM Number

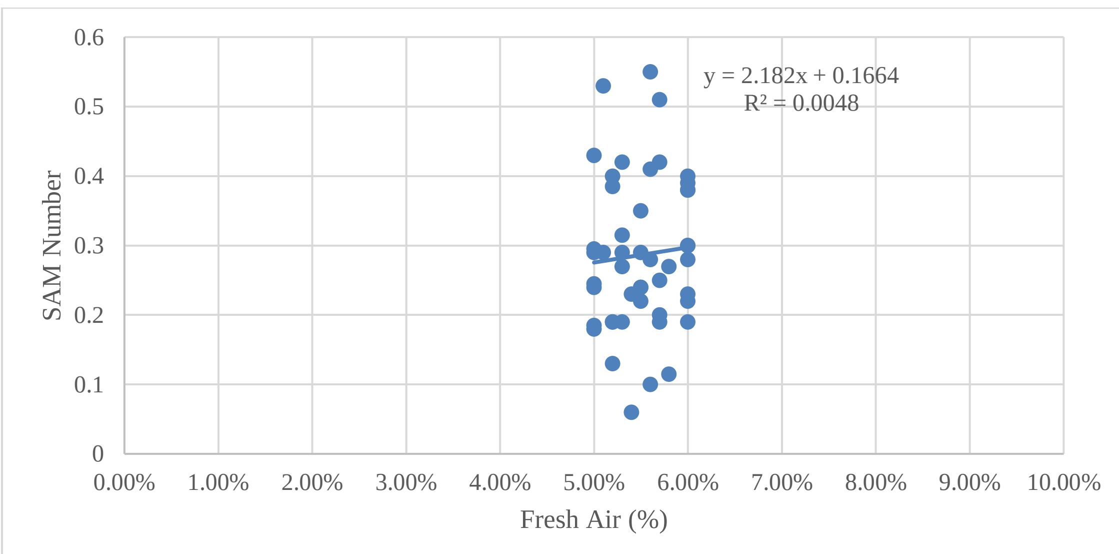

Figure 4.11: Fresh Air (%) vs. SAM Number

As can be seen in Figures 4.10 and 4.11, a fairly wide range of SAM numbers was measured for mixtures containing between 5 and 6% air content. This variability in the data may be the result of issues arising from use of the device (such as leaks), variability induced by different mixtures, materials, operators, environmental conditions, or other reasons. A report by Riding and Albahttiti (2016) found that between one SAM test to the next within the same site the coefficient of variation was 154% higher than that of the air content tests on average. Overall, the SAM test had a coefficient of variation of 56% throughout all of the samples taken while the air content had a coefficient of variation of 22% (Riding and Albahttiti 2016). The number of SAM operators used to collect this dataset is estimated to be approximately 10 people, likely contributing to the dispersion of the data. Although some users received training from the SAM developer, others learned via the online videos or from other users. Many agencies have reported improved results after additional training from the developer (Hall et al. 2019), and it is acknowledged that the change in user and device played a role in the dispersion observed in the data.

Figure 4.12 shows a trend for the SAM number to decrease significantly as fresh air contained within the fresh concrete increased. This does not match the trend observed in the NCDOT project's mixtures being graphed as can be seen in Figure 4.13. Figure 4.13 displays the test results for the NCDOT mixtures used in this project (red data markers) along with the OSU data from Ley et al. (2017). In this figure the narrow band of air content contained by the NCDOT mixtures can be observed in the middle of the graph while the data from OSU spreads out from approximately 1% to 10% air measured while the concrete was in a fresh state. As stated above, variability in the data obtained from testing of the NCDOT mixtures may be from a variety of sources. It is noted, however, that the spacing factors measured for the NCDOT mixtures were also greater than those obtained by Ley et al. (2017), and the increase in measured SAM number could therefore be expected.

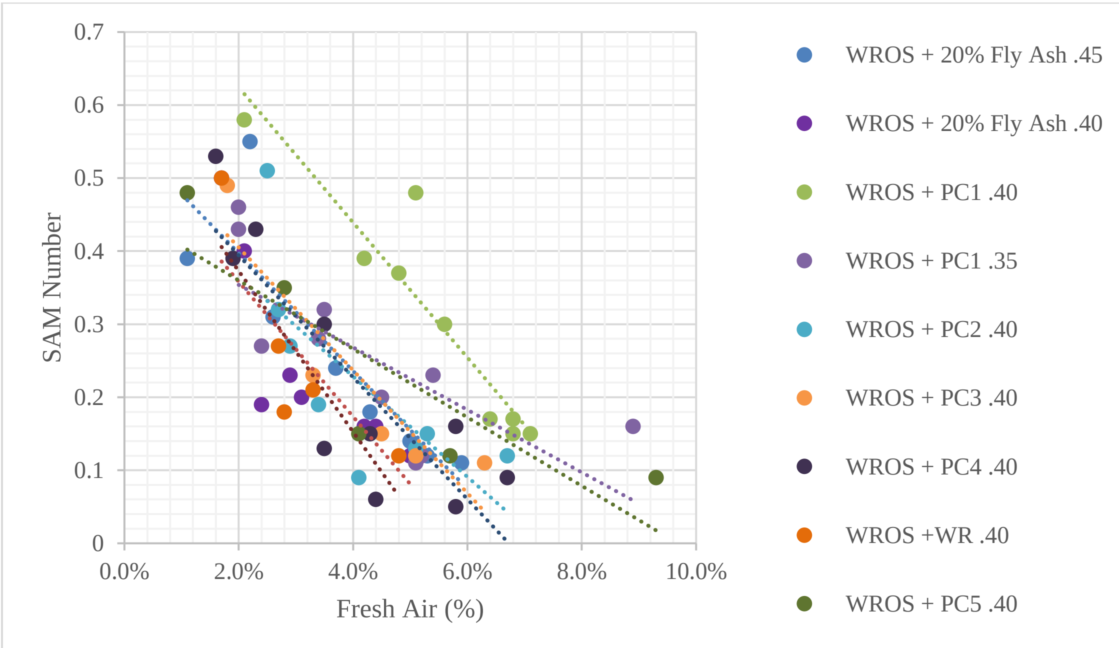

Figure 4.12: Fresh Air (%) vs. SAM Number - OSU data from Appendix of Ley et al. (2017)

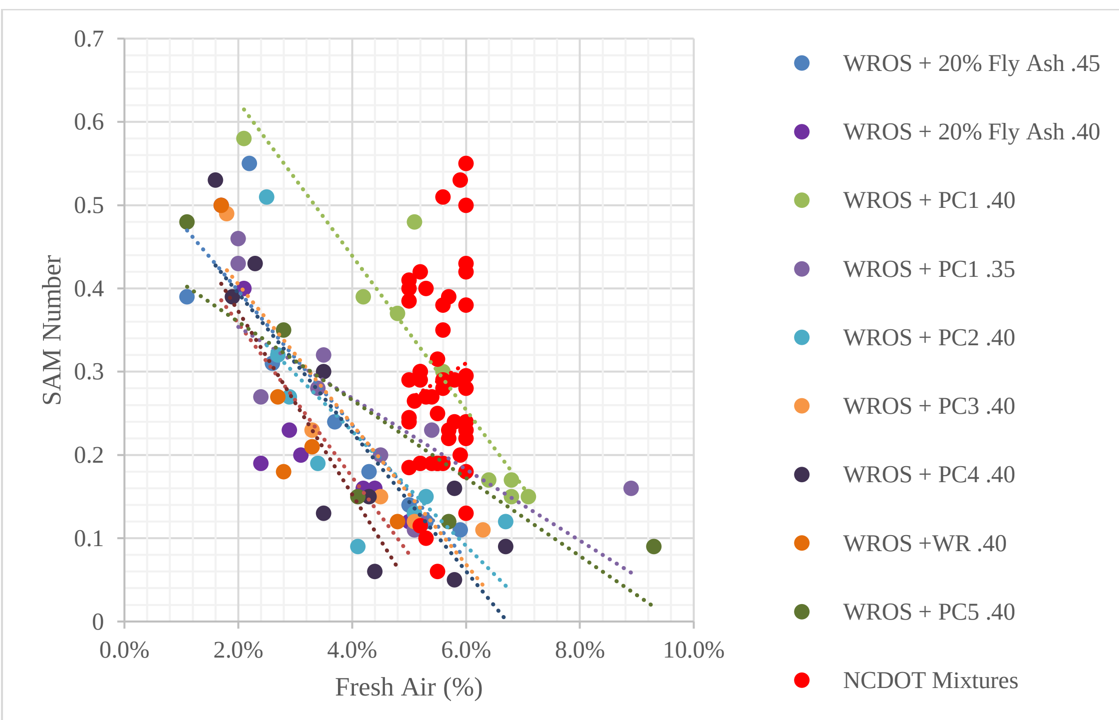

Figure 4.13: Fresh Air (%) vs. SAM Number - OSU data from Appendix of Ley et al. (2017) with NCDOT mixtures overlaid (red data markers)

4.4.2 Spacing Factor

ASTM C457 testing was performed on two samples cast in cardboard take-out food containers once the specimen was sufficiently aged to resist the forces encountered by sawing the sample in half. Of the 65 samples which had a spacing factor calculated, 29 were above the average of 0.0213 in. Of the samples which had above the average spacing factor 8 of 29 utilized fly ash while the variable w/cm ratio mixtures from 2018-14 and 2020-13 accounted for 10 of the 29 mixtures.

Previously in this document, the spacing factor was examined in comparison with the air percentage measured in fresh concrete. In this section of the document the spacing factor is compared to the durability factor and SAM number. Figure 4.14 shows the spacing factor (µm) graphed against the durability factor using data from Ley et al. (2017). In this graph the durability factor can be seen to decrease rapidly in the space between 200 µm and 400 µm with most mixtures at or before 200 µm having a durability factor above 80. The mixtures measured with a spacing factor of above 200 µm rapidly descend in the durability factor measured until they hit a general low at 400 µm and above with only random mixtures displaying a durability factor above 80 and the majority of mixtures being measured below 40. Figure 4.15 shows the same data from Figure 4.14 with NCDOT mixtures overlaid in red showing how few of the NCDOT mixtures failed ASTM C666. Note that the data shown with hollow red markers is from RP 2020-13 specimens where the durability factor was measured to be slightly greater than 100 due to the oscilloscope settings used.

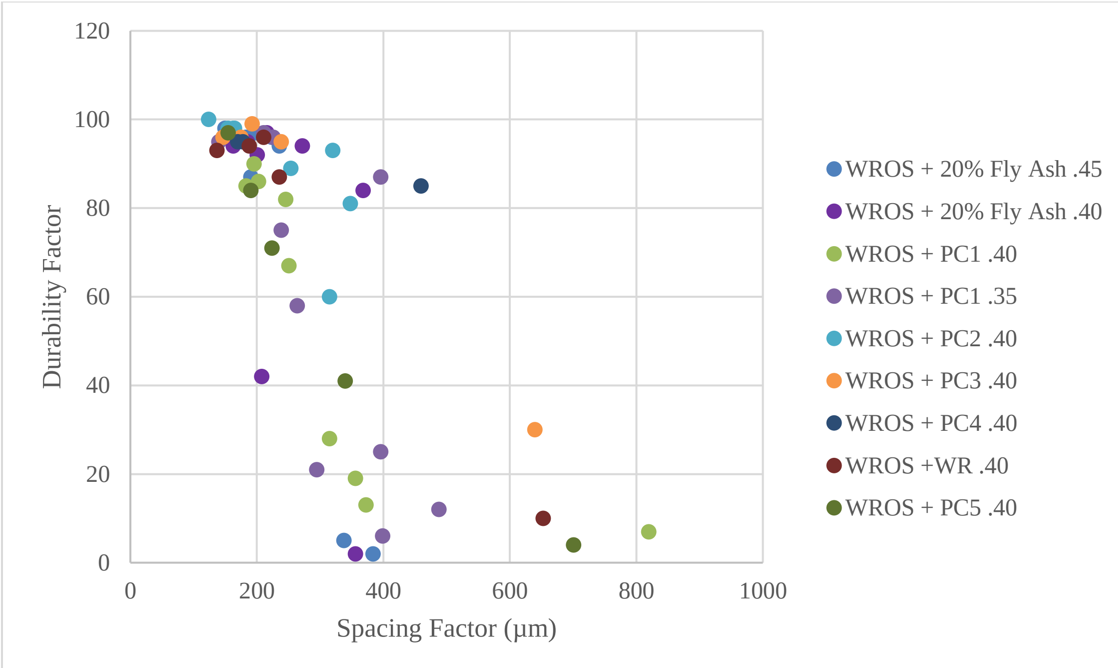

Figure 4.14: Spacing Factor (µm) vs. Durability Factor - OSU data from Appendix of Ley et al. (2017)

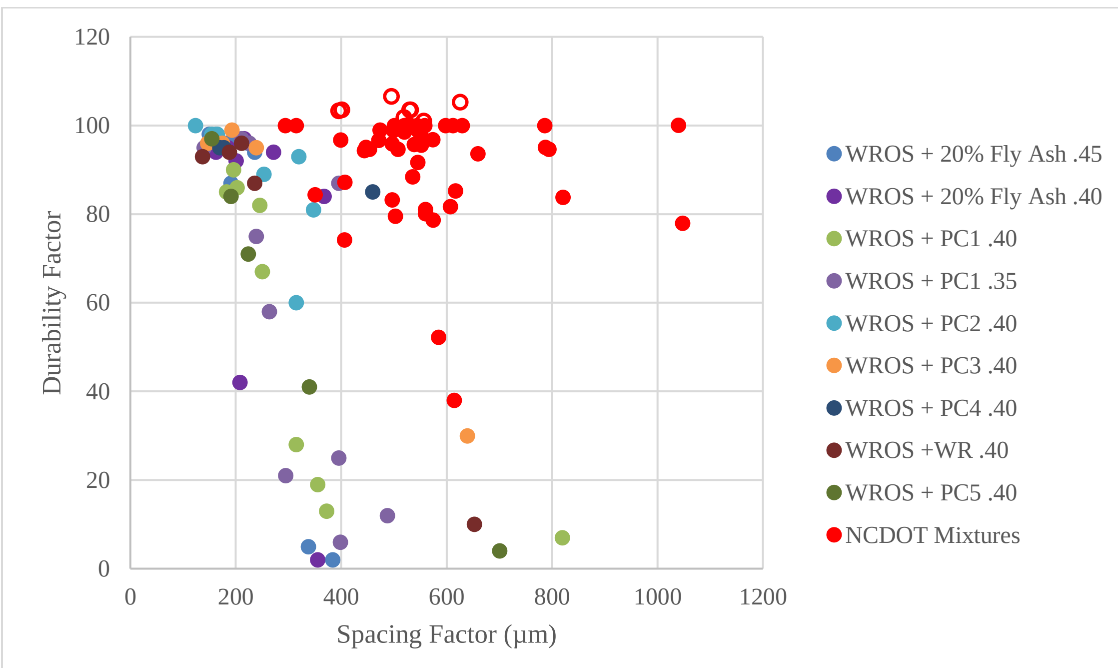

Figure 4.15: Spacing Factor (µm) vs. Durability Factor - OSU data from Appendix of Ley et al. (2017) with NCDOT mixtures overlaid (red data markers)

The data provided by OSU shows what seems to be a strong correlation between the SAM number and the spacing factor (µm) measured with the spacing factor increasing as the SAM number also increases. Figure 4.16 published by Ley et al. (2017)

shows two mixtures compared against each other one of which contains a superplasticizer (PC) while the other only contains a wood rosin AEA (WROS). While one mixture contains a superplasticizer the two have similar results when graphed. Figure 4.17 shows all of the data obtained by Ley et al. (2017) including data from FHWA labs and data obtained in the field rather than a lab. This data still demonstrates a strong correlation between the SAM number and the spacing factor.

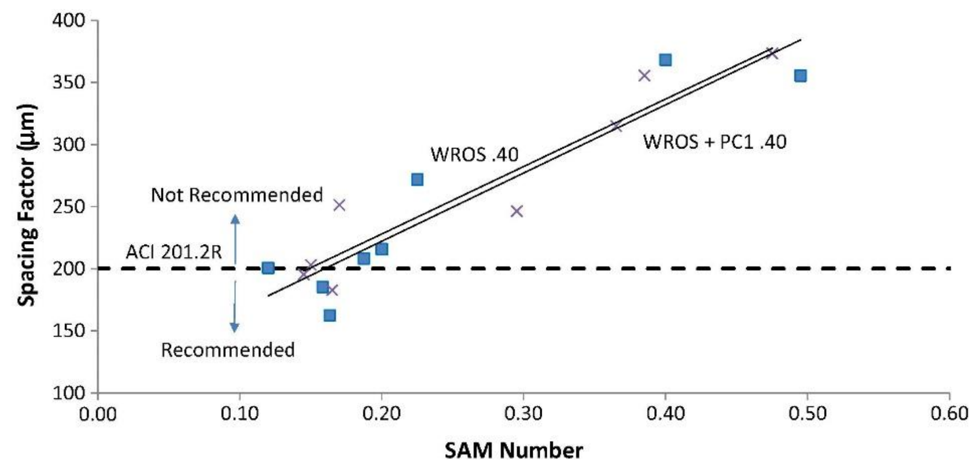

Figure 4.16: OSU SAM Number vs. Spacing Factor (µm) select mixtures (Ley et al. 2017)

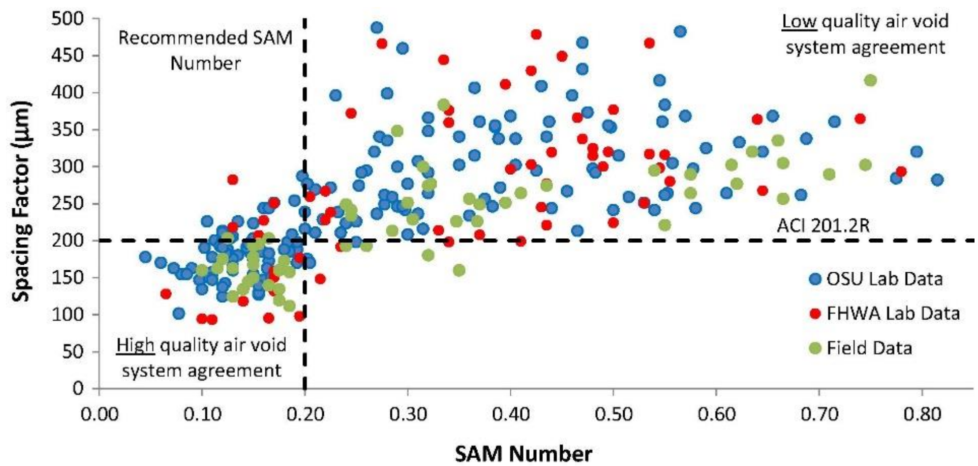

Figure 4.17: OSU SAM Number vs. Spacing Factor (µm) select mixtures (Ley et al. 2017)

Even without the field and FHWA data shown in Figure 4.17 the data obtained from OSU shows a general trend of increasing spacing factor as the SAM number increases as seen in Figure 4.18. The data found from the NCDOT mixtures (shown with red markers in Figure 4.19) notably exhibits spacing factors being higher in general when compared to the data acquired from OSU. This correlates with work by Ojo (2018) using mixtures with North Carolina materials.

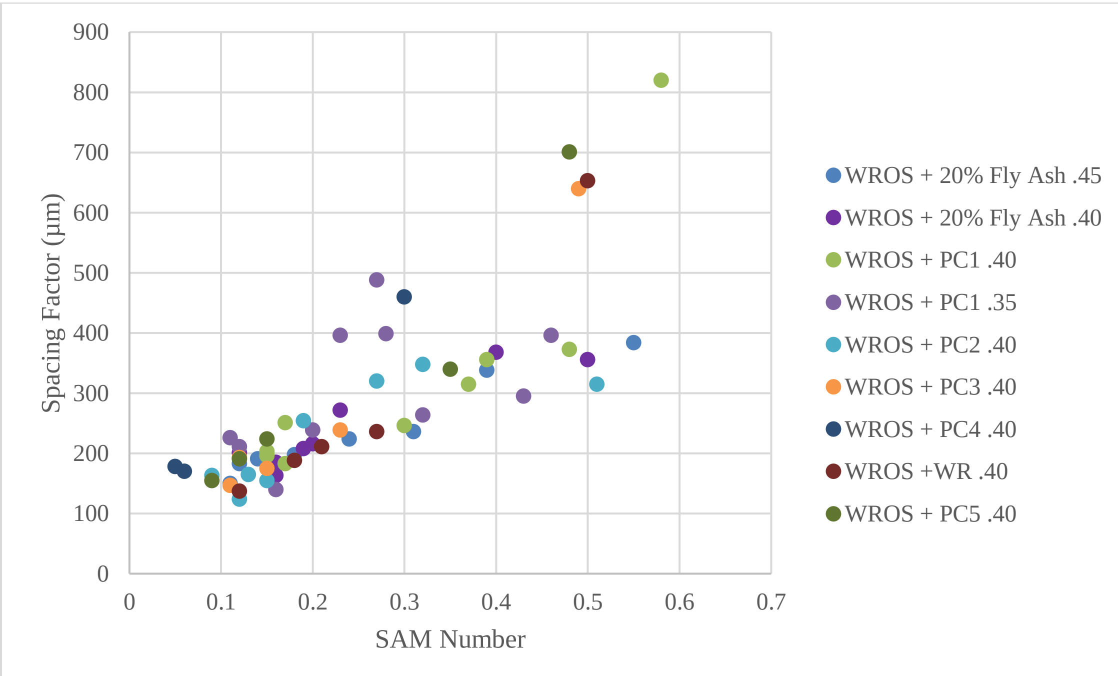

Figure 4.18: SAM Number vs. Spacing Factor (µm) - OSU data from Appendix of Ley et al. (2017)

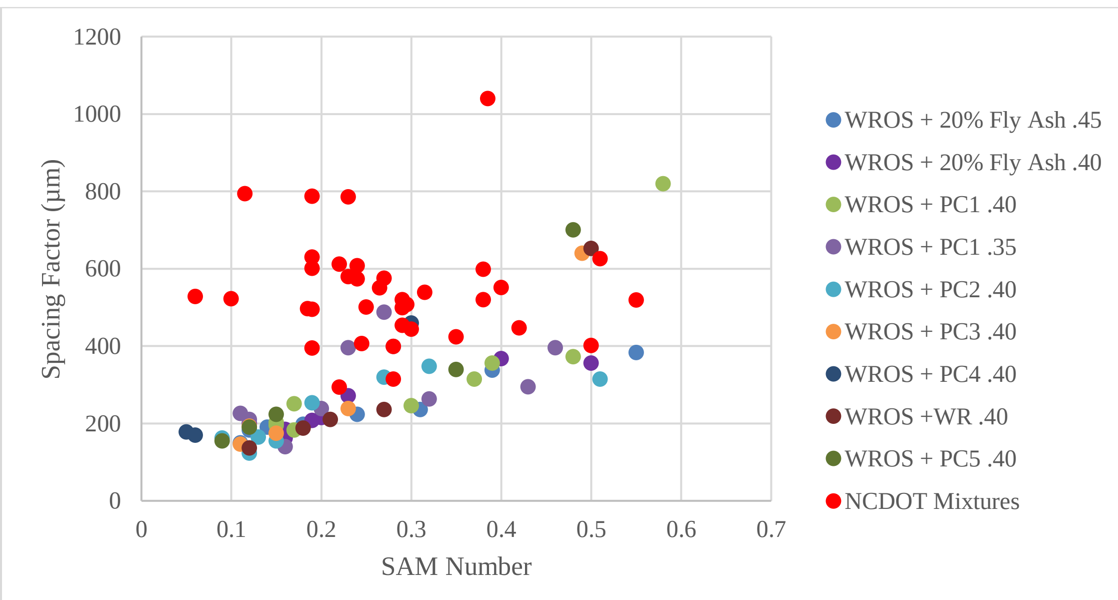

Figure 4.19: SAM Number vs. Spacing Factor (µm) - OSU data from Appendix of Ley et al. (2017) with NCDOT mixtures overlaid (red data markers)

Figure 4.20 shows the SAM number plotted against spacing factor for a study completed for a private entity using NCDOT mixtures. It is noted that some mixtures contained fly ashes that did not meet ASTM C168 in several mixtures. These mixtures appear to relate more closely to what the data from OSU suggests is the relationship between the SAM number and spacing factor.

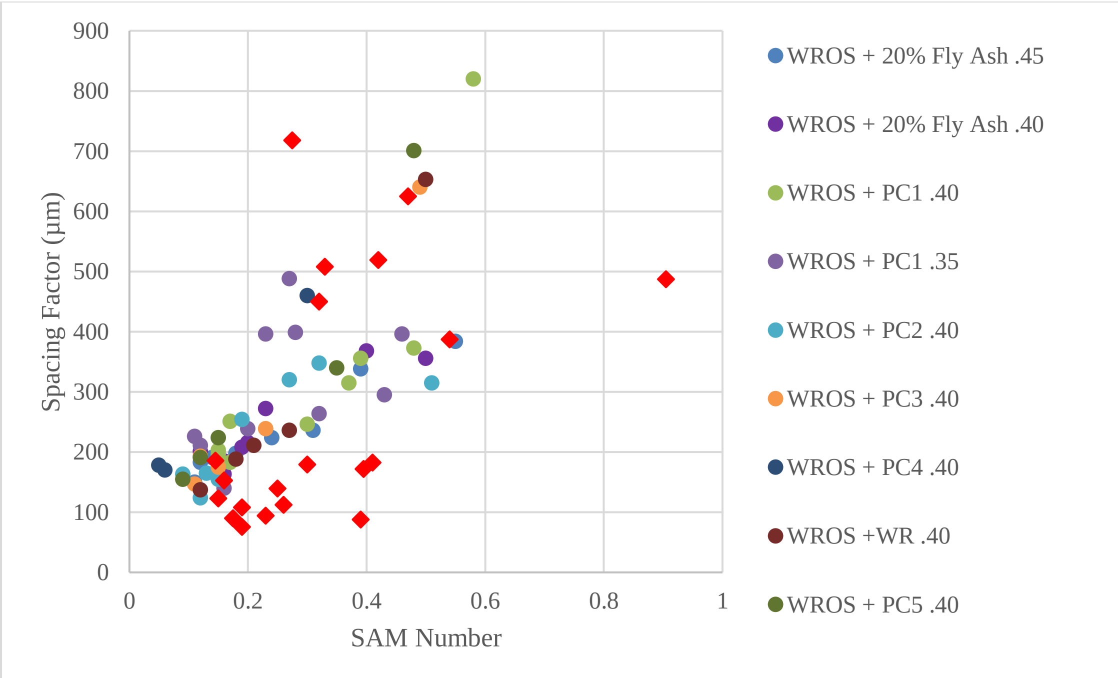

Figure 4.20: SAM Number vs. Spacing Factor (µm) – OSU data from Appendix of Ley et al. (2017) with NCDOT mixtures utilizing off spec fly ash overlaid (red data markers)

4.4.3 Durability Factor

ASTM C666 testing was performed on three 3in x 3in x 12in beams that had been wet cured for 14 days and then placed into a freezer to stop the curing process. As described in Section 3.9.2.2, a change in the oscilloscope settings during RP 2020-13 resulted in a loss of resolution on the fundamental frequency of these samples. Therefore, several samples from the RP 2020-13 project had a final (after 300 cycle) relative dynamic modulus than that of the initial reading, and therefore durability factors

(DF) slightly greater than 100. These samples will be shown as having a DF of 100 but will be marked with a hollow red circle to show which exceeded this limit.

Previously, the fresh air content and spacing factor of concrete mixtures was plotted against the durability factor. In this section the durability factor will be plotted with the SAM number of each mixture. The data from OSU shows a general drop in the durability factor as the SAM number approaches 0.4 as seen in Figure 4.21. This drop is similar to the drop measured when graphing the spacing factor (μm) vs the durability factor in Figure 4.14. The NCDOT mixtures did not exhibit a drop in durability factor with only 6 of the 57 mixtures with a durability factor being under a durability factor of 80. Of these 6 mixtures that fell under a durability factor of 80 only 2 were below a durability factor of 70. According to Brian Hunter, State Laboratory Engineer at NCDOT, North Carolina's bridge and pavement concrete mixtures have historically exhibited good freeze-thaw durability. UNC Charlotte's freeze-thaw laboratory tests of NCDOT mixtures have indeed supported this field observation, as can be seen in Figure 4.22. Note that the data shown with hollow red markers is from RP 2020-13 specimens where the durability factor was measured to be slightly greater than 100 due to the oscilloscope settings used.

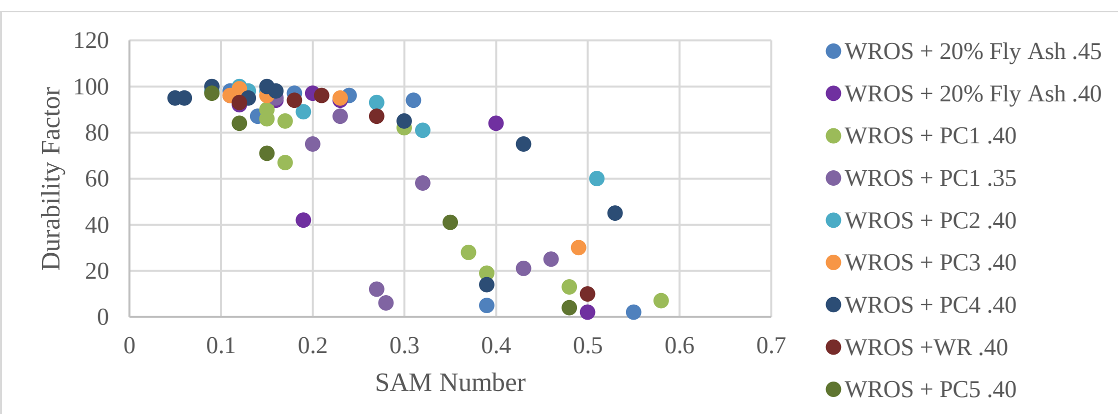

Figure 4.21: SAM Number vs. Durability Factor - OSU data from Appendix of Ley et al. (2017)

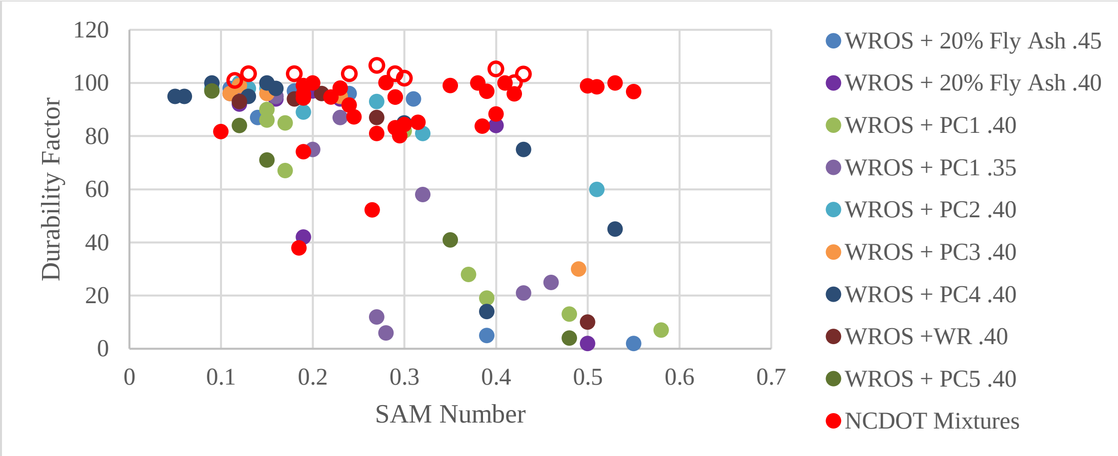

Figure 4.22: SAM Number vs. Durability Factor - OSU data from Appendix of Ley et al. (2017) with NCDOT mixtures overlaid (red data markers)

Figures 4.23, 4.24, and 4.25 show the results ASTM C666 from a previous project performed for a private client, which used off-spec fly ash (not meeting ASTM C618 requirements for Class F) in a typical NCDOT mixture. Findings from this project more closely aligned with the findings from Ley et al. (2017), but also aligned with NCDOT studies in that a majority of concrete mixtures that passed ASTM C666 testing. Figures 4.23, 4.24, and 4.25 shows the freeze-thaw performance test results for mixtures that contained off-spec fly ash from several sources, some treated with a treated them with a chemical compound to assist with air entrainment. Although the performance of mixtures containing fly ash from each source is different, mixtures containing air contents greater than 5% all had high (typically >90%) durability factors at the end of 300 freeze-thaw cycles (Ojo 2018).

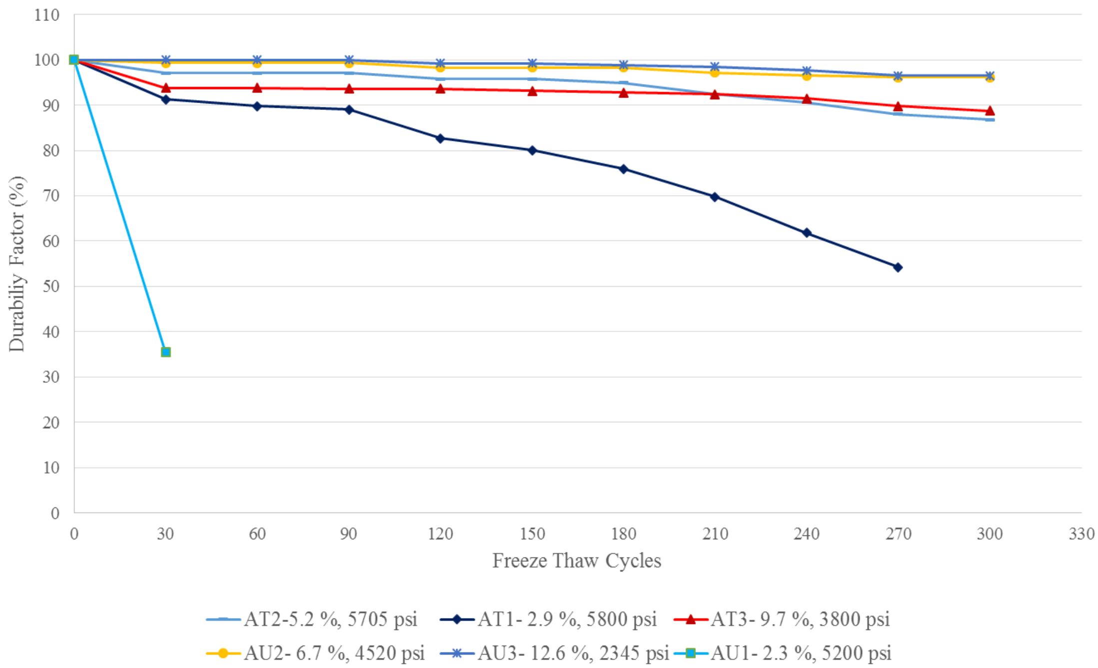

Figure 4.23: Previous NCDOT Mixtures ASTM C666 Testing Fly Ash A (Ojo 2018)

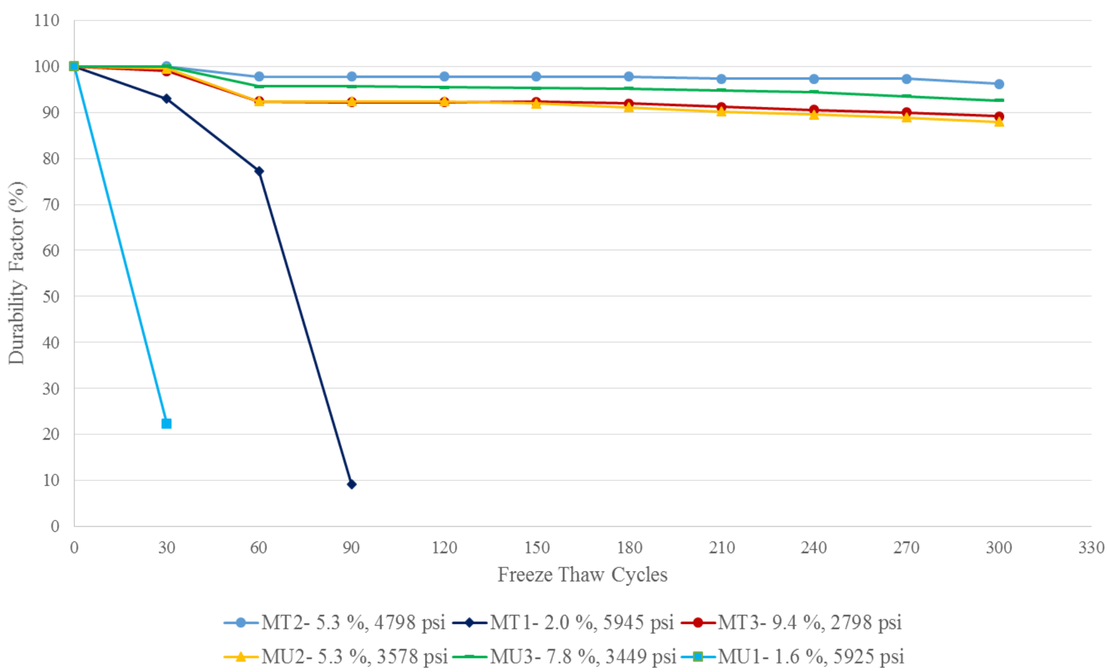

Figure 4.24: Previous NCDOT Mixtures ASTM C666 Testing Fly Ash M (Ojo 2018)

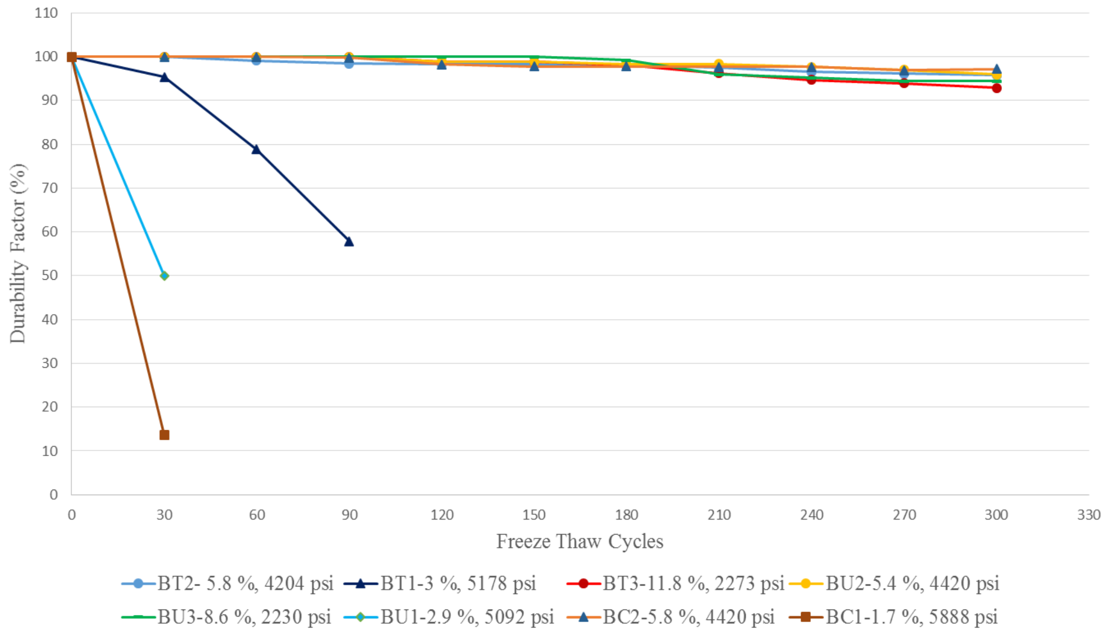

Figure 4.25: Previous NCDOT Mixtures ASTM C666 Testing Fly Ash B (Ojo 2018)

The mixtures in Figure 4.26 are the same mixtures used in all previous figures showing OSU data comparing a mixture using a PC and one containing no PC. These mixtures exhibit similar trends despite one containing a superplasticizer.

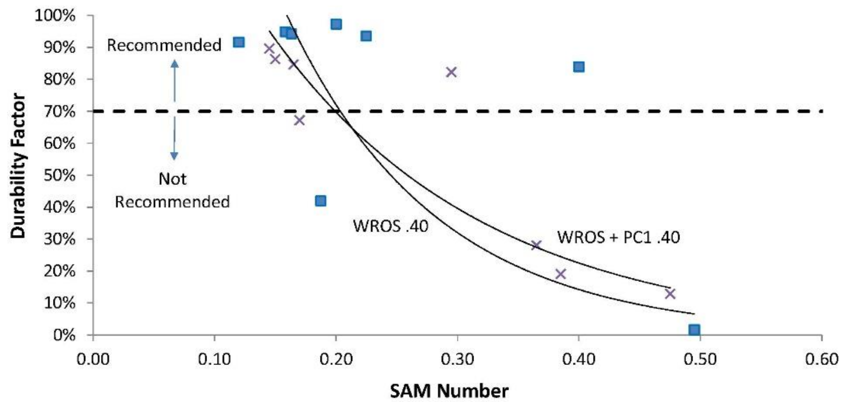

Figure 4.26: OSU SAM Number vs. Durability Factor select mixtures (Ley et al. 2017)

Along with comparing the durability factor to the SAM number, a comparison between the mass loss (%) and durability factor is shown in Figure 4.27 to demonstrate the relationship observed. In general, as the samples lost mass, a lower durability factor was measured. This is the expected outcome, since as the specimen loses mass, more of its pore structure is opened to the water it is placed in during the ASTM C666 Procedure A test. A visual inspection of all samples was also performed when the samples were tested for their dynamic modulus, and specimens typically exhibited progressive surface scaling only.

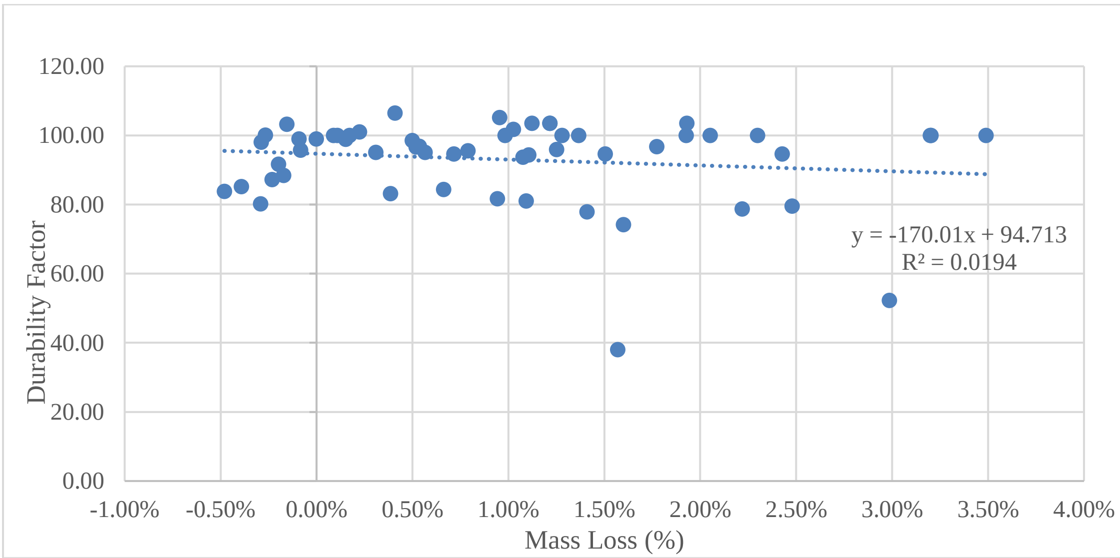

Figure 4.27: Mass Loss (%) vs. Durability Factor

4.4.4 Evaluation of Mixture Characteristics Influence on Spacing Factor

In this section, several mixture characteristics for NCDOT mixtures spanning the four projects described in Chapter 3 are plotted against the spacing factor. This was performed in order to evaluate whether a relationship exists between certain mixture characteristics and the spacing factor computed by the scanner technique of ASTM C457.

Figure 4.27 shows the paste content (%) graphed against the spacing factor for the NCDOT mixtures. The paste content of the samples exhibits a very weak positive correlation to the spacing factor measured. As can be seen in Figure 4.27, an increase in the paste content leading to an increase in the spacing factor measured.

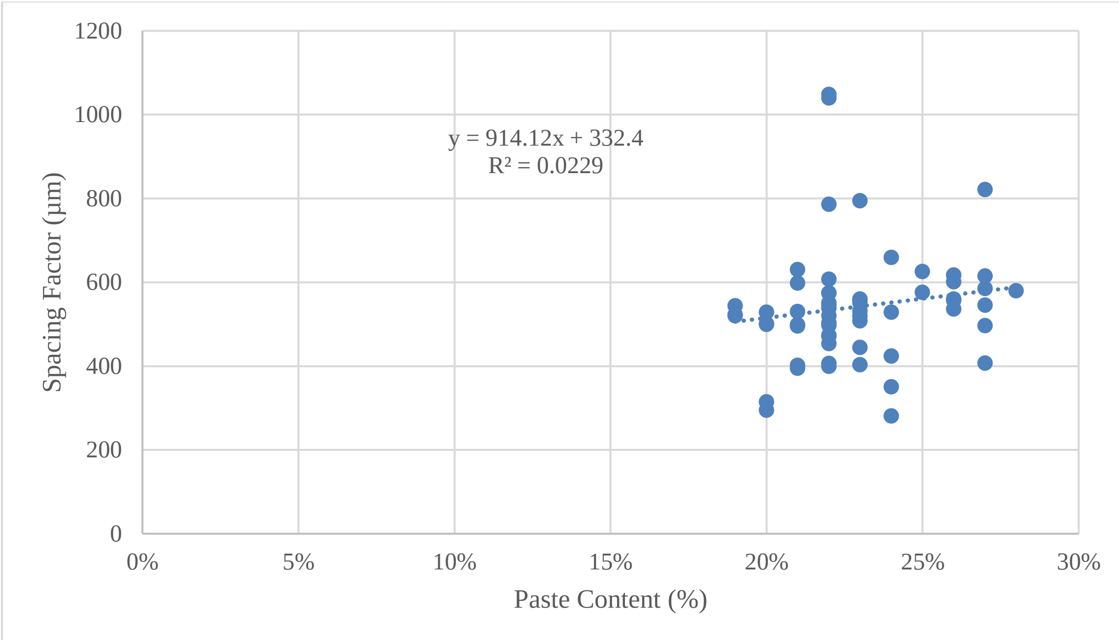

Figure 4.28: Paste Content (%) vs. Spacing Factor (µm)

The cementitious content of the mixtures also seems to be very weakly correlated with the spacing factor in much the same way the paste content is, as can be observed in Figure 4.25.

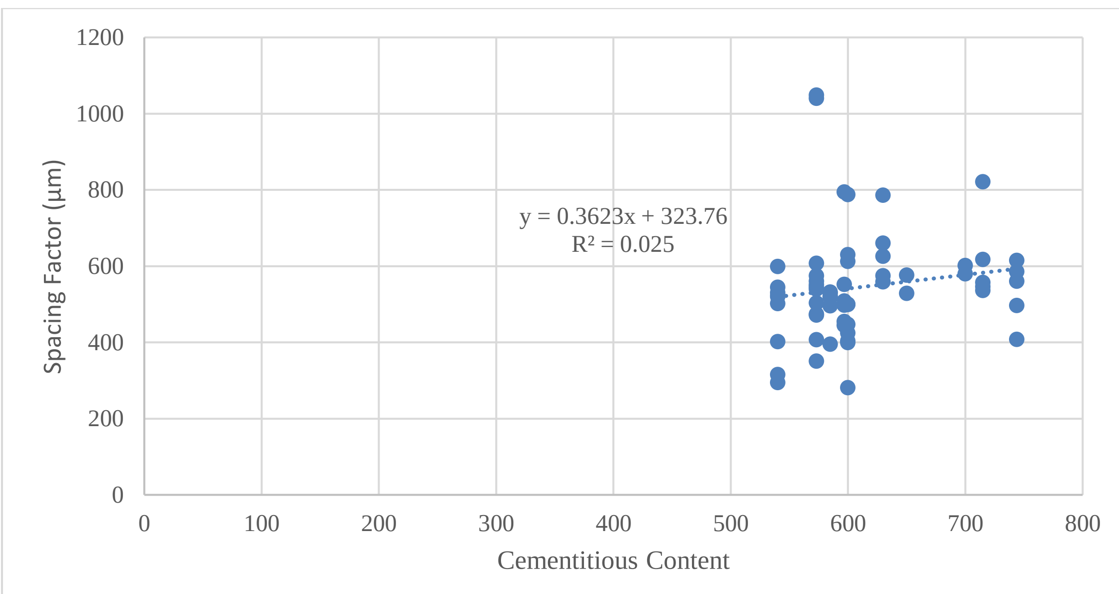

Figure 4.29: Cementitious Content vs. Spacing Factor (µm)

The w/cm ratio, however, did not show any discernable trend with spacing factor, as can be observed in Figure 4.29. Although no correlation was observed, the plot of w/cm ratio to the spacing factor has been shown below as a comparison to the weak correlations exhibited between cementitious content and spacing factor (Figure 4.27) and paste content and spacing factor (Figure 4.28).

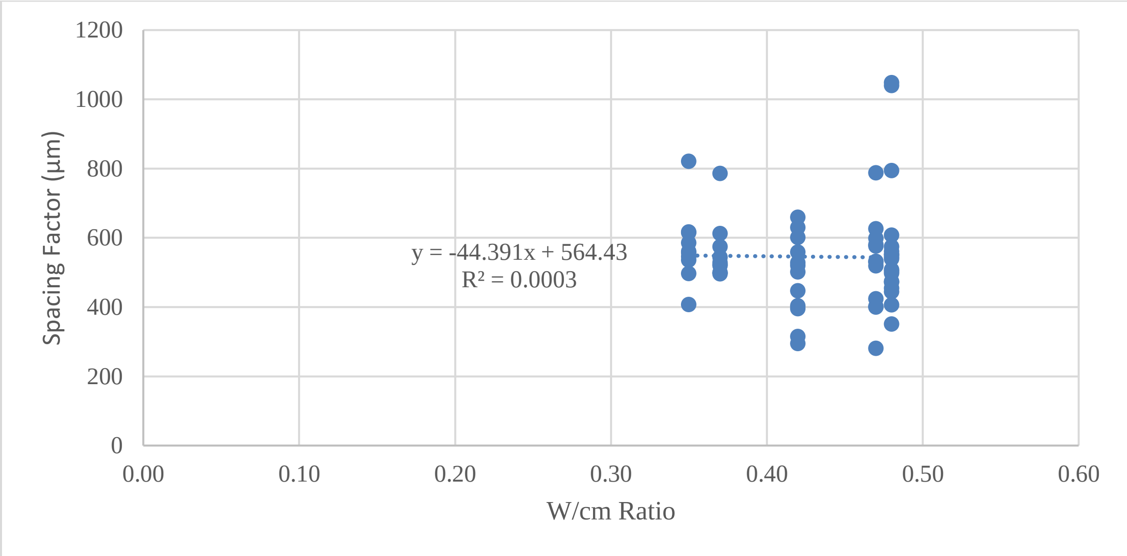

Figure 4.30: W/cm Ratio vs. Spacing Factor (µm)

The total percentage of mass of coarse and fine aggregates in each mixture were plotted against spacing factor in order to evaluate whether they had a noticeable correlation. These parameters were ultimately not included in this thesis as they also had no discernable correlation shown between them, and the spacing factor measured.

CHAPTER 5: DEVELOPMENT OF RECOMMENDED SAM SPECIFICATION

5.1 Introduction

This chapter provides a summary of current approaches, shadow targets, and specifications utilized by several state DOTs for SAM testing. The information from these states' agencies will be used to provide an overview of implementation approaches that have been used.

5.2 Relevant Current Requirements

To support use of the results from this research project in future work and to develop a preliminary SAM specification for NCDOT, a review of existing SAM specifications was undertaken. Along with a review of current state SAM specifications a review of the current AASHTO standard for the SAM is included.

5.2.1 AASHTO TP 118-17

The standard for the SAM test is AASHTO TP 118-17, which is referenced in AASHTO PP 84-20 (now AASHTO R 101). AASHTO TP 118-17 includes three separate testing methods; the first test method is to determine the air content of the sample tested, the second test is to determine the volume of the vessel, and the final and relevant test is to determine the SAM number of the sample tested. As discussed previously, the SAM number measures a durability characteristic of the concrete which is not an intrinsic value of the concrete. Since durability performance is influenced by the environmental stresses placed on the concrete, the SAM number is instead correlated to the spacing factor with a SAM number of 0.20 showing general agreement with a spacing factor of 0.008 in or 0.20 mm in some studies (Ley et al. 2017). Per AASHTO TP 118-

17, a correctly run test should have a SAM number between 0.03 and 0.82, and values found outside of this range should be considered a bad reading.

AASHTO PP 84-20 provides guidance for using and AASHTO TP 118-17 and interpreting the results. The prescriptive specification utilizing the SAM number calls for air content of 4 percent or greater and a SAM number less than or equal to 0.20 during mixture approval. AASHTO PP 84-20 recommends site acceptance criteria as detailed in Table 5.1 below.

Table 5.1: Concrete Acceptance Requirements (AASHTO PP 84-20)

SAM Acceptance Requirement (AASHTO TP 118)		
Action	Air Content (%)	SAM Number
Accept	≥4	<0.25
Modify	≥4	≥0.25 and ≤0.3
Reject	≥4	>0.3

5.2.2 Relevant State Approaches and Standards

Currently the SAM is being utilized in several states as well as some Canadian provinces. However, of the state specifications reviewed for this project, only Wisconsin had SAM requirements included in the standard specifications as a mixture design approval requirement (WisDOT 2022). At the time of this review, the Wisconsin DOT standard specifications includes a quality management plan requiring the SAM test be performed at least once per lot with the following exceptions: lots less than 4 sublots, high early strength concrete, special high early strength concrete, concrete pavement approach slabs, concrete masonry culverts, concrete masonry retaining walls, crash cushions, and concrete-filled steel grid floor. While the SAM number was a required measurement, no pay adjustment was required for an unsatisfactory test result, and recommendations for an acceptable SAM number were not included (WisDOT 2022).

At the time of this review, the New York DOT did not have a standard specification calling for the use of the SAM test but did include a special provision for SAM testing the during mixture design phase in section 501-3 (NYSDOT 2022).

Table 5.2: Design Mix Performance Criteria (NYSDOT)

Primary Application	Scaling, freeze/thaw, or shrinkage requirements
Superstructures: bridge decks, approach slabs, sidewalk and safety walk on decks, concrete barrier	ASTM C666 with DF > 90% or AASHTO TP 118 < 0.20 and paste factor < 27% per AASHTO PP-84
Substructures7: abutments, backwalls, wing walls, columns, pier caps, pedestals	ASTM C666 with DF > 90% or AASHTO TP 118 < 0.20 and paste factor < 27% per AASHTO PP-84
Thin structural applications, overlays	ASTM C666 with DF > 90% or AASHTO TP 118 < 0.20 and paste factor < 30% per AASHTO PP-84
Overhead sign bases, signal pole bases, and bases supporting overhead uses	ASTM C666 DF > 90% or AASHTO TP 118 ≤0.20
Sidewalks, gutters, curbs	ASTM C666 DF > 90% or AASHTO TP 118 ≤0.20
Barriers	ASTM C666 DF > 90% or AASHTO TP 118 ≤0.20
Headwalls, drainage elements, pipe inverts	ASTM C666 DF > 90% or AASHTO TP 118 ≤0.20

Colorado DOT has also created a special provision for the SAM test where all air entrained concrete produced for their projects will also need to have a SAM number reported when air testing is conducted for mixture design (CODOT 2021). This provision has been placed into section 601.05 of the standard specifications for projects that include a special provision.

West Virginia approved of using the SAM as a project specific special provision for mixture design acceptance. The criteria required for the mixture design is shown in Table 5.3 below.

Table 5.3: Design Mix Performance Criteria (WVDOT)

SAM Number	Required Action
Less than 0.25	Accept Concrete
0.25 to 0.30	Accept with Corrective Action Needed
Greater than 0.30	Reduced payment for concrete

The New York DOT approach appears to be useful as a guide, but performance targets may not be ideal, since the freeze-thaw cycles experienced in North Carolina and New York are likely very different due to the geographic distance.

As the AASHTO standard for performance engineered concrete for pavements (AASHTO PP 84) was recently approved as standard practice (now AASHTO R 101-22), the number of state agencies using the SAM test within their specifications may increase.

5.3 Development of Performance Targets for a SAM Specification

The original lab work completed by Ley et al. (2017) showed that beyond a SAM number of 0.30, a steep decline in the ability of the concrete to provide a durability factor above 80 in the ASTM C666 freeze-thaw test. With such a steep decline exhibited by the mixtures included to date, the OSU research team established a recommended of a SAM number of 0.20 to ensure adequate freeze-thaw performance of most mixtures. Of note, a SAM number of 0.20 is the target used by the New York DOT in their special provisions.

Other laboratories performing research on different types of concrete mixtures using materials from different geographic areas have had results that indicate a different SAM number may correlates to a recommended spacing factor and/or durability factor. In a study aimed to evaluate the SAM in Poland, Dabrowski et al. (2019) found that a SAM number of 0.40 provided a more accurate correlation to the desired spacing factor of 200 μm. These researchers indicated that a SAM number target of 0.20 was too restrictive, with only one of the tested mixtures included in their study achieving a SAM number of 0.20 or below while mixtures with a SAM number greater than 0.20- but less than 0.40 still exhibiting a desirable spacing factor. European countries do not use a rapid freeze-thaw test such as ASTM C666, so this study did not provide data to allow comparisons to be made with the durability factor. However, a SAM number of 0.40 had an apparent correlation to the content of microvoids deemed acceptable. Microvoids are air voids that are under 300 μm in size and have been shown to be a useful parameter in determining the quality of the microstructure of the air void system (Dabrowski et al. 2019).

One final lab's results will be used to help guide the specification for the SAM test in North Carolina and that is the work done by Ojo (2018) at UNC Charlotte. In these mixtures a SAM of 0.30 was found to encompass all but three mixtures that had a durability factor of 60 or higher which is the failure threshold for ASTM C666. As a disclaimer, the mixtures used by Ojo (2018) used fly ash that did not meet ASTM C618 in some mixtures. However, the mixtures and materials did provide useful insights into a wider range of air contents which the NCDOT-sponsored research did not provide due to the study design.

5.4 Summary of Findings

A limited number of state highway agencies have specifications or project special provisions for use of the SAM in their concrete infrastructure. The SAM number targets used by states in trial bases have typically aligned with the OSU research team and AASHTO PP 84 target of 0.20.

As part of a number of studies of NCDOT concrete mixtures, freeze-thaw testing per Procedure A of ASTM C666 was performed on mixtures with a wide range of w/cm, SCM contents, aggregate sources, and other factors. These mixtures have exhibited highly favorable freeze-thaw durability performance in the laboratory, with DF typically greater than 80 at 300 cycles. With these favorable durability factors in the ASTM C666 test, a less conservative SAM number (e.g., greater than 0.20) should be an appropriate preliminary target for NCDOT project special provisions for the SAM until additional field and laboratory data is collected and analyzed. It is therefore recommended that NCDOT use a SAM number of 0.30 in shadow specifications for future projects, along with requirements for total air content aligned with their current specifications 6.0% ± 1.5%. In environments experiencing significant freeze-thaw, such as in the mountains, it could be worthwhile to for NCDOT to consider specifying a higher air content range of 6 to 8%, consistent with other states with similar environments.

CHAPTER 6: CONCLUSIONS AND FUTURE WORK

6.1 Introduction

In support of the NCDOT's larger effort in the FHWA's PEM initiative, this thesis presents the results of analysis of structural and pavement concrete produced using typical North Carolina materials and mixtures to evaluate the fresh and hardened air void system characteristics and freeze thaw durability performance. A range of different mixture proportions and mixture characteristics used as part of several NCDOT projects offered the opportunity to explore the effect different mixture components and characteristics each might have on the entrained air void system and freeze-thaw performance of the concrete.

The overall objective of this work was to identify performance targets to support of the development of a proposed SAM specification for use by the NCDOT to improve the durability performance of concrete pavements and structures in freeze-thaw environments. Results of the laboratory testing and analysis to support identification of target SAM numbers that NCDOT's pavement and structural mixtures could reasonably meet with conventional mixtures that exhibit the required mechanical properties and durability performance. Findings of a review of other state agency specifications for use of the SAM for highway concrete were paired with results from a privately funded study of North Carolina concrete mixtures to help inform selection of a performance target. As such, all conclusions and recommendations presented herein should be considered a preliminary step in the NCDOT's movement towards PEM specifications and a more durable and sustainable concrete infrastructure.

6.2 Conclusions

Laboratory testing of the 24 mixtures batched for this thesis along with test results from several past projects using concrete representative of NCDOT mixtures provided valuable information regarding the characteristics which influence the freeze-thaw durability of a mixture. The key findings from the laboratory testing and analysis are listed below:

- NCDOT structural and pavement mixtures batched and tested as part of a series of research studies are very resistant to freeze-thaw stresses. After 300 cycles of ASTM C666 testing, only 6 of the 56 mixtures exhibited a durability factor below 80 and only 2 falling below ASTM C666's performance threshold durability factor of 60.
- The historically used spacing factor limit of 0.008 in (200 μm) appears to be too conservative for use of NCDOT in specification development. Many mixtures exhibiting good to excellent freeze-thaw durability performance in the ASTM C666 test had spacing factors that exceeded this target. Since most concrete mixtures included in this study exhibited durability factors greater than 80, a proposed target spacing factor could not be identified.
- Fresh air content exhibited a reasonable correlation to the spacing factor and durability factor found during testing.
- The SAM numbers obtained during studies of NCDOT concrete at UNC Charlotte exhibited a lesser correlation to the durability factor. The strong relationship between SAM number and spacing factor observed in other studies was not observed based on findings of this work. Variability in the SAM measurements was likely increased due to use of multiple devices, operators, and materials. Variability also exists in the spacing

factor measurements, which could have affected the ability to observe meaningful correlations.

6.3 Recommendations for Future Work

The findings of this study were significantly limited by the range of air contents (5 to 6%) used in the mixtures. A more comprehensive study should be performed using a wider range of air contents (such as 2% to 10%). Analysis of field-produced concrete should also be paired with additional laboratory testing of to further explore the SAM number, in hopes of expanding the types of materials and mixtures used to identify the performance target. Future research projects to support NCDOT's PEM initiatives could further explore the spacing factor, SAM number and durability factor that correlates to adequate performance in both the field and laboratory.

REFERENCES

American Association of State Highway and Transportation Officials (AASHTO). (2019). “Standard Practice for Developing Performance Engineered Concrete Pavement Mixtures.” PP 84-19, American Association of State Highway and Transportation Officials, Washington, DC.

American Association of State Highway and Transportation Officials (AASHTO). (2022). “Standard Test Method for Characterization of the Air-Void System of Freshly Mixed Concrete by the Sequential Pressure Method” R 101-22, American Association of State Highway and Transportation Officials, Washington, DC.

American Concrete Institute (2016). Guide to Durable Concrete. ACI 201.2R-16. Farmington Hills, MI.

American Concrete Institute (2012). Chemical Admixtures for Concrete. ACI Education Bulletin E4-12. Farmington Hills, MI.

ASTM International. C39/C39M-21 Standard Test Method for Compressive Strength of Cylindrical Concrete Specimens. West Conshohocken, PA; ASTM International, 2021. doi: https://doi.org/10.1520/C0039_C0039M-21

ASTM International. C78/C78M-21 Standard Test Method for Flexural Strength of Concrete (Using Simple Beam with Third-Point Loading). West Conshohocken, PA; ASTM International, 2021. doi: https://doi.org/10.1520/C0078_C0078M-21

ASTM International. C138/C138M-17a Standard Test Method for Density (Unit Weight), Yield, and Air Content (Gravimetric) of Concrete. West Conshohocken, PA; ASTM International, 2017. doi: https://doi.org/10.1520/C0138_C0138M-17A

ASTM International. C143/C143M-20 Standard Test Method for Slump of Hydraulic-Cement Concrete. West Conshohocken, PA; ASTM International, 2020. doi: https://doi.org/10.1520/C0143_C0143M-20

ASTM International. C150/C150M-20 Standard Specification for Portland Cement. West Conshohocken, PA; ASTM International, 2020. doi: https://doi.org/10.1520/C0150_C0150M-20

ASTM International. C157/C157M-17 Standard Test Method for Length Change of Hardened Hydraulic-Cement Mortar and Concrete. West Conshohocken, PA; ASTM International, 2017. doi: https://doi.org/10.1520/C0157_C0157M-17

American Society for Testing and Materials (ASTM). (2018). ASTM Standard C192/C192M-18 "Standard Practice for Making and Curing Concrete Test Specimens in the Laboratory." ASTM International, West Conshohocken, PA. DOI: 10.1520/C0192_C0192M-18. www.astm.org

ASTM International. C215-19 Standard Test Method for Fundamental Transverse, Longitudinal, and Torsional Resonant Frequencies of Concrete Specimens. West Conshohocken, PA; ASTM International, 2019. doi: https://doi.org/10.1520/C0215-19

ASTM International. C231/C231M-17a Standard Test Method for Air Content of Freshly Mixed Concrete by the Pressure Method. West Conshohocken, PA; ASTM International, 2017. doi: https://doi.org/10.1520/C0231_C0231M-17A

American Society for Testing and Materials (ASTM). (2016). ASTM Standard C457/C457M-16 "Standard Test Method for Microscopical Determination of Parameters of the Air-Void System in Hardened Concrete." ASTM International, West Conshohocken, PA. DOI: 10.1520/C0457_C0457M-16. www.astm.org

ASTM International. C511-19 Standard Specification for Mixing Rooms, Moist Cabinets, Moist Rooms, and Water Storage Tanks Used in the Testing of Hydraulic Cements and Concretes. West Conshohocken, PA; ASTM International, 2019. doi: https://doi.org/10.1520/C0511-19

ASTM International. C618-19 Standard Specification for Coal Fly Ash and Raw or Calcined Natural Pozzolan for Use in Concrete. West Conshohocken, PA; ASTM International, 2019. doi: https://doi.org/10.1520/C0618-19

American Society for Testing and Materials (ASTM). (2015). ASTM Standard C666/C666M-15 “Standard Test Method for Resistance of Concrete to Rapid Freezing and Thawing.” ASTM International, West Conshohocken, PA. DOI: 10.1520/C0666_C0666M-15. www.astm.org

American Society for Testing and Materials (ASTM). (2017). ASTM Standard C685/C685M-17 “Standard Specification for Concrete Made by Volumetric Batching and Continuous Mixing.” ASTM International, West Conshohocken, PA. DOI: 10.1520/C0685_C0685M-17. www.astm.org

Appropedia.org. 2021. BubbleCounter - Appropedia: The sustainability wiki. [online] Available at: <https://www.appropedia.org/BubbleCounter> [Accessed 7 April 2021].

Biggers, R. B. (2019). “Development of a Surface Resistivity Specification for Durable Concrete” (Master Thesis), University of North Carolina at Charlotte.

Blanchard, E. H. (2016). “Determination and Evaluation of Inputs for Portland Cement Concrete Pavement to Support Local Calibration of MEPDG for North Carolina” (Master Thesis), University of North Carolina at Charlotte

Cackler, T., Harrington, D., Taylor, P.C. (2017). “Performance Engineered Mixtures (PEM) for Concrete Pavements.” CP Road Map MAP Brief, April 2017. National Concrete Pavement Technology Center. Ames, IA.

Cavalline, T. L., Tempest, B. Q., Biggers, R. B., Lukavsky, A. J., McEntyre, M. S., and Newsome, R. A. (2020). Durable and Sustainable Concrete Through Performance Engineered Concrete Mixtures. Report No. FHWA/NC/2018-14

Cavalline, T. L., Tempest, B. Q., Blanchard, E. H., Medlin, C. D., and Chimmula, R. R. (2018). Improved Data for Mechanistic-Empirical Pavement Design for Concrete Pavements. Report No. FHWA/NC/2015-03.

Cavalline, T. L., Tempest, B. Q., Leach, J. W., Newsome, R. A., Loflin, G. D., and Fitzner, M. J. (2019). Internal Curing of Concrete Using Lightweight Aggregate. Report No. FHWA/NC/2016-06.

Claisse, P. A., Transport Properties of Concrete: Measurements and Applications, Elsevier, 2014.

Colorado Department of Transportation (CDOT). 2021. Standard Special Provisions: Section 601: Concrete Mix Designs

Concrete.org. 2021. How is the air content of freshly mixed concrete determined?. [online] Available at: <https://www.concrete.org/tools/frequentlyaskedquestions.aspx?faqid=823> [Accessed 17 February 2021].

Dabrowski, M., Glinicki, M. A., Dziedzic, K., and Anotlik, A. (2019). “Validation of sequential pressure method for evaluation of the content of microvoids in air entrained concrete,” Construction and Building Materials, 227.

Economic Development Research Group, Inc. (2016). “Failure to Act: Closing the Infrastructure Investment Gap for America’s Economic Future.” American Society of Civil Engineers. Reston, VA.

Fagerlund, G. (2004). “A service life model for international frost damage in concrete.” Rep. TVBM-3119, Div. of Building Technology, Lund Institute of Technology, Lund, Sweden.

Felice, R., Freeman, J. M., and Ley, M. T. (2014). “Durable Concrete with Modern Air-Entraining Admixtures,” Concrete International 36(8), 37-45.

Hall, H., LeFlore, J., Staffileno, C., Fennell, M., and Ley, T. (2019). "Update on the Super Air Meter." Presented at the Spring 2019 meeting of the National Concrete Consortium. April 25, 2019. Denver, Colorado. Available at: https://intrans.iastate.edu/events/spring-2019-national-concrete-consortium/

Hallet, B., Walder, J. S., and Stubbs, C. W. (1991). "Weathering by Segregation Ice Growth in Microcracks at Sustained Sub-zero Temperatures: Verification from an Experimental Study Using Acoustic Emissions" Permafrost and Periglacial Processes, 2, 283-300.

Hearn, N., Hooton, R. D., and Nokken, M. R., "Pore Structure, Permeability, and Penetration Resistance Characteristics of Concrete" Significance of Tests and Properties of Concrete & Concrete-Making Materials, ASTM International, West Conshohocken, PA, 2006, 238-252.

Hover, K., 1993 'Why is there Air in Concrete', http://www.concreteconstruction.net/_view-object?id=00000153-964c-dbf3-a177-967ddaf60000

Hover, K. C., 1998, "Concrete Mixture Proportioning with Water-reducing Admixtures to Enhance Durability: A Quantitative Model." Cement and Concrete Composites, 20(1998), 113-119.

Kosmatka, S. H., Kerkhoff, B., and Panarese, W. C., Design and Control of Concrete Mixtures, EB001, 14th edition, Portland Cement Association, Skokie, Illinois, USA, 2002, 358 pages.

Ley, M.T. and Tabb, B., 2014. "A Test Method to Measure the Freeze Thaw Durability of Fresh Concrete using Overpressure," T&DI Congress 2014: Planes, Trains, and Automobiles, 79-87.

Ley, M. T., Welchel, D., Peery, J., Khatibmasjedi, S., and LeFlore, J. (2017). "Determining the air-void distribution in fresh concrete with the Sequential Air Method," Construction and Building Materials, 150, 723-737.

Lilek, J. (2017). "Roadway deicing in the United States: How a few industrial minerals supply a vital transportation service." American Geosciences Institute. Alexandria, VA. https://www.americangeosciences.org/sites/default/files/CI_Factsheet_2017_3_Deicing_170712.pdf [accessed 2-01-2021].

Mehta, P. and Monteiro, P. (2006). Concrete: Microstructure, Properties, and Materials. McGraw-Hill, New York, NY

Neville, A. M. (2013). Properties of Concrete. Pearson Education Limited, London, UK

New York Department of Transportation (NYSDOT). 2022. Special Specifications: Section 501: Portland Cement Concrete – Performance Mixture Design and Quality Control. Albany, New York

North Carolina Department of Transportation (NCDOT). (2018). Section 1000, Portland Cement Concrete Production and Delivery. https://connect.ncdot.gov/resources/safety/Signing%20and%20Delineation%20Library/2018_Division_10.pdf

Ojo, T., O. (2018). "Performance of Portland Cement Concrete Containing Chemically Beneficiated High Loss on Ignition Fly Ashes with Air Entrainment" (Master Thesis), University of North Carolina at Charlotte.

Peppin, S. S. L. and Style, R. W. (2013). "The Physics of Frost Heave and Ice-Lens Growth," Vadose Zone Journal 12(1), 1-12. https://doi.org/10.2136/vzj2012.0049

Peterson, K. W., Swartz, R. A., Sutter, L. L., and Van Dam, T. J. (2001). "Hardened Concrete Air Void Analysis with a Flatbed Scanner" Transportation Research Record, 1775, 36-43.

Pigeon, M. and Pleau, R. (1995). Durability of Concrete in Cold Climates. E & FN Spon, London, UK

Powers, T.C. (1958). Structure and Physical Properties of Hardened Portland Cement Paste. Journal of the American Ceramic Society, 41: 1-6. https://doi.org/10.1111/j.1151-2916.1958.tb13494.x

Powers, T. C., and Helmuth, R. A. (1953). "Theory of Volume Changes in Hardened Portland Cement Paste During Freezing," Proceedings, Highway Research Board, V. 32, 1953, pp. 285-297.

Powers, T.C., Copeland, L.E., and Mann, H.M. (1959). "Capillary continuity or discontinuity in cement pastes". Journal of the PCA Research and Development Laboratories, 1959. 1(2): p. 38-48.

Ram, P., Dam, T. V., Sutter, L., Anzalone, G., and Smith, K. (2012). Field Study of Air Content Stability in the Slipform Paving Process. Report No. WHRP 0092-11-06

Rixom, R. and Mailvaganam, N. (1999). "Chemical Admixtures for Concrete 3rd ed. E & FN Spon, London, UK

Setzer, M. J. (2001). "Micro-Ice-Lens Formation in Porous Solid," Journal of Colloid and Interface Science 243,193–20.1 doi: 10.1006/jcis.2001.7828

Welchel, David. (2014). "Determining the Air-Void Distribution of Fresh Concrete with the Sequential Pressure Method" (Master Thesis), Oklahoma State University, https://hdl.handle.net/11244/299670

Wisconsin Department of Transportation (WisDot). 2022. Standard Specification for Highway and Structure Construction: Section 715: QMP Concrete Pavement and Structures. Madison, Wisconsin.

Tanesi, J. and Meininger, R. (2006). Freeze-Thaw Resistance of Concrete with Marginal Air Content. Report No. FHWA-HRT_06-117.

Theilgard P. (2022). “Optimized Aggregate Gradation Concrete Mixtures with Cementitious Material Reduction” (Master Thesis), University of North Carolina at Charlotte.

Transportation Research Board (TRB). (2013). Durability of Concrete. Transportation Research Circular No. E-C171. TRB Committee AFN30. Transportation Research Board, Washington, DC.